NUREG/CR-3391, Vol. 1
HEDL-TME 83-21

LWR PRESSURE VESSEL SURVEILLANCE DOSIMETRY IMPROVEMENT PROGRAM

QUARTERLY PROGRESS REPORT
JANUARY 1983 - MARCH 1983

Hanford Engineering Development Laboratory

Prepared by
E.P. Lippincott
W.N. McElroy

Prepared for the U.S. Nuclear Regulatory Commission

GPO Printed copy price: $4.50

NUREG/CR-3391, Vol. 1
HEDL-TME 83-21
R5

LWR PRESSURE VESSEL SURVEILLANCE DOSIMETRY IMPROVEMENT PROGRAM

QUARTERLY PROGRESS REPORT JANUARY 1983 - MARCH 1983

NUREG/CR--3391-Vol.1

DE84 004657

Hanford Engineering Development Laboratory

Operated by Westinghouse Hanford Company
P.O. Box 1970 Richland, WA 99352
A Subsidiary of Westinghouse Electric Corporation

Prepared by
E.P. Lippincott
W.N. McElroy

Manuscript Completed: September 1983
Date Published: November 1983

Prepared for Division of Engineering Technology
Office of Nuclear Regulatory Research
U.S. Nuclear Regulatory Commission
Washington, DC 20555
NRC FIN No. B5988

PREVIOUS REPORTS IN LWR-PV-SDIP SERIES

NUREG/CR-0038	HEDL-TME 78-4	July 1977 - September 1977
NUREG/CR-0127	HEDL-TME 78-5	October 1977 - December 1977
NUREG/CR-0285	HEDL-TME 78-6	January 1978 - March 1978
NUREG/CR-0050	HEDL-TME 78-7	April 1978 - June 1978
NUREG/CR-0551	HEDL-TME 78-8	July 1978 - September 1978
NUREG/CR-0720	HEDL-TME 79-18	October 1978 - December 1978
NUREG/CR-1747	HEDL-TME 80-73	October 1979 - September 1980*
NUREG/CR-1240, Vol. 1	HEDL-TME 79-41	January 1979 - March 1979
NUREG/CR-1240, Vol. 2	HEDL-TME 80-1	April 1979 - June 1979
NUREG/CR-1240, Vol. 3	HEDL-TME 80-2	July 1979 - September 1979
NUREG/CR-1240, Vol. 4	HEDL-TME 80-3	October 1979 - December 1979
NUREG/CR-1291	HEDL-SA-1949	October 1978 - December 1979*
NUREG/CR-1241, Vol. 1	HEDL-TME 80-4	January 1980 - March 1980
NUREG/CR-1241, Vol. 2	HEDL-TME 80-5	April 1980 - June 1980
NUREG/CR-1747	HEDL-TME 80-73	October 1979 - December 1980*
NUREG/CR-1241, Vol. 3	HEDL-TME 80-6	October 1980 - December 1980
NUREG/CR-2345, Vol. 1	HEDL-TME 81-33	January 1981 - March 1981
NUREG/CR-2345, Vol. 2	HEDL-TME 81-34	April 1981 - June 1981
NUREG/CP-0029	HEDL-SA-2546	October 1980 - September 1981*
NUREG/CR-2345, Vol. 4	HEDL-TME 81-36	October 1981 - December 1981
NUREG/CR-2805, Vol. 1	HEDL-TME 82-18	January 1982 - March 1982
NUREG/CR-2805, Vol. 2	HEDL-TME 82-19	April 1982 - June 1982
NUREG/CR-2805, Vol. 3	HEDL-TME 82-20	October 1981 - September 1982*
NUREG/CR-2805, Vol. 4	HEDL-TME 82-21	October 1982 - December 1982

*Annual Reports

FOREWORD

The Light Water Reactor Pressure Vessel Surveillance Dosimetry Improvement Program (LWR-PV-SDIP) has been established by NRC to improve, test, verify, and standardize the physics-dosimetry-metallurgy, damage correlation, and the associated reactor analysis methods, procedures and data used to predict the integrated effect of neutron exposure to LWR pressure vessels and their support structures. A vigorous research effort attacking the same measurement and analysis problems exists worldwide, and strong cooperative links between the US NRC-supported activities at HEDL, ORNL, NBS, and MEA-ENSA and those supported by CEN/SCK (Mol, Belgium), EPRI (Palo Alto, USA), KFA (Jülich, Germany), and several UK laboratories have been extended to a number of other countries and laboratories. These cooperative links are strengthened by the active membership of the scientific staff from many participating countries and laboratories in the ASTM E10 Committee on Nuclear Technology and Applications. Several subcommittees of ASTM E10 are responsible for the preparation of LWR surveillance standards.

The primary objective of this multilaboratory program is to prepare an updated and improved set of physics-dosimetry-metallurgy, damage correlation, and associated reactor analysis ASTM Standards for LWR pressure vessel and support structure irradiation surveillance programs. Supporting this objective are a series of analytical and experimental validation and calibration studies in "Standard, Reference, and Controlled Environment Benchmark Fields," research reactor "Test Regions," and operating power reactor "Surveillance Positions."

These studies will establish and certify the precision and accuracy of the measurement and predictive methods recommended in the ASTM Standards and used for the assessment and control of the present and end-of-life (EOL) condition of pressure vessel and support structure steels. Consistent and accurate measurement and data analysis techniques and methods, therefore, will be developed, tested, and verified along with guidelines for required neutron field calculations used to correlate changes in material properties with the characteristics of the neutron radiation field. It is expected that the application of the established ASTM Standards will permit the reporting of measured material property changes and neutron exposures to an accuracy and precision within bounds of 10 to 30%, depending on the measured metallurgical variable and neutron environment.

The assessment of the radiation-induced degradation of material properties in a power reactor requires accurate definition of the neutron field from the outer region of the reactor core to the outer boundaries of the pressure vessel. Problems with measuring neutron flux and spectrum are associated with two distinct components of LWR irradiation surveillance procedures: 1) proper application of calculational estimates of the neutron exposure at in- and ex-vessel surveillance positions, various locations in the vessel wall and ex-vessel support structures, and 2) understanding the relationship between material property changes in reactor vessels and their support structures, and in metallurgical test specimens irradiated in test reactors and at accelerated neutron flux positions in operating power reactors.

The first component requires verification and calibration experiments in a variety of neutron irradiation test facilities including LWR-PV mockups, power reactor surveillance positions, and related benchmark neutron fields. The benchmarks serve as a permanent reference measurement for neutron flux and fluence detection techniques, which are continually under development and widely applied by laboratories with different levels of capability. The second component requires a serious extrapolation of an observed neutron-induced mechanical property change from research reactor "Test Regions" and operating power reactor "Surveillance Positions" to locations inside the body of the pressure vessel wall and to ex-vessel support structures. The neutron flux at the vessel inner wall is up to one order of magnitude lower than at surveillance specimen positions and up to two orders of magnitude lower than at test reactor positions. At the vessel outer wall, the neutron flux is one order of magnitude or more lower than at the vessel inner wall. Further, the neutron spectrum at, within, and leaving the vessel is substantially different.

In order to meet the reactor pressure vessel radiation monitoring requirements, a variety of neutron flux and fluence detectors are employed, most of which are passive. Each detector must be validated for application to the higher flux and harder neutron spectrum of the research reactor "Test Region" and to the lower flux and degraded neutron spectrum at "Surveillance Positions." Required detectors must respond to neutrons of various energies so that multigroup spectra can be determined with accuracy sufficient for adequate damage response estimates. Detectors being used, developed, and tested for the program include radiometric (RM) sensors, helium accumulation fluence monitor (HAFM) sensors, solid state track recorder (SSTR) sensors, and damage monitor (DM) sensors.

The necessity for pressure vessel mockup facilities for physics-dosimetry investigations and for irradiation of metallurgical specimens was recognized early in the formation of the NRC program. Experimental studies associated with high and low flux versions of a PWR pressure vessel mockup are in progress in the US, Belgium, and the United Kingdom. The US low flux version is known as the ORNL Poolside Critical Assembly (PCA), and the high flux version is known as the ORR Poolside Facility (PSF). Both are located at Oak Ridge, Tennessee. As specialized benchmarks, these facilities will provide well-characterized neutron environments where active and passive neutron dosimetry, various types of LWR-PV and support structure neutron field calculations, and temperature-controlled metallurgical specimen exposures are brought together. The two key low flux pressure vessel mockups in Europe are known as the Mol-Belgium-VENUS and Winfrith-United Kingdom-NESDIP facilities. The VENUS facility is to be used for PWR core source and azimuthal lead factor studies, while NESDIP is to be used for PWR cavity and azimuthal lead factor studies.

The results of the measurement and calculational strategies outlined here will be made available for use by the nuclear industry as ASTM Standards. Federal Regulation 10CFR50 already requires adherence to several ASTM Standards that establish a surveillance program for each power reactor and incorporate metallurgical specimens, physics-dosimetry flux-fluence monitors and neutron field evaluation. Revised and new standards in preparation will be carefully updated, flexible, and, above all, consistent.

CONTENTS

FIGURES

TABLES

TABLES (Cont'd)

ACRONYMS

AOTS	Argonne Optical Track Scanner
ANL	Argonne National Laboratory
ASEM	Automated Scanning Electron Microscope
ASTM	American Society for Testing and Materials
BSR	Bulk Shielding Reactor
BWR	Boiling Water Reactor
EPRI	Electric Power Research Institute
ESP	Emulsion Scanning Processor
FBR	Fast Breeder Reactor
FFTF	Fast Flux Test Facility
FSAR	Final Safety Analysis Report
HEDL	Hanford Engineering Development Laboratory
HOTS	Hanford Optical Track Scanner
IRL	Industrial Research Laboratory
LWR	Light Water Reactor
MFR	Magnetic Fusion Reactor
NDTT	Nil Ductility Transition Temperature
NRC	Nuclear Regulatory Commission
NRE	Nuclear Research Emulsion
ORNL	Oak Ridge National Laboratory
ORR	Oak Ridge Research Reactor (ORNL)
PCA	Poolside Critical Assembly
PROM	Programmable Read Only Memory
PSF	Poolside Facility (ORNL)
PV	Pressure Vessel
PWR	Pressurized Water Reactor
QA	Quality Assurance
RI	Rockwell International
SDIP	Surveillance Dosimetry Improvement Program
SDMF	Simulated Dosimetry Measurement Facility
SEM	Scanning Electron Microscope
SRM	Standard Reference Material

ACRONYMS (Cont'd)

SSC	Simulated Surveillance Capsule
SSTR	Solid-State Track Recorder
TLD	Thermoluminescent Dosimeter
TS	Thermal Shield
UK	United Kingdom
WRSR	Water Reactor Safety Research

ACKNOWLEDGMENTS

The following organizations are presently participating in the Light Water Reactor Pressure Vessel Surveillance Dosimetry Improvement Program (LWR-PV-SDIP) and will periodically contribute written reports, experimental data, or calculations.

Atomic Energy Research Establishment (AERE-H), Harwell, UK

Babcock & Wilcox Company (B&W), USA

Battelle Memorial Institute (BMI), Columbus Laboratory, USA

Brookhaven National Laboratory (BNL), USA

Centre d'Étude de l'Energie Nucléaire - Studiecentrum Voor Kernenergie (CEN/SCK), Mol, Belgium

Centre d'Études Nucléaires de Saclay (CEA, Saclay), Gif-sur-Yvette, France

Combustion Engineering, Inc. (CE), USA

EG&G ORTEC, USA

Electric Power Research Institute (EPRI), USA

Engineering Services Associates (ENSA), USA

Fracture Control Corporation (FCC), USA

General Electric Vallecitos Nuclear Center (GE-VNC), USA

Hanford Engineering Development Laboratory (HEDL), USA

Institüt für Kernenergetik und Energiesysteme der Universitat Stuttgart (IKE), Stuttgart, Germany

IRT Corporation (IRT), USA

Italian Atomic Power Authority (ENEL), Italy

Japan Atomic Energy Research Institute (JAERI), Japan

Kernforschungsanlage Jülich Gmbh (KFA), Germany

Kraftwerk Union, Germany

Materials Engineering Associates (MEA), USA

National Bureau of Standards (NBS), USA

Oak Ridge National Laboratory (ORNL), USA

Radiation Research Associates (RRA), USA

Rockwell International Energy Systems Group (RI-ESG), USA

Rolls-Royce and Associates Limited (RRAL), Derby, UK

Science Applications Incorporated (SAI), USA

Ship Research Institute (SRI), Japan

Southwest Research Institute (SWRI), USA

University of Arkansas (UA), USA

University of California, Santa Barbara (UCSB), USA

University of Tennessee (UT), USA

University of Tokyo, Japan

Westinghouse Electric Corporation - Nuclear Technology Division (W-NTD), USA

Westinghouse Electric Corporation - Research and Development Division (W-R&D), USA

SUMMARY

HANFORD ENGINEERING DEVELOPMENT LABORATORY (HEDL)

A list of planned NUREG reports is presented in Table S-1. These reports address individual and combined pressurized water reactor (PWR) and boiling water reactor (BWR) physics-dosimetry-metallurgy issues. These will provide a reference base of information to support the preparation of new set of LWR ASTM Standards (Figures S-1 and S-2).

Formulas are given for use in estimating the uncertainty in the calculated value of the shift in the 30 ft•lb Charpy temperatures, when the calculated shift is found using trend curve formulas recently described in the present series of reports. Covariance matrices are supplied for use in conjunction with previously developed trend curve formulas.

The status of three computer-controlled systems for quantitative track measurements is reviewed. Two systems, the Hanford optical track scanner (HOTS) and an automated scanning electron microscope (ASEM), are used for scanning solid state track recorders (SSTR). The third system, the emulsion scanning processor (ESP), is an interactive system used to measure the length of proton tracks in nuclear research emulsions (NRE). Current limitations of these systems for quantitative track scanning are presented. Experimental uncertainties attained with these computer-controlled systems are described using results obtained from reactor neutron dosimetry.

OAK RIDGE NATIONAL LABORATORY (ORNL)

Additional data and comparisons from the coupled neutron-gamma calculations for the PCA 12/13 configuration have been compiled. These calculations were reported in the April-June 1982 Quarterly, and additional tables are included in this report.

The evaluation of the physics-dosimetry of the 4th series of NRC-HSST experiments has been completed. A summary of the results is included in this report. Details will be published in two ORNL/TM reports.

A Blind Test has been promulgated for the prediction of metallurgical test results in the surface, 1/4T, and 1/2T capsules in the PSF-PV metallurgical irradiation experiment. ORNL has provided the neutron-physics calculation and other technical information to be distributed to the participants of the Blind Test.

The status of two ASTM standards for which ORNL has the lead is as follows:

- E706 (IIA) - "Application of Neutron Spectrum Adjustment Methods" is currently being balloted at the Society level.
- E706 (II) - "Analysis and Interpretation of Physics-Dosimetry Results for Test Reactors" is being balloted at the E10 Committee level.

TABLE S-1

PROGRAM DOCUMENTATION

LWR-PV-SDIP Program No.	NRC Report No.	Report No.	Issue Date	Editors
NUREG 1	NUREG/CR-3318	HEDL-TME 83-14	January 1984	W. N. McElroy
NUREG 2	NUREG/CR-3320, Vol. 1	HEDL-TME 84-1	June 1984	W. N. McElroy F. B. K. Kam
NUREG 3	NUREG/CR-3320, Vol. 2	HEDL-TME 84-2	June 1984	W. N. McElroy F. B. K. Kam
NUREG 4	NUREG/CR-3319	HEDL-TME 83-15	September 1983	W. N. McElroy
NUREG 5	NUREG/CR-3320, Vol. 3	HED1-TME 85-XX	March 1985	W. N. McElroy F. B. K. Kam
NUREG 6	NUREG/CR-3320, Vol. 4	HEDL-TME 85-XX	June 1985	W. N. McElroy F. B. K. Kam
NUREG 7	NUREG/CR-3321	HEDL-TME 85-XX	September 1985	W. N. McElroy F. B. K. Kam J. Grundl E. F. McGarry
NUREG 8	NUREG/CR-3322	HEDL-TME 86-XX	September 1986	W. N. McElroy F. B. K. Kam
NUREG 9	NUREG/CR-3323, Vol. 1 Vol. 2	CEN-R-XX	 September 1983 September 1984	A. Fabry W. N. McElroy E. D. McGarry
NUREG 10	NUREG/CR-3324, Vol. 1 Vol. 2	CEN-R-XX	 September 1983 September 1984	J. Butler A. Austin W. N. McElroy
NUREG 11	NUREG/CR-3325	CEN-R-XX	September 1983	Ph. Van Asbroeck R. Hawthorne A. Fabry
NUREG 12	NUREG/CR-3326	HEDL-TME 86-XX	September 1986	W. N. McElroy F. B. K. Kam
NUREG 13	NUREG/CR-	HEDL-TME 84-XX	September 1984	W. N. McElroy R. Gold
NUREG 14	NUREG/CR-3324, Vol. 3	AERE-XX	September 1985	J. Butler A. Austin W. N. McElroy
NUREG 15	NUREG/CR-3324, Vol. 4	AERE-XX	September 1986	J. Butler A. Austin W. N. McElroy

NUREG Report 1 (Issue Date: January 1984)
LWR-PV SURVEILLANCE DOSIMETRY IMPROVEMENT PROGRAM:
PCA DOSIMETRY IN SUPPORT OF THE PSF PHYSICS-DOSIMETRY-METALLURGY EXPERIMENTS
(4/12, 4/12 + SSC configurations and update of 8/7 and 12/13 configurations)
W. N. McElroy, Editor

This document will provide reference physics-dosimetry information needed to support the analysis of the PSF metallurgical experiments. It will also provide updated and supplemental data in support of the previous publication: "PCA Experiments and Blind Test," NUREG/CR-1861, HEDL-TME 80-87, July 1981.

NUREG Report 2 (Issue Date: June 1984)
LWR-PV SURVEILLANCE DOSIMETRY IMPROVEMENT PROGRAM:
PSF PHYSICS-DOSIMETRY-METALLURGY EXPERIMENTS

Part I - PSF Physics-Dosimetry Characterization Program
W. N. McElroy and F. B. K. Kam, Editors

This document will provide reference startup physics-dosimetry information in support of the PSF metallurgical experiments.

NUREG Report 3 (Issue Date: June 1984)
LWR-PV SURVEILLANCE DOSIMETRY IMPROVEMENT PROGRAM:
PSF PHYSICS-DOSIMETRY-METALLURGY EXPERIMENTS

Part II - PSF Simulated Surveillance Capsule (SSC) Metallurgical Program
W. N. McElroy and F. B. K. Kam, Editors

This document will provide reference metallurgical information on measured property changes in a number of different pressure vessel and reference steels for a simulated surveillance capsule (SSC) location for two different neutron exposures of $\sim 2 \times 10^{19}$ and $\sim 4 \times 10^{19}$ n/cm^2 (E > 1.0 MeV); i.e., for tests SSC-1, and SSC-2, respectively.

NUREG Report 4 (Issue Date: September 1983)
LWR-PV SURVEILLANCE DOSIMETRY IMPROVEMENT PROGRAM:
LWR POWER REACTOR SURVEILLANCE PHYSICS-DOSIMETRY DATA BASE COMPENDIUM
W. N. McElroy, Editor

This loose-leaf document will provide new and/or re-evaluated exposure parameter values (fluence E > 1.0 MeV, dpa, etc.) for individual surveillance capsules removed from operating PWR and BWR power plants -- all in support of the development and applications of the NRC-MPC-EPRI-ASTM metallurgical data bases. The document will be revised annually as information in new and old surveillance reports is re-evaluated with the FERRET-SAND and other developed methodologies.

NUREG Report 5 (Issue Date: March 1985)
LWR-PV SURVEILLANCE DOSIMETRY IMPROVEMENT PROGRAM:
PSF PHYSICS-DOSIMETRY-METALLURGY EXPERIMENTS

Part III - PSF Simulated Pressure Vessel Capsule (SPVC) and Simulated Void Box Capsule (SVBC) Physics-Dosimetery Program
W. N. McElroy and F. B. K. Kam, Editors

This document will provide reference in-situ physics-dosimetry information in support of the PSF metallurgical experiments.

NUREG Report 6 (Issue Date: June 1985)
LWR-PV SURVEILLANCE DOSIMETRY IMPROVEMENT PROGRAM:
PSF PHYSICS-DOSIMETRY-METALLURGY EXPERIMENTS

Part IV - PSF Simulated Pressure Vessel Capsule (SPVC) and Simulated Void Box Capsule (SVBC) Metallurgy Program
W. N. McElroy and F. B. K. Kam, Editors

This document will provide reference metallurgical information on measured property changes in a number of different pressure vessel and reference steels for simulated PV locations at the inner surface, 1/4 T and 1/2 T positions of a PWR PV wall mockup. The corresponding neutron exposures for the 2 year irradiation are $\sim 4 \times 10^{19}$, $\sim 2 \times 10^{19}$, and $\sim 1 \times 10^{19}$ n/cm^2, respectively, for a ~550°F irradiation temperature.

This document will also provide reference metallurgical information on measured property changes in a number of different pressure vessel support structure and reference steels for a simulated ex-vessel cavity neutron exposure of $\sim 5 \times 10^{17}$ n/cm^2 (E > 1.0 MeV) for a ~95°F irradiation temperature (based on preliminary ORNL calculations, as yet unsubstantiated by measurements).

NUREG Report 7 (Issue Date: September 1985)
LWR-PV SURVEILLANCE DOSIMETRY IMPROVEMENT PROGRAM:
PSF SURVEILLANCE DOSIMETRY MEASUREMENT FACILITY (SDMF)
W. N. McElroy, F. B. K. Kam, J. Grundl and E. D. McGarry, Editors

This will be a loose-leaf volume of results to certify the accuracy of exposure parameter and perturbation effects for surveillance capsules removed from PWR and BWR power plants. It will be updated periodically, as required.

NUREG Report 8 (Issue Date: September 1986)
LWR-PV SURVEILLANCE DOSIMETRY IMPROVEMENT PROGRAM:
LWR TEST REACTOR PHYSICS-DOSIMETRY DATA BASE COMPENDIUM
W. N. McElroy and F. B. K. Kam, Editors

This will be a loose-leaf volume of results from FERRET-SAND, LSL, and other least square type code analyses of physics-dosimetry for US (BSR, PSF, SUNY-NSTF [Buffalo], Virginia, etc.), UK (DIDO, HERALD, etc.), Belgium

(BR-2, etc.), France (Melusine, etc.), Germany (FRJ1, FRJ2, etc.), and other participating countries. It will provide needed and consistent exposure parameter values (fluence E > 1.0 MeV, dpa, etc.) and uncertainties for correlating test reactor property change data with that obtained from PWR and BWR power plant surveillance capsules. That is, with data from NUREG Report 4, these two reports will serve as a reference physics-dosimetry data base for the correlation and application of power and research reactor derived steel irradiation effects data.

NUREG Report 9 (Issue Date: September 1983, Vol.1 and September 1984, Vol. 2)
LWR-PV SURVEILLANCE DOSIMETRY IMPROVEMENT PROGRAM:
VENUS PWR CORE SOURCE AND AZIMUTHAL LEAD FACTOR EXPERIMENTS AND CALCULATIONAL TESTS
A. Fabry, W. N. McElroy and E. D. McGarry, Editors

This document will provide VENUS-derived reference physics-dosimetry information on active, passive, and calculational dosimetry studies involving CEN/SCK, HEDL, NBS, ORNL, and other LWR program participants.

NUREG Report 10 (Issue Date: September 1983, Vol. 1 and September 1984, Vol. 2)
LWR-PV SURVEILLANCE DOSIMETRY IMPROVEMENT PROGRAM:
NESDIP PWR CAVITY AND AZIMUTHAL LEAD FACTOR EXPERIMENTS AND CALCULATIONAL TESTS
J. Butler, M. Austin, A. Fudge and W. N. McElroy, Editors

This document will provide NESDIP-derived reference physics-dosimetry information on active, passive, and calculational dosimetry studies involving Winfrith, CEN/SCK, HEDL, NBS, and other LWR program participants.

NUREG Report 11 (Issue Date: September 1983)
LWR-PV SURVEILLANCE DOSIMETRY IMPROVEMENT PROGRAM:
PSF SIMULATED SURVEILLANCE CAPSULE (SSC) RESULTS-CEN/SCK/MEA
A. Fabry and R. Hawthorne, Editors

This document will provide CEN/SCK/MEA metallurgical information and results for the Mol, Belgium, PV steel irradiated in the SSC position for the ORR-PSF physics-dosimetry-metallurgy experiments.

NUREG Report 12 (Issue Date: September 1986)
LWR-PV SURVEILLANCE DOSIMETRY IMPROVEMENT PROGRAM:
LWR TEST REACTOR IRRADIATED NUCLEAR PRESSURE VESSEL AND SUPPORT STRUCTURE STEEL DATA BASE COMPENDIUM
W. N. McElroy and F. B. K. Kam, Editors

This will be a loose-leaf volume of information and results for selected metallurgical experiments performed in the US (BSR, PSF, SUNY-NSTF [Buffalo], Virginia, etc.), UK (DIDO, HERALD, etc.), Belgium (BR-2, etc.),

France (Melusine, etc.), Germany (FRJ1, FRJ2, etc.), and other participating countries. It will provide needed and consistent Charpy, upper shelf energy, tensile, compression, hardness, etc., property change values and uncertainties. These metallurgical data will be combined with the corresponding NUREG Report 8 physics-dosimetry data to provide 1) a more precisely defined and representative research reactor physics-dosimetry-metallurgy data base, 2) a better understanding of the mechanisms causing neutron damage, and 3) tested and verified exposure data and physical damage correlation models; all of which are needed to support the preparation and acceptance of the ASTM E706(IE) Damage Correlation and ASTM E706(IIF) ΔNDTT with Fluence Standard.

NUREG Report 13 (Issue Date: September 1984)
GUNDREMMINGEN PHYSICS-DOSIMETRY-METALLURGY PROGRAM
W. N. McElroy and R. Gold, Editors

This document provides results that support the NRC fracture mechanics analysis of the pressure vessel base metal at Gundremmingen. Compression and micro-hardness metallurgical and dosimetry specimens will be obtained as a function of distance through the PV wall. Previous capsule and cavity physic-dosimetry-metallurgy Gundremmingen results will be correlated with new in-wall vessel results. Appropriate PSF results will be used to help NRC obtain the best possible overall data correlations.

NUREG Report 14 (Issue Date: September 1985)
NESDIP PWR CAVITY AND AXIMUTHAL LEAD FACTOR EXPERIMENTS AND CALCULATIONAL TESTS - TWENTY-CENTIMETER CAVITY RESULTS
J. Butler, A. Austin and W. N. McElroy, Editors

This document provides NESDIP 20-cm cavity-derived reference physics-dosimetry data on active, passive, and calculational dosimetry studies involving Winfrith, RR&A, HEDL, ORNL, NBS, CEN/SCK, and other LWR program participants. (It may be issued as a UK report with LWR-PV-SDIP contributions.)

NUREG Report 15 (Issue Date: September 1986)
NESDIP PWR CAVITY AND AXIMUTHAL LEAD FACTOR EXPERIMENTS AND CALCULATIONAL TESTS - HUNDRED-CENTIMETER CAVITY RESULTS
J. Butler, A. Austin and W. M. McElroy, Editors

This document provides NESDIP 100-cm cavity-derived reference physics-dosimetry data on active, passive, and calculational dosimetry studies involving Winfrith, RR&A, HEDL, ORNL, NBS, CEN/SCK, and other LWR program participants. (It may be issued as a UK report with LWR-PV-SDIP contributions.)

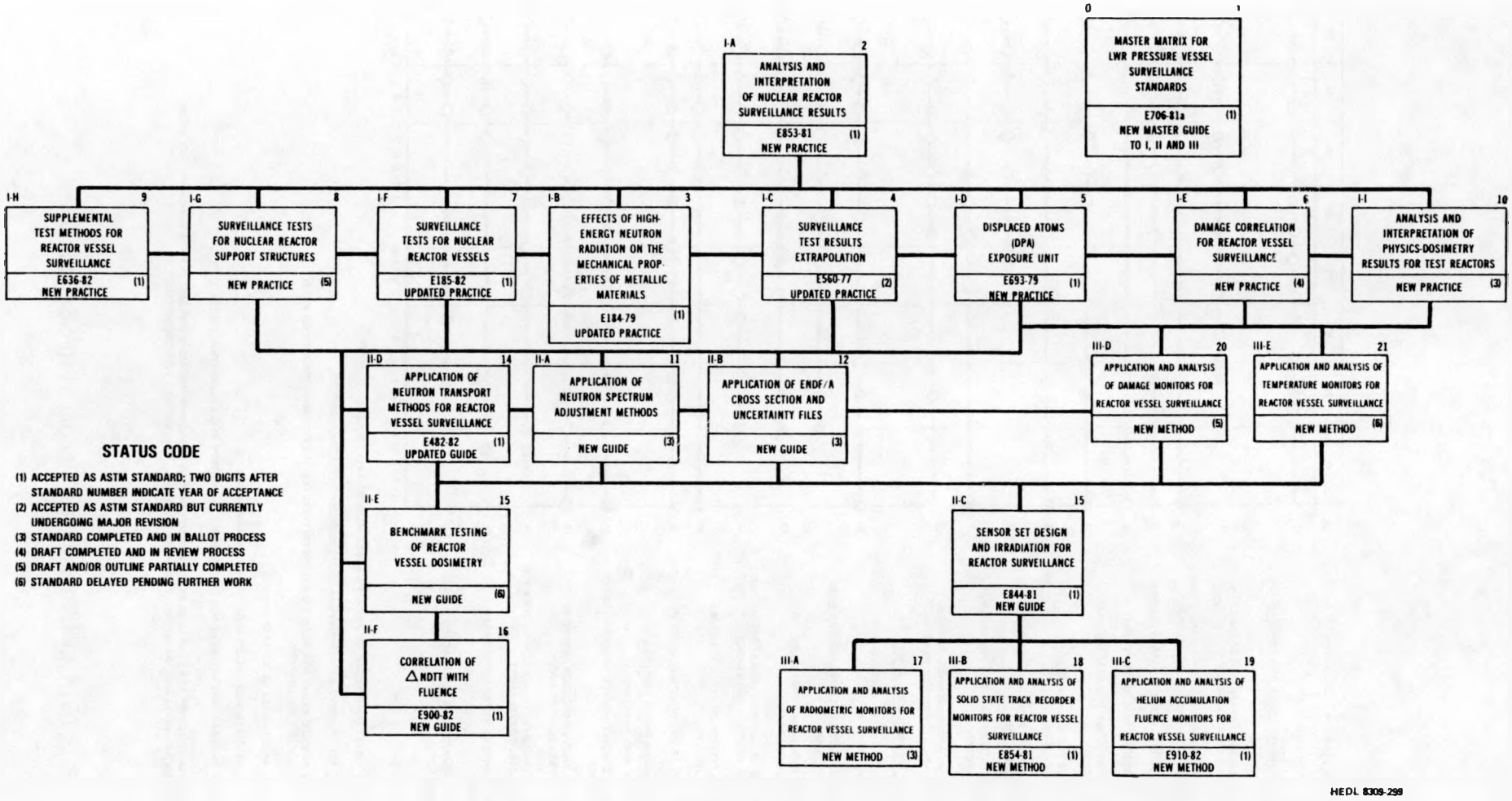

FIGURE S-1. ASTM Standards for Surveillance of LWR Nuclear Reactor Pressure Vessels and Support Structures.

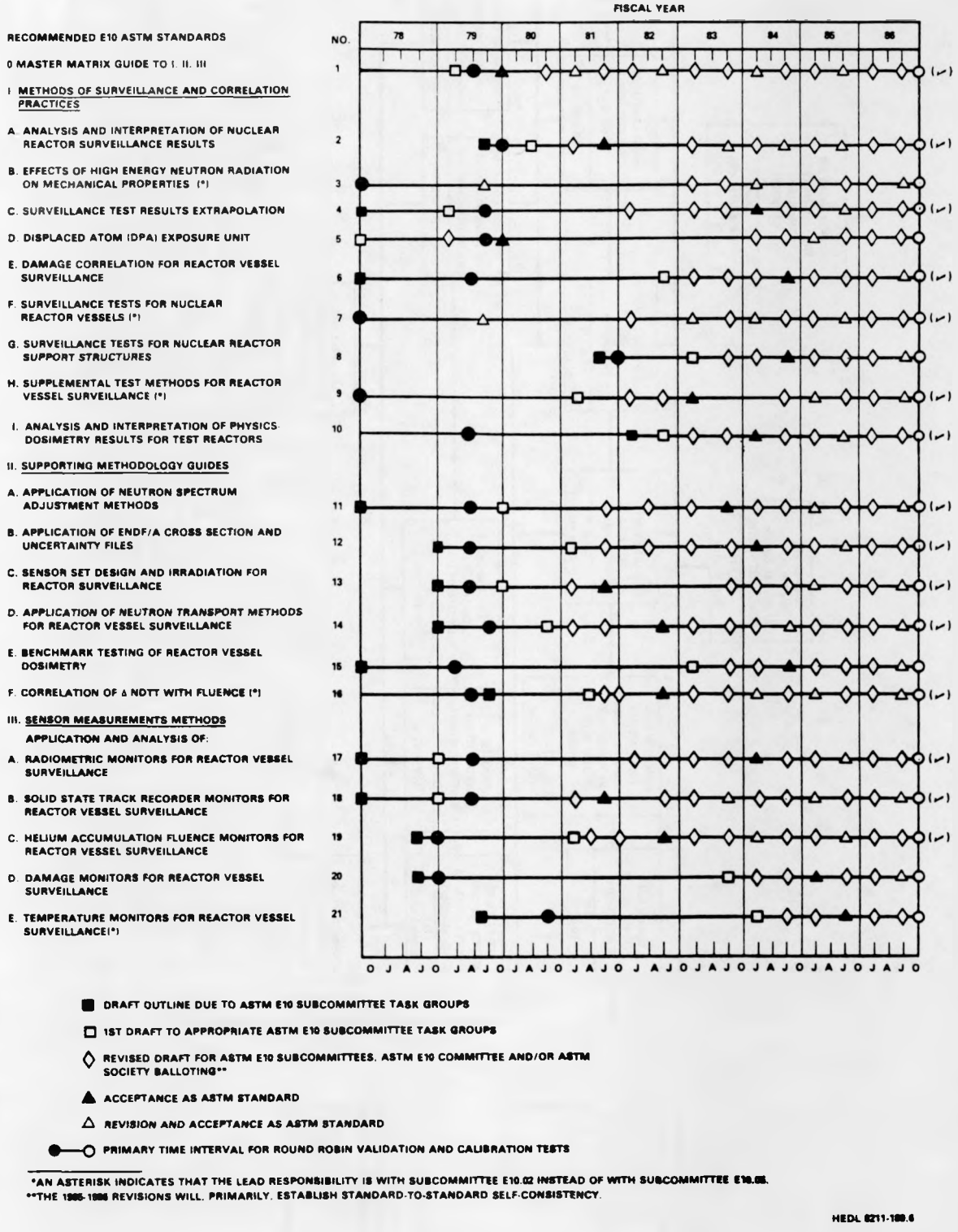

FIGURE S-2. ASTM LWR Standards Preparation Schedule.

HANFORD ENGINEERING DEVELOPMENT LABORATORY

(HEDL)

A. ERROR ESTIMATIONS IN APPLICATIONS OF CHARPY TREND CURVE FORMULAS

G. L. Guthrie - HEDL

Objective

The objective of the present work is to provide useful methods for estimating the uncertainty in a predicted shift in the 30 ft·lb Charpy transition temperature when the transition temperature shift has been calculated from formulas of the types developed in recent reports in the present series.

Summary

Formulas are given for use in estimating the uncertainty in the calculated value of the shift in the 30 ft·lb Charpy temperatures, when the calculated shift is found using trend curve formulas recently described in the present series of reports. Covariance matrices are supplied for use in conjunction with previously developed trend curve formulas. Use of the recommended methods results in uncertainty estimates that depend on the material form (weld or plate), composition, fluence, fluence uncertainty, and composition uncertainties. An example of the application of the formulas is provided for the user. For a typical case using a formula for a combined PWR weld and plate data set of 138 points (with copper, nickel, and fluence uncertainties of approximately 17%, 12%, and 30%, respectively), an uncertainty (1σ) of 35.6°F (16%) is obtained for a calculated trend curve shift of 221.6°F for a fluence ($E > 1.0$ MeV) of about 1.5×10^{19}.

Accomplishments and Status

The usual method of assigning an uncertainty to a calculated item is to supply an estimate of the square root of the expectation value of the square of the error. This can be done for the trend curve formulas recently developed in this series of reports, provided that several simplifying assumptions are made: 1) all errors and uncertainties are small enough that linear approximations are valid, 2) all distribution functions are "normal" in form, and 3) particular pairs of items are independent (uncorrelated). An example is the pair consisting of the expected error in the $\log_e$ of the fluence and the expected error in the copper concentration for a particular application of a trend curve formula. When the indicated assumptions are made, the theory of linear least squares error estimation is available for application to the problem. To satisfy the assumption about normal distributions of errors and to maintain consistency with the previous work, $\log_e(\phi t)$ is used as the independent exposure variable, rather than ϕt itself. This is because the trend curve formulas have been derived under the assumption of a log normal distribution in fluence errors (i.e., there is a normal distribution of errors in $\log_e$ of the fluence).

To briefly review the existing theory on error estimation, first assume:

$$\Delta T = f(P_i, V_j) \qquad (1)$$

where:

ΔT = Charpy shift
f = Some functional expression chosen by the analyst
P_i = Parameters (i = 1, 2, 3, etc.)
V_j = Variables (j = 1, 2, 3)

The parameters are the adjustable constants that have taken on "best" values found in a least squares fit to a data base, and the variables are items associated with the specimen and its irradiation. Possible variables are the chemical concentrations and $\log_e(\phi t)$ in a given application.

Taking differentials in Eq. (1) at any set of values for the P_i and V_j, the error in ΔT is

$$\delta(\Delta T) = \sum_i \frac{\partial f}{\partial p_i}\delta(P_i) + \sum_j \frac{\partial f}{\partial V_j}\delta(V_j) \qquad (2)$$

where $\delta(\Delta T)$ is the error in ΔT caused by all the errors $\delta(P_i)$ in the parameters and the errors $\delta(V_j)$ in the independent variables.

For any particular set of values for the $\delta(P_i)$ and $\delta(V_j)$, the square of $\delta(\Delta T)$ can be obtained by squaring both sides of Eq. (2). The expectation value of $\delta^2(\Delta T)$ is then the sum of the expectation values of all the terms resulting from squaring the right hand side of Eq. (2).

We find

$$\overline{\delta^2(\Delta T)} = \sum\sum \frac{\partial f}{\partial P_k}\frac{\partial f}{\partial P_l}\,\overline{\delta P_k \cdot \delta P_l} + \sum_j \left(\frac{\partial f}{\partial V_j}\right)^2 \cdot \overline{\delta^2(V_j)} \qquad (3)$$

where the bar denotes an expectation value.

In the first set of terms, the factors $\partial f/\partial P_k$ and $\partial f/\partial P_l$ can be directly calculated from the formula f in any given application. The factor $\overline{\delta P_K \cdot \delta P_l}$ is by definition the covariance matrix of the parameters in the formula. In the second set of terms, $(\partial f/\partial Vj)^2$ can be directly calculated from the trend curve formula, and $\overline{\delta^2(V_j)}$ is an estimate of an expected value of the square

of the errors in the variable V_j. This must be obtained from a knowledge of the uncertainties in chemistry, fluence, and any other relevant variables appearing in the function f. Cross terms of the type

$$\text{Cross Term (1)} = \frac{\partial f}{\partial V_m} \frac{\partial f}{\partial V_n} \overline{\delta(V_m) \cdot \delta(V_n)} \tag{4}$$

have been omitted on the assumption that V_m and V_n are independent, and the errors are uncorrelated so that the expectation value of the product is zero.

Cross terms of the type

$$\text{Cross Term (2)} = \frac{\partial f}{\partial P_k} \frac{\partial f}{\partial V_i} \overline{\delta(P_k) \cdot \delta(V_i)} \tag{5}$$

have been omitted since the parameters P_k are derived from a reference data base, while the V_i are the variables in a particular application, possibly not even part of the same data base. Thus, P_k and V_i are independent, and the separate errors in Eq. (5) are uncorrelated so that each product term has an expectation value of zero.

The covariance matrix of the parameters, in a local linear approximation, is available from the theory of linear least squares (Ma71). For a linear problem, the covariance matrix is given by

$$C_{ij} = \left(\frac{R_k \, W_{kl} \, R_l}{N-P} \right) \left(\psi^T_{im} \, W_{mn} \, \psi_{nj} \right)^{-1} \tag{6}$$

where a repeated index indicates a summation and

W_{kl} = Weight matrix for the observations
R_k = Column matrix of residuals
ψ = So-called "design" matrix, which is the matrix of the original set of overdetermined equations
ψ^T = Matrix transpose

In Eq. (6), (N-P) is the number of equations minus the number of parameters or the degrees of freedom.

The quantity $\sigma^2 = R_k \, W_{kl} \, R_l / (N-P)$ (7)

is simply the estimate of the square of the standard deviation for the fit, and is a single scalar number.

The quantity $Q_{ij} = \left(\psi^T_{in} \, W_{mn} \, \psi_{nj} \right)^{-1}$, (8)

which is a part of Eq. (6), is a matrix that must be obtained by inversion. It is worth noting that any arbitrary scale factor in W cancels in Eq. (6) since it appears in the numerator of Eq. (7) and appears as an inverse in Eq. (8).

The ψ_{im} matrix of the linear problem is replaced by the Jacobian matrix in a situation involving a linear approximation. A numerical approximation Jacobian is available in the output of commonly used nonlinear least squares computer packages. Thus it is possible to compute a covariance matrix [Eq. (6)] for any given trend curve formula derived from any given data base, merely by obtaining the Jacobian counterpart of ψ from the numerical approximation performed by the nonlinear computer package, and then computing

$$C_{ij} = \sigma^2 \left(J^T \, W \, J \right)^{-1} \tag{9}$$

The acquisition of the remaining required items in Eq. (3) is straightforward, but perhaps tedious in some cases. The methods indicated above have been applied to a combined plate-weld formula developed in late 1982.

The Charpy shift formula is

$$\Delta T = \left[-28.47 + 421.3 \, Cu + 449.25 \, Cu \cdot \text{Tanh} \left(0.2769 \, Ni/Cu \right) \right] \cdot \left(\frac{\phi t}{10^{19}} \right)^{0.262 \, - \, 0.0308 \, \log_e \left(\phi t / 10^{19} \right)} \tag{10}$$

To put this equation in a form consistent with the theory discussed, it must be re-written so that the fluence term appears in the form

$$\text{Fluence factor} = \exp\left(EK + FK^2 \right) \tag{11}$$

where:

$K = \log_e \left(\phi t / 10^{19} \right)$

E and F = Adjustable parameters having values E = 0.262 and F = -0.0308 in Eq. (10)

With only moderate difficulty, the above form can be shown to be identical to the fluence term in Eq. (10), but the form of Eq. (11) allows the analyst to work with the variable $K = \log_e$ (fluence), so that the variable (K)

appearing in the calculations has a "normal" distribution of errors. In this form, the entire trend curve formula is

$$\Delta T = \left[A + B \cdot Cu + C \cdot Cu \, \text{Tanh}\left(D \cdot \frac{Ni}{Cu}\right)\right] \cdot \exp\left(EK + FK^2\right) \quad (12)$$

The parameters A through F were determined by a least squares fit to 138 data points, resulting in the values shown in Eq. (10). The covariance matrix for parameters A through F is given in Table HEDL-1.

TABLE HEDL-1

COVARIANCE MATRIX FOR PARAMETERS

0.4246+002	-0.3176+003	-0.2974+003	0.4515+000	-0.4431-002	0.6528-002
-0.3176+003	0.3760+004	0.1752+004	-0.5109+001	-0.4201-001	-0.2407-001
-0.2974+003	0.1752+004	0.4284+004	-0.4301+001	0.1059+000	-0.6689-001
0.4515+000	-0.5109+001	-0.4301+001	0.9119-002	0.2702-004	-0.9320-004
-0.4431-002	-0.4201-001	0.1059+000	0.2702-004	0.2049-003	-0.5668-004
0.6528-002	-0.2407-001	-0.6689-001	-0.9320-004	-0.5668-004	0.1065-003

The formal derivatives required in Eq. (3) are given by

$$\frac{\partial f}{\partial A} = \exp\left(EK + FK^2\right) \quad (13)$$

$$\frac{\partial f}{\partial B} = Cu \cdot \frac{\partial f}{\partial A} \quad (14)$$

$$\frac{\partial f}{\partial C} = \text{Tanh} \cdot D \cdot \frac{Ni}{Cu} \cdot \frac{\partial f}{\partial B} \quad (15)$$

$$\frac{\partial f}{\partial D} = C \cdot Ni \left[\cosh\left(\frac{D \cdot Ni}{Cu}\right)\right]^{-2} \frac{\partial f}{\partial A} \quad (16)$$

$$\frac{\partial f}{\partial E} = K \cdot f \quad (17)$$

$$\frac{\partial f}{\partial F} = K \cdot \frac{\partial f}{\partial E} \quad (18)$$

$$\frac{\partial f}{\partial (Cu)} = \frac{\partial f}{\partial A} \cdot \left[B + C \, \text{Tanh}\left(\frac{D \, Ni}{Cu}\right) - \frac{D \cdot C \cdot Ni}{Cu} \cosh^{-2}\left(\frac{D \cdot Ni}{Cu}\right)\right] \quad (19)$$

$$\frac{\partial f}{\partial (Ni)} = C \cdot D \cdot \frac{\partial f}{\partial A} \cdot \left[\cosh\left(\frac{D \cdot Ni}{Cu}\right)\right]^{-2} \quad (20)$$

$$\frac{\partial f}{\partial K} = \frac{\partial f}{\partial E} \cdot \left(\frac{E}{K} + 2F\right) \qquad (21)$$

The standard deviation for the fitting procedure was $\sigma = 20.31°F$.

A program was written to calculate an error estimate for ΔT of Eq. (10), using the method of Eq. (3) together with Table HEDL-1 and the formulas of Eqs. (13) through (21). The input variables used in a test run were

Cu = (0.3 $\pm$ 0.05) wt% - (approximately 17% 1σ uncertainty)

Ni = (0.65 $\pm$ 0.075) wt% - (approximately 12% 1σ uncertainty)

Fluence = 1.5×10^{19} (uncertain by 30% [1σ] of the reported value)

The resulting uncertainty in ΔT was 35.6°F, and the calculated shift was 221.6°F.

Formulas for required derivatives, together with covariance tables for recently developed formulas are given below.

Formula Pair Number 1 (Gu83):

$$\Delta T(\text{Weld}) = \left[\, x(1) + x(2) \cdot Cu + x(3) \cdot Ni \,\right] \left(\frac{\phi t}{10^{19}}\right)^N$$

where:

$$N = x(4) + x(5) \log_e \frac{\phi t}{10^{19}} \qquad (22a)$$

and

$$\Delta T(\text{plate}) = \left\{ x(6) + x(7) \cdot Cu + x(8) \cdot Cu \cdot \text{Tanh} \left[x(9) \cdot \frac{Ni}{Cu} \right] \right\} \left(\frac{\phi t}{10^{19}}\right)^N$$

where:

$$N = x(10) + x(11) \log_e \left(\frac{\phi t}{10^{19}}\right) \qquad (22b)$$

Best values for the "x" parameters are:

x(1) = 15.01	x(6) = -37.85
x(2) = 329.2	x(7) = 541.6
x(3) = 139.6	x(8) = 523.2
x(4) = 0.2899	x(9) = 0.303
x(5) = -0.04522	x(10) = 0.2723
	x(11) = -0.04795

The parameters are consistent with wt%, fluence in n/cm^2 ($E > 1.0$ MeV), and °F. The standard deviations for the two parts of the formula are 27.17°F for the weld formula and 15.54°F for the plate formula. The covariance matrix is given by

0.189+003	-0.762+003	0.211+000	-0.108-001	0.422-001
-0.762+003	0.423+004	-0.417+003	0.499-001	-0.258+000
0.211+000	-0.417+003	0.227+003	0.140-001	-0.495-001
-0.108-001	0.499-001	0.140-001	0.564-003	-0.191-003
0.422-001	-0.258+000	-0.495-001	-0.191-003	0.271-003

for x(1) through x(5) and by

0.499+002	-0.373+003	-0.274+003	0.372+000	0.592-003	0.102-001
-0.373+003	0.498+004	0.102+004	-0.569+001	-0.168+000	0.288-001
-0.274+003	0.102+004	0.355+004	-0.212+001	0.232+000	-0.162+000
0.372+000	-0.569+001	-0.212+001	0.877-002	0.715-004	-0.236-003
0.592-003	-0.168+000	0.232+000	0.715-004	0.414-003	-0.147-003
0.102-001	0.288-001	-0.162+000	-0.236-003	-0.147-003	0.185-003

for x(6) through x(11). The covariance matrix elements connecting parameters x(N), where $N \leq 5$ and x(M), where $M \geq 6$ are not zero, but they do not enter into any error estimates, since any given ΔT formula can contain only one of the two sets (weld or plate). The necessary partial derivatives for formula pair number 1 are given below.

Welds:

$$\frac{\partial f}{\partial x(1)} = \exp\left[x(4) \cdot K + x(5) \cdot K^2 \right]$$

where:

$$K = \log_e\left(\frac{\phi t}{10^{19}} \right)$$

$$\frac{\partial f}{\partial x(2)} = Cu \cdot \frac{\partial f}{\partial x(1)}$$

$$\frac{\partial f}{\partial x(3)} = Ni \cdot \frac{\partial f}{\partial x(1)}$$

$$\frac{\partial f}{\partial x(4)} = K \cdot f$$

$$\frac{\partial f}{\partial x(5)} = K^2 \cdot f$$

$$\frac{\partial f}{\partial Cu} = x(2) \cdot \frac{\partial f}{\partial x(1)}$$

$$\frac{\partial f}{\partial Ni} = x(3)\,\frac{\partial f}{\partial x(1)}$$

$$\frac{\partial f}{\partial K} = f \cdot \left[x(4) + 2 \cdot K \cdot x(5) \right]$$

Plates:

$$\frac{\partial f}{\partial x(6)} = \exp\left[x(10) \cdot K + x(11) \cdot K^2 \right]$$

$$\frac{\partial f}{\partial x(7)} = Cu\,\frac{\partial f}{\partial x(6)}$$

$$\frac{\partial f}{\partial x(8)} = Cu \cdot \mathrm{Tanh}\left[x(9)\,\frac{Ni}{Cu} \right] \cdot \frac{\partial f}{\partial x(6)}$$

$$\frac{\partial f}{\partial x(9)} = x(8) \cdot Ni \left\{ \cosh\left[\frac{x(9) \cdot Ni}{Cu} \right] \right\}^{-2} \frac{\partial f}{\partial x(6)}$$

$$\frac{\partial f}{\partial x(10)} = K \cdot f$$

$$\frac{\partial f}{\partial x(11)} = K^2 \cdot f$$

$$\frac{\partial f}{\partial Cu} = \frac{\partial f}{\partial x(6)} \cdot \left\{ x(7) + x(8)\,\tanh\left[\frac{x(9) \cdot Ni}{Cu} \right] - \frac{x(8) \cdot x(9)\,Ni}{Cu}\,\cosh^{-2}\left[\frac{x(9)\,Ni}{Cu} \right] \right\}$$

$$\frac{\partial f}{\partial Ni} = x(8) \cdot x(9) \cdot \frac{\partial f}{\partial x(6)} \cdot \cosh^{-2}\left[\frac{x(9) \cdot Ni}{Cu} \right]$$

$$\frac{\partial f}{\partial K} = f \cdot \left[x(10) + 2 \cdot K \cdot x(11) \right]$$

Formula Pair Number 2 (Gu83):

$$\Delta T(\mathrm{weld}) = \left[x(1)\,Cu + x(2)\sqrt{CuNi} + x(3)Ni \right] \left(\frac{\phi t}{10^{19}} \right)^{N}$$

where:

$$N = x(4) + x(5) \cdot K$$

$$K = \log_e \left(\frac{\phi t}{10^{19}} \right).$$

$$\Delta T(\text{Plate}) = \left\{ x(6) + x(7)\,Cu + x(8)\tanh\left[x(9)\,\frac{Ni}{Cu}\right]\right\} \cdot \left(\frac{\phi t}{10^{19}}\right)^{N}$$

where:

$$N = x(10) + x(11) \cdot K$$

$$K = \log_e\left(\frac{\phi t}{10^{19}}\right).$$

The best parameter values for this pair are given by:

x(1) = 582.	x(6) = -37.8
x(2) = -322.3	x(7) = 539.8
x(3) = 261.3	x(8) = 522.1
x(4) = 0.2868	x(9) = 0.30421
x(5) = -0.0472	x(10) = 0.2718
	x(11) = -0.0457

and the covariance matrix is given by:

0.106+005	-0.157+005	0.551+004	-0.207+000	-0.128-001
-0.157+005	0.262+005	-0.989+004	0.342+000	-0.117+000
0.551+004	-0.989+004	0.396+004	-0.111+000	-0.595-002
-0.207+000	0.342+000	-0.111+000	0.558-003	-0.190-003
-0.128-001	-0.117+000	-0.595-002	-0.190-003	0.258-003

for x(1) through x(5), and by

0.485+002	-0.363+003	-0.264+003	0.363+000	0.516-003	0.986-002
-0.363+003	0.488+004	0.956+003	-0.559+001	-0.166+000	0.285-001
-0.264+003	0.956+003	0.343+004	-0.202+001	0.226+000	-0.160+000
0.363+000	-0.559+001	-0.202+001	0.864-002	0.712-004	-0.227-003
0.516-003	-0.166+000	0.226+000	0.712-004	0.400-003	-0.140-003
0.986-002	0.285-001	-0.160+000	-0.227-003	-0.140-003	0.179-003

for x(6) through x(11). The standard deviations are 26.42°F for the weld formula and 15.56°F for the plate formula. The necessary derivatives for the plate part of the formula are formally the same as those given for pair number one. For the weld part of the formula, the derivatives follow:

$$\frac{\partial f}{\partial x(1)} = Cu \cdot \exp\left[x(4) \cdot K + x(5) \cdot K^2\right]$$

$$\frac{\partial f}{\partial x(2)} = (Cu \cdot Ni)^{1/2} \cdot \exp\left[x(4) \cdot K + x(5) \cdot {}^{2}K \right]$$

$$\frac{\partial f}{\partial x(3)} = Ni \cdot \exp\left[x(4) \cdot K + x(5) \cdot K^2 \right]$$

$$\frac{\partial f}{\partial x(4)} = K \cdot f$$

$$\frac{\partial f}{\partial x(5)} = K^2 \cdot f$$

$$\frac{\partial f}{\partial Cu} = \left[x(1) + \frac{x(2)}{2} \cdot \sqrt{\frac{Ni}{Cu}} \right] \exp\left[x(4) \cdot K + x(5) \cdot K^2 \right]$$

$$\frac{\partial f}{\partial Ni} = \left[x(3) + \frac{x(2)}{2} \cdot \sqrt{\frac{Cu}{Ni}} \right] \exp\left[x(4) \cdot K + x(5) \cdot K^2 \right]$$

$$\frac{\partial f}{\partial K} = f \cdot \left[x(4) + 2 \cdot K \cdot x(5) \right]$$

Actual Application of Theory

All of the information required for the calculation of an error estimation is contained in the preceeding material. The error estimation is based on Eq. (3). This equation can be used to calculate an expectation value, $\delta^2(\Delta T)$, in any given case. Let us take for example, the second equation pair (Formula Pair Number 2), and apply the formula of Eq. (3) to a weld. Eq. (3) has two summations that contribute to $\delta^2(\Delta T)$. The first came from the uncertainties in the parameters in the weld formula, and the second came from the uncertainties in the variables associated with the given specimen and irradiation.

The first summation (actually a double summation) can be regarded as a matrix multiplication. The analyst must take the data associated with the particular problem (Cu concentration, Ni concentration, $\log_e$ (fluence), etc.) and obtain a numerical matrix containing all the values of

$$D_{ke} = \frac{\partial f}{\partial P_k} \frac{\partial f}{\partial P_e} .$$

For instance, the element D_{13} of the matrix is $\partial f/\partial x(1) \cdot \partial f/\partial x(3)$. Using the defined formulas, we find the expression for $\partial f/\partial x(1)$ and $\partial f/\partial x(3)$ and obtain a numerical value for D_{13}, and similarly for all 25 elements of D. Then the D matrix is multiplied by the weld covariance matrix [covariance elements connecting parameters x(1) through x(5)]. This gives us the first term of Eq. (3). To obtain the second term of Eq. (3),

estimates are obtained for the squares of the uncertainties in the experimental variables, $(\delta V)^2$, and the formulas defined in the text for the various $\partial f/\partial V_j$ are used to compute the numerical value of the second term.

Of course since the computation depends on the chemical composition and exposure for each individual irradiation, it would be worthwhile to write a computer program for the computation if it was anticipated that more than a few individual estimates of $\overline{\delta^2(\Delta T)}$ would ultimately be calculated.

When the formalism above is used to predict a charpy shift value, it should be noted that the calculated uncertainty is the uncertainty in the "true" value of the shift. If the analyst wants the uncertainty in the value of a measured shift, then the uncertainty of the measurement must be added in quadrature. This remark also applies if there is an "inherent variability" in the material such that two identical materials with identical sets of input variables produce two noticeably different shifts.

Conclusions

The derived formalism gives more rigorous, but yet reasonable and relatively easily derived results, based on current state of the art, needs, and knowledge. The method has several advantages over the previous practice of merely stating a single standard deviation for all cases. These advantages are:

- Separate results can be found for plates and welds if separate formulas are used.
- The estimated error depends on the values and uncertainties of the variables, such as Cu content, Ni content and fluence.
- It is not necessary to assume that the uncertainty in the variables of the application are the same as the uncertainties of the variables in the data base used to derive the parameter values.

Plans for Future Work

No additional work in this area is contemplated except that the necessary formal derivatives and covariance matrices will be developed for any new trend curve formulas derived by the author.

References

(Gu83) G. L. Guthrie, "Charpy Trend Curve Formulas Derived from an Expanded Surveillance Data Base," LWR-PV-SDIP Quarterly Progress Report, October 1982 - December 1982, NUREG/CR-2805, Vol. 4, HEDL-TME 82-21, Hanford Engineering Development Laboratory, Richland, WA, pp. HEDL-3 - HEDL-13, July 1983.

(Ma71) B. R. Martin, Statistics for Physicists, Sec. 8.1.2, Academic Press, New York, NY, 1971.

B. STATUS OF AUTOMATED NUCLEAR SCANNING SYSTEMS

Raymond Gold, J. H. Roberts, C. C. Preston, J. P. McNeece and F. H. Ruddy - HEDL

Objective

The objective is to provide instrumentation systems for quantitative scanning of solid state track recorders (SSTR) and nuclear research emulsions (NRE) irradiated in light water reactor pressure vessel (LWR-PV) environments. SSTR and NRE are applied in LWR-PV neutron dosimetry over an enormous range of flux/fluence from low-power benchmark mockups to high-power actual on-line LWR commercial power plants. See for example, ASTM E854-81, "Standard Method for Application and Analysis of Solid State Track Recorder (SSTR) Monitors for Reactor Surveillance" (As82b), which was prepared within the "Master Matrix for LWR-PV Surveillance Standards, ASTM E706-81a (As82). Cost-effective dosimetry for the LWR-PV Surveillance Dosimetry Improvement Program (SDIP) requires automation of different NRE and SSTR scanning tasks to the fullest possible extent.

Summary

Present day minicomputers and microprocessors enable a range of automation, from partial to total, of tasks once thought beyond approach. The status of three computer controlled systems for quantitative track measurements is reviewed. Two systems, the Hanford optical track scanner (HOTS) and an automated scanning electron microscope (ASEM), are used for scanning solid state track recorders (SSTR). The third system, the emulsion scanning processor (ESP), is an interactive system used to measure the length of proton tracks in nuclear research emulsions (NRE).

Current limitations of these systems for quantitative track scanning are presented. Experimental uncertainties attained with these computer-controlled systems are described using results obtained from reactor neutron dosimetry.

Accomplishments and Status

Track methods have been successfully applied over a remarkable domain of scientific activities. Rather than remaining stagnant, this diversity continues to expand as new techniques with solid state track recorders (SSTR) continue to evolve. This broad applicability is based on many significant attributes of SSTR. The general applicability of track techniques for neutron dosimetry is based upon two particular attributes perhaps more than any others, namely enormous dynamic range and high accuracy.

Experimental uncertainty in applying track techniques for absolute measurements can be as low as 1-2% (1σ) if care is exercised. This capability was demonstrated using manual scanning techniques (Go68, Ro68a). However, manual track counting is very labor-intensive, time-consuming, and carries a risk of observer bias. Consequently, elimination of the human element is highly desirable for precise track measurements.

A tacit goal underlying efforts to automate track scanning has been to maintain the high experimental accuracy already attained with manual scanning techniques. Ideally, one desires the reduced labor and costs afforded by automation, while still maintaining already demonstrated standards of accuracy. In national and international nuclear energy programs, current goals call for attainment of the highest possible accuracy levels (Gc80f). Hence, for reactor neutron dosimetry, automated systems for SSTR and nuclear research emulsions (NRE) cannot compromise accuracy standards already available through manual scanning.

In contrast with accuracy, automated methods can enlarge the range of applicability of track techniques by extending quantitative measurements to higher track densities than can be accurately scanned with manual techniques. Indeed, the high sensitivity of SSTR leads to a serious track density limitation for high-neutron flux/fluence experiments because of track pile-up. However, it has already been shown that this pile-up limitation is allayed using the Buffon Needle method of track scanning (Go82). The Buffon Needle method is, in turn, particularly well suited for automated scanning systems. More recently, it has been demonstrated that the random sampling procedure of the Buffon Needle method can be replaced by sampling on a fixed network or grid of points on the SSTR surface (Gr83a). Gray has rigorously derived the probability distribution for fixed grid sampling and proven this result through comparison with experiment down to the level of approximately 1% (1σ). Moreover, fixed grid sampling provides significantly more alleviation from pile-up effects than even the Buffon Needle method. Using such techniques, automation promises to render practical many key experiments for power reactor environments that were previously not feasible.

The Hanford optical track scanner (HOTS) is described in the next section, with emphasis given to advances that have been achieved relative to earlier SSTR automation efforts. The automated scanning electron microscope (ASEM) system, which is devoted to high-power/high-fluence reactor experiments, is presented in the following section. In the last section, the interactive emulsion scanning processor (ESP) system is described. Improvements in NRE neutron dosimetry are illustrated using experimental results obtained through application of the ESP system.

Hanford Optical Track Scanner (HOTS)

Although considerable effort has been expended by many groups in attempts to automate track scanning, overall progress has been slow. A spark counting method applicable with plastic SSTR such as Makrofol or Lexan has been successfully demonstrated (Cr69, La69), but possesses severe limitations for precision work. Detailed investigations (Co70, Co72a) reveal accuracy of roughly 10%-20% for this technique, provided track density is limited to $<10^3/cm^2$.

A more sophisticated automation system, using an optical microscope under computer control, was developed at Argonne National Laboratory (ANL) (Co69, Co72, Go71). This Argonne optical track scanner (AOTS) system has demonstrated comparable accuracy to manual scanning for plastic SSTR of the polycarbonate resin variety such as Makrofol, Lexan, etc. (Co72, Go72).

Although this AOTS system did establish that SSTR automation was possible at an accuracy level comparable with human observations, severe limitations arose. Extreme difficulty was originally encountered using mineral track recorder materials, such as mica with any degree of reliability or reproducibility. Subsequent efforts by (Co75) have overcome these difficulties in scanning mica SSTR. A track density limit of roughly 10^5 tracks/cm^2 was established, beyond which SSTR accuracy could be seriously compromised. System speed was approximately 10 h/cm^2, which provides a relatively slow processing rate of 1-2 SSTR/day.

The AOTS system was the first microscope system ever built that possessed automatic focussing capability. It was transferred to HEDL to meet the overall dosimetry needs of the U.S. fast breeder reactor (FBR), light water reactor (LWR), and magnetic fusion reactor (MFR) energy programs. During the past two years, major hardware modifications have been undertaken to improve the utility of this system, which is now called the Hanford optical track sensor (HOTS).

While the microscope remains little changed from the original AOTS, major improvements have been made in both the imaging system and computer control modules (Mc83). Figure HEDL-1 is a photograph delineating the components of the HOTS system. The specimen stage moves on linear ball bearings. Movements of the stage in the X and Y directions are made by two independent stepping motors of 800 steps/revolutions coupled to a micrometer screw of 40 threads/inch. Positioning accuracy is a ± 1 motor step. A third stepping motor having 200 steps/revolution provides for focus control.

A major improvement in converting the optical image into a digital format compatible for computer analysis is the use of a high-resolution videcon camera. The camera replaces the original photomultiplier tube imaging system. Conversion of the optical image to digital format is accomplished with the internal high-speed digitizer of the camera controller. The maximum resolution of the videcon system is 1024 x 1024 pixels per frame. Current computer memory capacity limits the resolution to 256 x 512 pixels per frame. Each pixel is converted to a digital value over the range 0-255 with zero representing a completely dark image. An entire frame can be digitized and stored in the computer memory in approximately 250 milliseconds. Once the frame image is stored, high speed data analysis begins and the stage moves to the next location. Control of the entire system as well as data analysis is accomplished with the LSI 11/23 computer. The lower 32K words of memory are used for program storage, and upper 64K words are used to store a digitized frame image. In addition to controlling the automatic scan operation, a stepping motor interface provides for inputs from two joysticks. The joysticks allow for manual operation of the stage for initial alignment and set-up of the SSTR specimen.

Control of the entire system is accomplished with a program written in FORTRAN and DEC assembly language. All data analysis routines are written in assembly language due to the speed intensive nature of this task. The control program consists of six basic modules that provide for initial set-up and alignment, input of required parameters, image digitizing, stage movement, autofocusing, and track correlation.

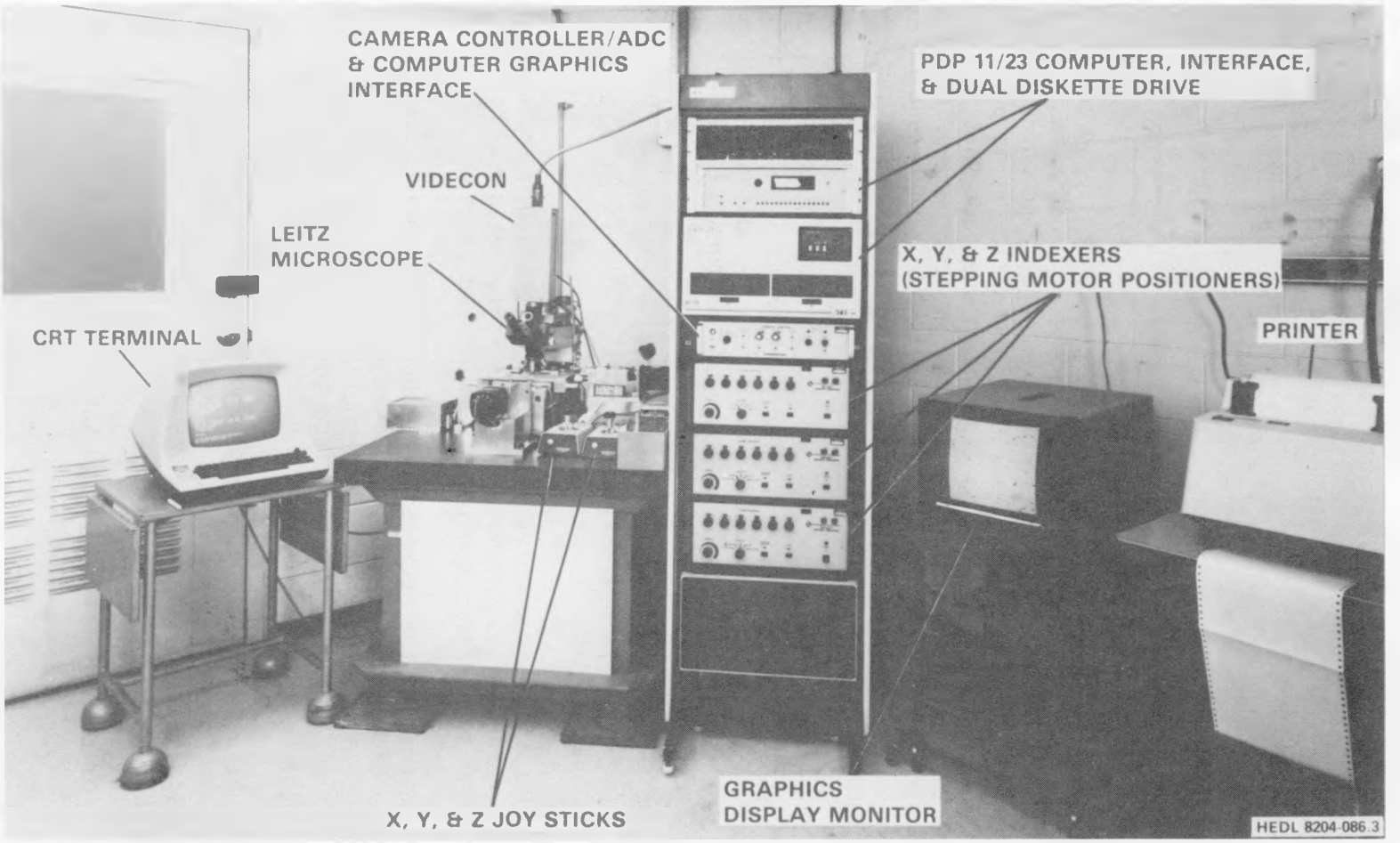

FIGURE HEDL-1. Photograph of the Hanford Optical Track Scanner (HOTS) System.

Before the control program begins, the user inputs the event detection threshold, the focus check frequency, and the diameter of the SSTR area to be scanned. The event detection threshold is based on a user input multiplier (0-1) and the average pixel intensity (0-255). The average pixel intensity is computed by averaging 8192 randomly selected pixels whose intensity exceeds the event threshold. The threshold for event detection is then recomputed as the product of the average value and the user input multiplier. A user input of 0.9 is most commonly used. Periodically during the scan, an autofocus routine is used to optimize the image contrast. The routine is based on the maximum opacity criterion introduced by Conn and Gold (Co72).

The most time-consuming operation performed by the control program is the correlation of the events into tracks. It is for this reason that all the correlation routines are written in assembly language. The correlation routines are based on the technique described in (Co72). It is possible to extend this technique to the present system due to the fact that the frame image can be reconstructed into single line scan images. An additional routine was required to keep track of events that end on the boundaries of each frame. This routine correctly accounts for tracks that continue into one or more frames.

After the scan is completed, tracks are grouped by area (pixels) so that a track size histogram can be produced. These histograms are similar to those obtained with the AOTS system. A nonlinear regression analysis program is used to fit the histogram data to an equation of the form

$$F(x) = ae^{-bx} + \frac{c}{(x - d)^2 + e} + \frac{f}{(x - g)^2 + h} \quad , \qquad (1)$$

where x is the track area in pixels, a, b, c, d, e, f, and h are parameters to be determined, and F(x) is the number of tracks for each x. For low-track density, $\sim 10^5$ tracks/cm^2, the third term can be omitted.

The first term represents the decreasing exponential function that is characteristic of the background seen on unexposed mica samples. The second and third terms represent the track area distribution. Figure HEDL-2 illustrates a typical track size histogram obtained from the HOTS and the excellent fit provided by Eq. (1).

The HOTS system has been calibrated using procedures completely analogous to the earlier calibration work carried out for the AOTS system (Go72). If one plots N, the fissions/cm^2 against the average values of N_O, the tracks/cm^2, for each sample, the data is found to give a good fit to the paralyzable counter model. This model predicts the relationship where $\langle\alpha\rangle$ is the average area for pile-up of tracks in the sample. By using a nonlinear

$$N_O = N\, e^{-\langle\alpha\rangle N} \quad , \qquad (2)$$

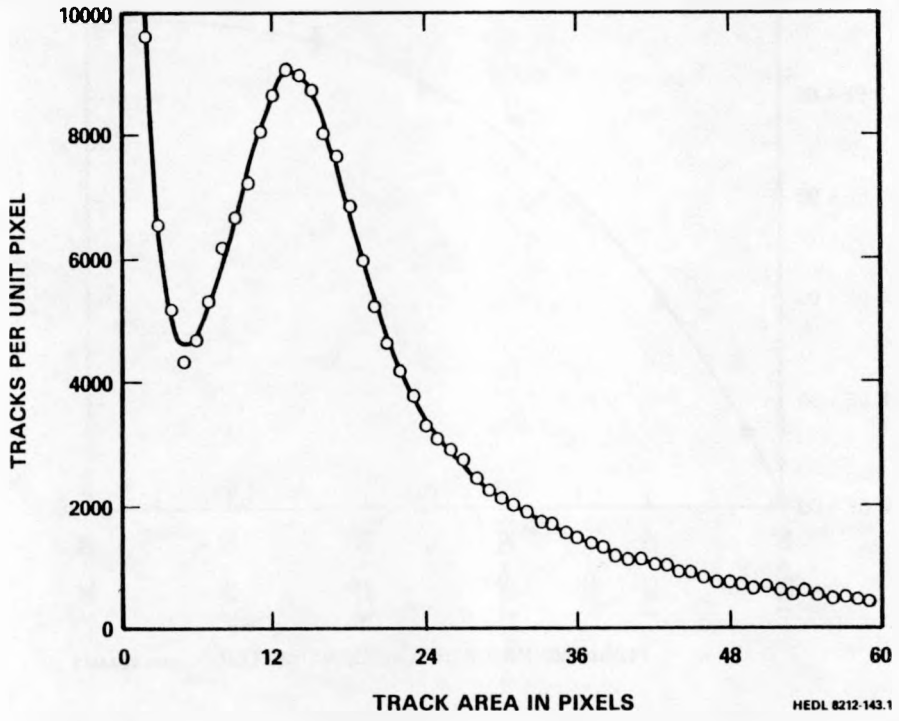

FIGURE HEDL-2. Typical Track Area Distribution for a Mica SSTR Sample Exposed to a Thin Deposit of an Actinide Element and Etched in 40% HF for 45 min at 22 ± 0.2°C. The data were fit to the functions given in Eq. (1).

regression analysis code, the value of $\langle\alpha\rangle$ was found to be 1.5592 x 10^{-6} cm^2, with a relative sigma of 0.014. The excellent fit to the paralyzable counter model is shown in Figure HEDL-3. Considerably greater detail on the HOTS system operation (Mc83) and calibration (Ro83) is now available in a special issue of Nucl. Tracks.

The processing time on the HOTS varies with track density from about 45 minutes for a density of approximately 4 x 10^4 tracks/cm^2 up to about 150 minutes for a density of approximately 7 x 10^5 tracks/cm^2. The increased time for higher track densities follows from the need to correlate more events into tracks. The reproducibility for repeated scans of SSTR on the HOTS system is at the 2% (1σ) level. These enhanced features greatly increase the cost effectiveness of SSTR applications in reactor dosimetry. Consequently, when sufficient tracks are available for counting, statistics are no longer a problem; other sources of uncertainty will then dominate the overall experimental error.

Automated Scanning Electron Microscope (ASEM)

A block diagram of the ASEM system in current use at HEDL is shown in Figure HEDL-4. The system is essentially a video digitizer with a programmable

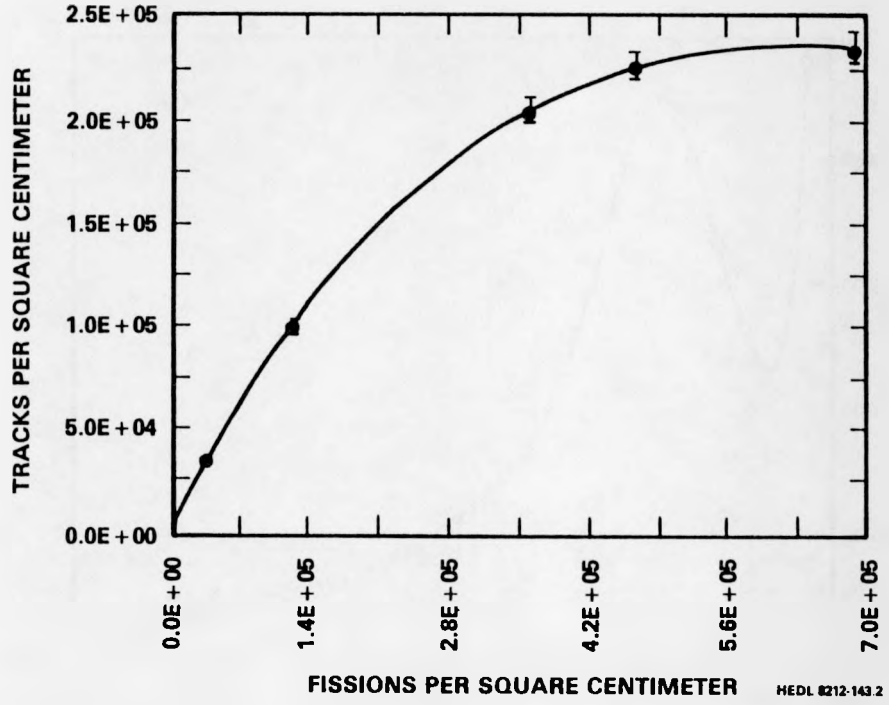

FIGURE HEDL-3. Track Densities Obtained from Fitting the Track Area Distribution to Eq. (1) Plotted Against the Known Fission Densities for Mica Samples Exposed to a Calibrated Fission Source. The data have been fit to the paralyzable counter model expressed by Eq. (2).

trigger circuit. The computer can instruct the trigger circuit to store data from any selected video line. Data are stored in the buffer memory and may, in turn, be read into the PDP 11/03 at a slower rate. The data acquired by the PDP 11/03 can then be transmitted to a larger computer for storage on disk or magnetic tape for analysis. A PE3220 computer is utilized for this task.

Automation of a scanning electron microscope (SEM) for track scanning eliminates the mechanical motion inherent in the stage of an automated optical microscope, thus an improvement in speed accrues. Since the electron beam is scanned across the SSTR surface in TV raster fashion, reproducibility and reliability are vastly improved by elimination of any mechanical motion.

In addition to improved reproducibility and reliability, a SEM offers a much higher magnification range and, hence, covers a much greater dynamic range of track density than is possible in optical microscopy. These two factors together with the much greater depth of focus of a SEM should provide quantitative data of greater accuracy, especially for high-flux or high-fluence neutron dosimetry experiments in power reactors.

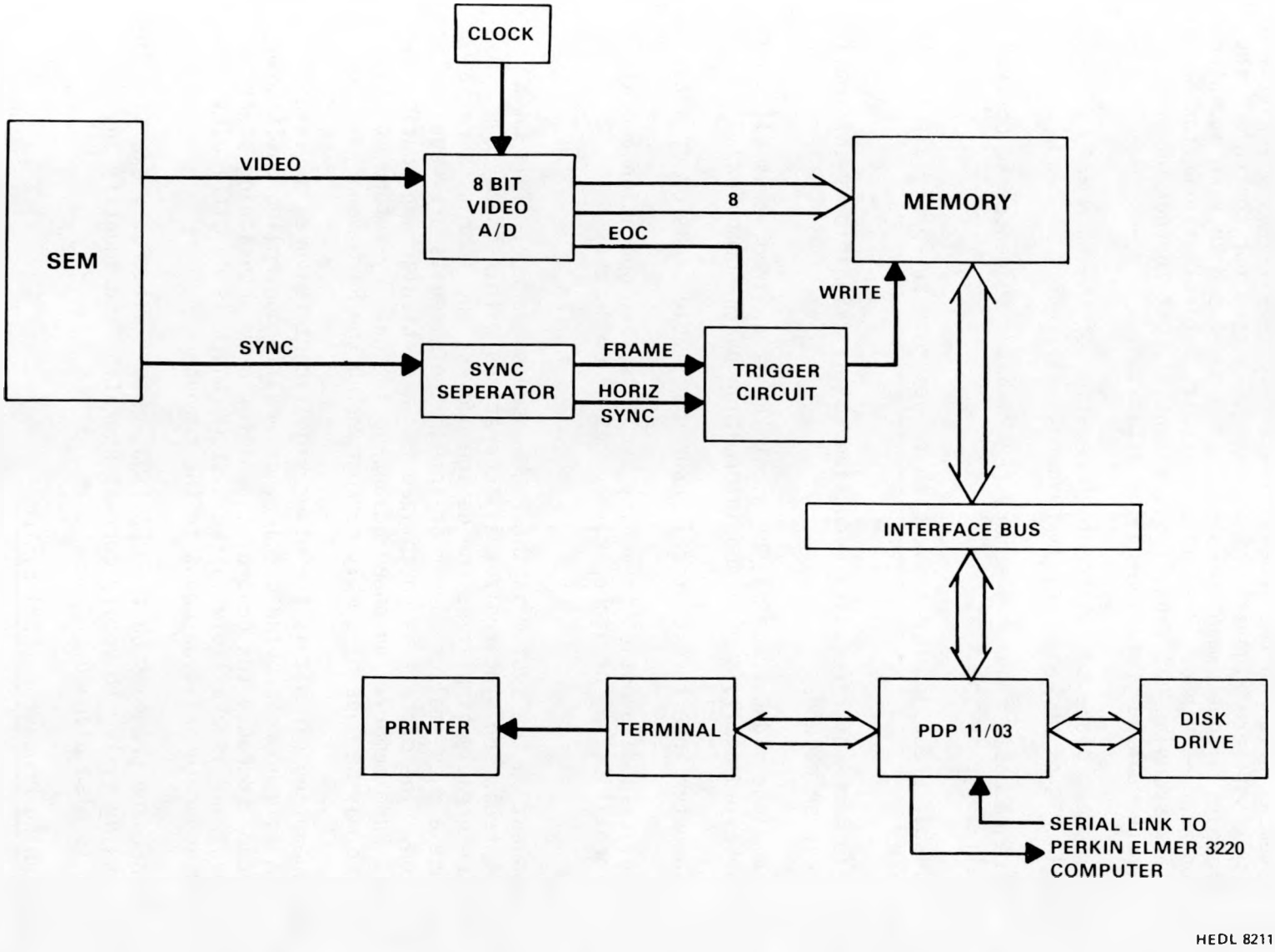

FIGURE HEDL-4. Block Diagram of the Automated Scanning Electron Microscope (ASEM) System.

In contrast with the HOTS and ESP systems, which are in routine use, the ASEM is still under development. A detailed description of progress with the ASEM system is given in the special issue of J. Nucl. Tracks for greater detail (Pr83). Software algorithms have been developed for control of the SEM. For example, a code named BUFFON is being developed to take advantage of the Buffon Needle method. Preliminary results indicate the Buffon Needle method of track scanning has significant potential, but further work is necessary before routine operation can be established.

Current development plans to ennance the operation of the ASEM are illustrated in Figure HEDL-5. Key improvements will be:

- Programmable read-only memory (PROM)-based sequencer to control all logic in the system
- 14-bit precision D/A conversion to generate sweep signals for the SEM
- A/D comparator for data reduction so only significant information need be recorded
- Complete video frame may be digitized if desired, thus allowing detailed analysis of video information by the computer
- Computer interface protocol ensures reliable transfer of data
- Built-in diagnostics to verify proper system operation and allow identification of improperly operating components

The key component in the system is the PROM-based sequencer. This unit completely controls and synchronizes all operations within the system. Use of this device greatly simplifies the design process and increases reliability because a much smaller number of integrated circuits are required for implementation. The circuit is customized for a particular application by programming a PROM memory. An added advantage is that any future modification desired may be made by simply reprogramming the PROM memory.

The sweep generating circuit is the other significant feature. A 14-bit precision D/A is used to provide precise, externally controlled positioning of the SEM beam. Because the central signal for beam positioning starts as a digital count and is available in the system, there is no difficulty providing an accurate position count to the computer.

Diagnostic software programs on the DEC 1103, which would fully exercise the signal processing system to verify correct operation and identify any malfunction, is also planned.

Emulsion Scanning Processor (ESP) System

Because of the diverse utility of NRE in scientific research, many groups nave developed special instrumentation systems to aid in the task of

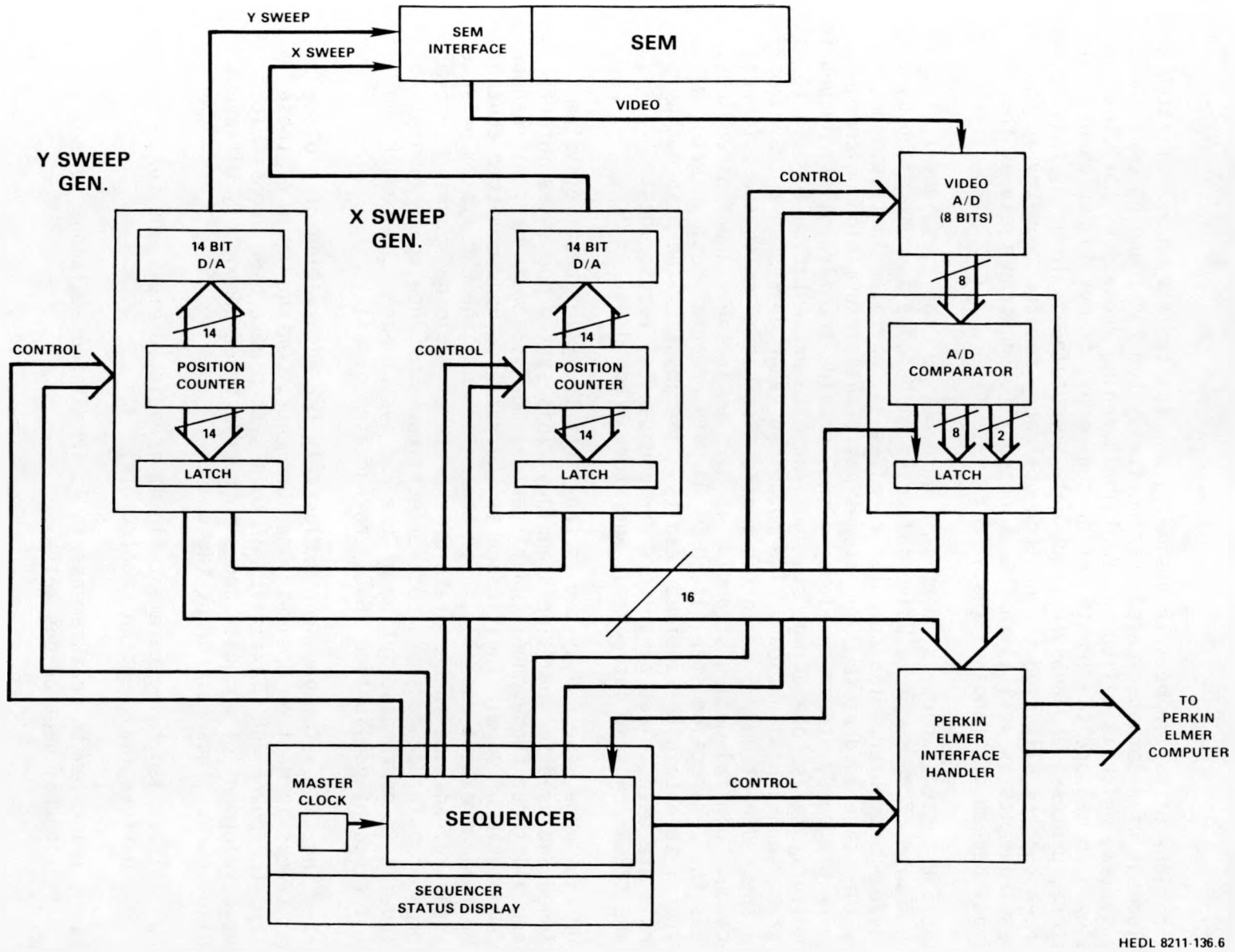

FIGURE HEDL-5. Block Diagram of the Advanced Automated Scanning Electron Microscope (ASEM) System Under Development.

emulsion scanning. A review text (Ba63) on NRE summarizes earlier NRE-instrumentation activities. More recently, a Russian group has developed an emulsion scanning instrumentation system for fast neutron measurements (Be72).

Applications of NRE in neutron dosimetry and spectrometry have motivated the development of a computer-based interactive system for scanning emulsions. This system, which is called the Emulsion Scanning Processor (ESP), has been developed to measure the lengths of proton-recoil tracks in NRE as well as to store, process, and analyze track data so obtained. To date, this system has been successfully used for neutron dosimetry and spectrometry in FBR and LWR environments as well as in the standard ^{252}Cf neutron field at the National Bureau of Standards (NBS).

In the ESP system, which is shown in Figure HEDL-6, the X, Y, and Z (focus) stage motion of a motorized Universal Zeiss microscope is controlled by a PDP 11/03-L computer. The computer receives all operator instructions, moves the stage as directed, and stores positional information on command. Software programs, stored on floppy disks, provide the flexibility needed to conveniently tailor operating, storage, and data presentation formats to fit different scanning situations. The motorized stage possesses a travel of 75 mm in the X-direction, 25 mm in the Y-direction, and 4 mm in the Z (focus) direction. Digital motion step size is 0.25 μm in the X and Y directions, whereas the Z-direction step size 0.05 μm. An operator must interact with the system to obtain the desired results. The joystick and push button controls are used to set parameters and boundaries, focus, locate tracks, measure track lengths, categorize, and store track data.

To our knowledge, the ESP system is the first truly interactive system developed and used for emulsion scanning. This system possesses interfaces between all three fundamental constituent elements, namely man, microscope, and computer. Of equal significance is the reliance upon computer control to the maximum extent possible. For these reasons, the ESP system provides a substantial advance in the state-of-the-art of emulsion scanning systems in terms of both accuracy and cost-effectiveness. Since space limitations preclude an in-depth description of the ESP system here, the reader should consult a recent publication (Go83) for greater details.

To date, the ESP system has been exclusively for observation of proton-recoil tracks in neutron dosimetry measurements. On the basis of these efforts, the power and flexibility of this system have been demonstrated by the development of computer codes to handle three completely different scanning tasks. These different tasks are:

- Track length measurements in 4π irradiated emulsions for differential neutron spectrometry
- Track length measurements in 4π irradiated emulsions for integral neutron dosimetry

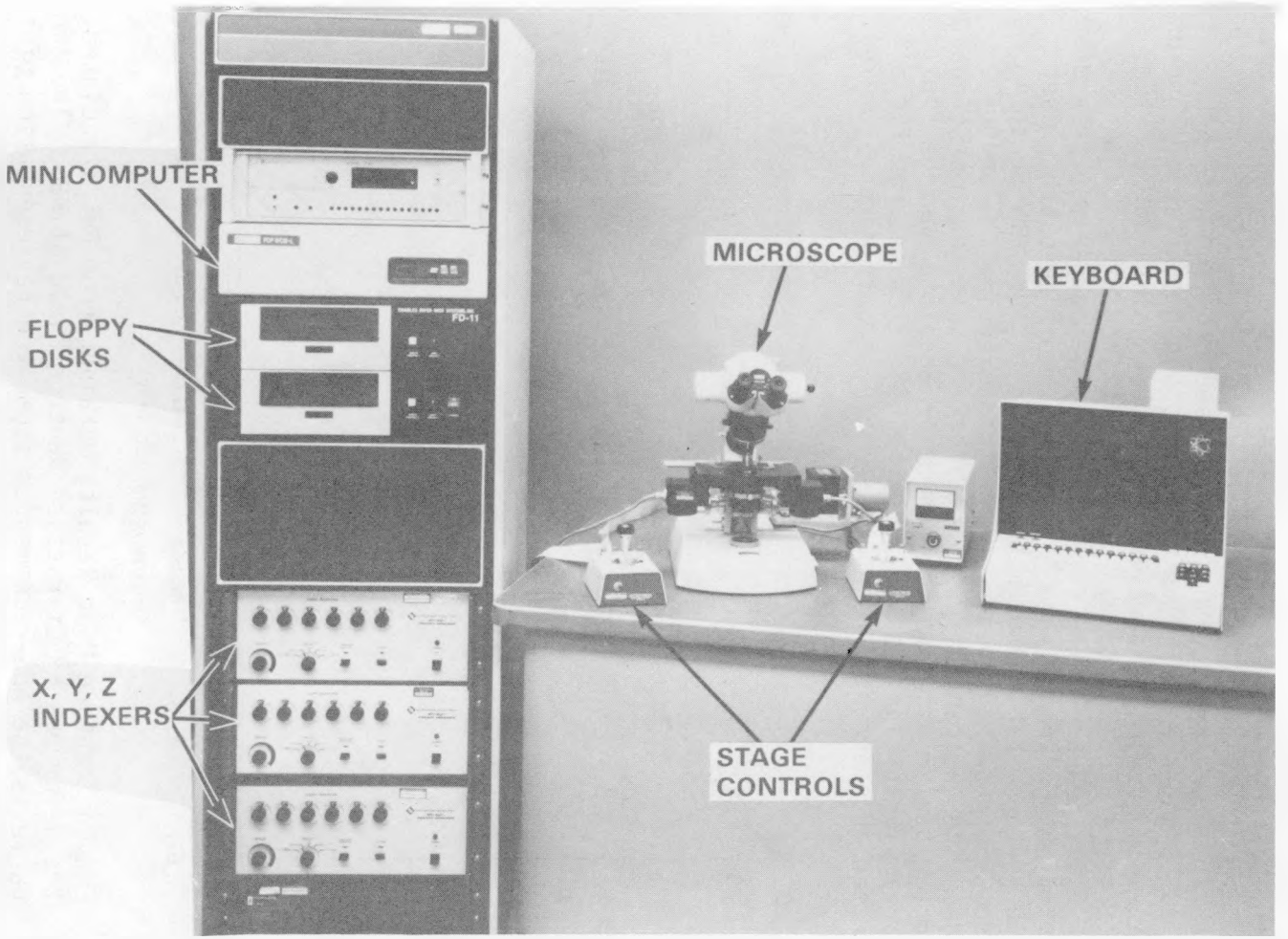

FIGURE HEDL-6. Photograph of the Interactive Emulsion Scanning Processor (ESP) System.

- Track length measurements in emulsions irradiated in collimated or undirectional neutron beams for differential neutron spectrometry

These scanning tasks correspond to operation of the ESP system in different modes, namely differential mode scanning, integral mode scanning, and end-on scanning, respectively. Differential mode scanning has been used for NRE differential neutron spectrum measurements in the Fast Flux Test Facility (FFTF) at startup (Go81). Indeed, these efforts led to the first experimental confirmation of the existence of angular anisotropy in the neutron field within a reactor core. Integral mode scanning has been used for NRE integral proton-recoil reaction rate measurements in the LWR pressure vessel mockup at the pool critical assembly (PCA) in Oak Ridge National Laboratory (ORNL) (Go81d,e). The end-on scanning mode has been applied with NRE exposed in the NBS Standard ^{252}Cf fission neutron benchmark field. End-on irradiations can be conveniently carried out in this point source ^{252}Cf neutron field. Figure HEDL-7 displays results obtained from scanning approximately 2×10^3 tracks in the end-on mode. The comparison presented in Figure HEDL-7 with the recommended ^{252}Cf spectrom is absolute. Over the energy range of these NRE measurements, from about 0.8 MeV up to 10 MeV, the NRE observed ^{252}Cf neutron spectrum is within experimental uncertainty of the absolute neutron intensity claimed for this neutron standard benchmark field (Gr75b, Gr78). This agreement in absolute neutron flux intensity is particularly significant since the NBS ^{252}Cf neutron field has been calibrated independently using the manganese bath method (Gr77b).

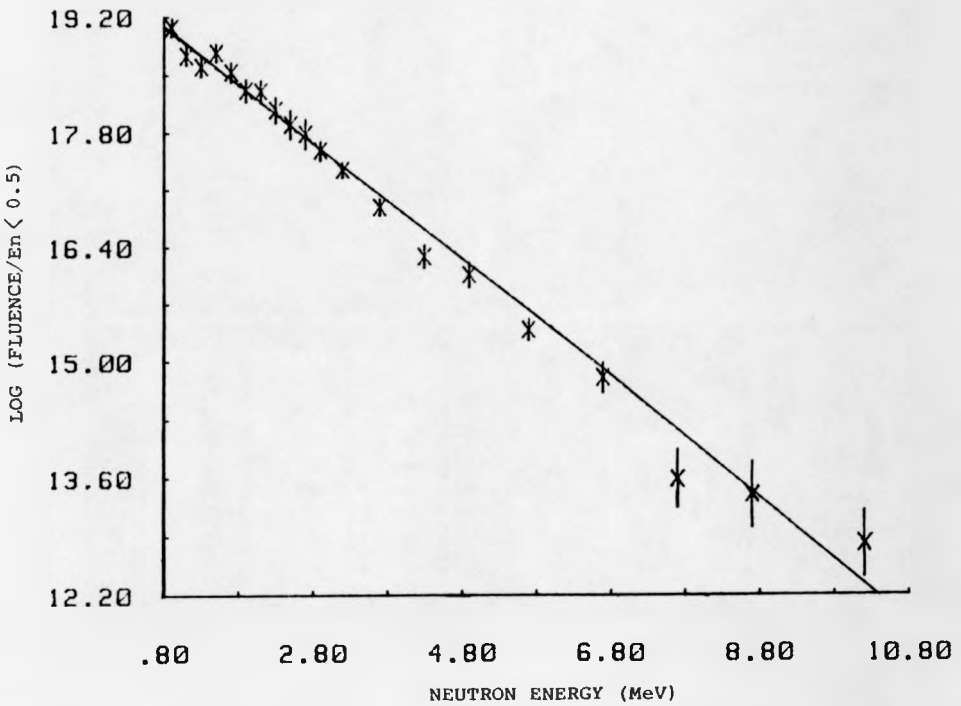

FIGURE HEDL-7. End-on Scanning Mode Results Obtained from NRE irradiated in the Reference ^{252}Cf Fission Neutron Field at NBS. The smooth curve is the NBS-recommended segmented representation of the ^{252}Cf spectrum (Gr75, Gr78). The comparison is absolute.

Sources of uncertainty arising in absolute NRE neutron spectrometry are summarized in Table HEDL-2. In contrast with the first five sources of uncertainty listed in Table HEDL-2, which are systematic, the range measurement uncertainty does not introduce any systematic bias into NRE neutron spectrometry. Hence, this range measurement uncertainty, or the corresponding energy uncertainty, must be classified as a random uncertainty. Since these systematic uncertainties are independent, the quadrature uncertainty for all systematic effects in NRE neutron spectrometry comes to roughly 5%. Nevertheless, it must be stressed that Table HEDL-2 is restricted to uncertainties which arise in the NRE experimental technique. Additional uncertainties can arise in neutron irradiations, such as exist in the irradiation exposure time t and the absolute reactor power. The existence of such additional uncertainties must be recognized and treated separately.

The ESP system provides a substantial advance in the state-of-the-art of emulsion scanning in terms of both accuracy and cost-effectiveness. The uncertainty in track length measurements with this system is approximately 0.52 μm (1σ), which is an improvement of about a factor of 4 over the earlier automation efforts of (Be72). While emulsion scanning rates vary for the different modes of system operation, scanning rates of 30 to 40 tracks/hour have been typically obtained. This rate represents an increase by a factor of 3 to 4 over the scanning rates attained in the earlier work of (Be72).

TABLE HEDL-2

UNCERTAINTY ESTIMATES FOR ABSOLUTE NEUTRON SPECTROMETRY WITH NUCLEAR RESEARCH EMULSIONS

Source of Uncertainty	Approximate Uncertainty (1σ)
Proton range straggling	2%
Proton energy based on range-energy relation	2%
Hydrogen density in the emulsion	3%
Elastic scattering cross section σ_{np} (E)	1%
Volume of emulsion scanning with ESP system	2%
Range measurements with the ESP system	0.5 μ

Expected Future Accomplishments

HOTS

A number of improvements are currently being implemented on the HOTS system. Methods for improving reproducibility are being implemented. Finer control of focus as well as improved autofocusing will be incorporated to improve discrimination between tracks and imperfections in both mineral and plastic SSTR. Imperfections in mica present problems in accurate track counting at low track densities. Methods of alleviating this problem, such as software routines for track shape discrimination, will be explored. Preliminary studies of track diameter measurements in ^{39}Cr polymer show promise, but finer focus control is necessary to attain accurate results. Software improvements currently underway are frame-by-frame correction for track pile-up (for SSTR possessing non-uniform track density) and subframe corrections for variations in frame (videcon) illumination.

ASEM

The ASEM will be applied in scanning high-track density SSTR and the limitations of the Buffon Needle method and alternative sampling methods will be established.

ESP

Design plans to convert the interactive ESP system to a fully automated system will be initiated. The highest priority of this new design will be to fully automate integral mode scanning.

References

(As82) ASTM E706-81a, "Master Matrix for LWR Pressure Vessel Surveillance Standards," 1982 Annual Book of ASTM Standards, Part 45, "Nuclear Standards," American Society for Testing and Materials, Philadelphia, PA, 1982.

(As82b) ASTM E854-81, "Standard Method for Application and Analysis of Solid State Track Recorder (SSTR) Monitors for Reactor Surveillance," 1982 Annual Book of ASTM Standards, Part 45, "Nuclear Standards," American Society for Testing and Materials, Philadelphia, PA, 1982.

(Ba63) W. H. Barkas, "Techniques and Theories," Nuclear Research Emulsions, Vol. I, Academic Press, New York, NY, 1963.

(Be72) G. E. Belovitiskii et al., "Measurement of the Spectra of Fast Neutrons (∿14 MeV) with High-Energy Resolution with the Aid of Nuclear Emulsions - Automation of the Measurements," Proc. (Trudy) of the P. N. Lebedev Physics Institute, Nuclear Reactions and Interaction of Neutrons and Matter, Vol. 63, pp. 109-119, Nanka Press, Moscow, USSR, 1972.

(Co69) C. E. Cohn, R. Gold and T. W. Pienias, "Computer-Controlled Microscope for Scanning Fission Track Plates," Trans., Am. Nucl. Soc. 12, p. 68, 1969.

(Co70) F. J. Congel et al., "Automatic System for Counting Etched Holes in Thin Dielectric Plastics," Trans. Am. Nucl. Soc. 13, p. 419, 1970.

(Co72) C. E. Cohn and R. Gold, "Computer-Controlled Microscope for Automatic Scanning of Solid-State Nuclear Track Recorders," Rev. Sci. Instrum. 42, pp. 12-17, 1972.

(Co72a) F. J. Congel et al., "Automatic System for Counting Etched Holes in Thin Dielectric Plastics, Nucl. Instrum. Methods 100, pp. 247-252, 1972.

(Co75) C. E. Cohn and R. J. Armani, "Automatic Scanning of Mica Track Recorders," Rev. Sci. Instrum. 46, pp. 18-19, 1975.

(Cr69) N. G. Cross and L. Tommasino, Proc. of the International Topical Conf. on Nuclear Track Registration in Insulating Solids and Applications, Univ. of Clermont, Clermont-Ferrand, France, Vol. I, p. 73, 1969.

(Go68) R. Gold, R. J. Armani and J. H. Roberts, "Absolute Fission Rate Measurements with Solid-State Track Recorders," Nucl. Sci. Eng. 34, p. 13, 1968.

(Go71) R. Gold and C. E. Cohn, "Analysis of Automatic Fission Track Scanning Data, Trans. Am. Nucl. Soc. 14, p. 500, 1971.

(Go72) R. Gold and C. E. Cohn, "Analysis of Automatic Fission Track Scanning in Solid-State Nuclear Track Recorders," Rev. Sci. Instrum. 43, pp. 18-28, 1972.

(Go80f) R. Gold, F. H. Ruddy, and J. H. Roberts, "Applications of Solid-State Track Recorders in US Nuclear Reactor Energy Programs," Proc. of the 10th International Conference on Solid-State Nuclear Track Detectors, Lyons, France, July 2-7, 1979, pp. 533-547, Pergamon Press, Oxford, UK, 1980.

(Go81) R. Gold and J. H. Roberts, "Nuclear Emulsion Neutron Spectrometry in FFTF," Trans. Am. Nucl. Soc. 39, p. 896, December 1981.

(Go81d) R. Gold, J. H. Roberts, F. H. Ruddy, C. C. Preston and C. A. Hendricks, "Proton-Recoil Observations for Integral Neutron Dosimetry," Proc. of the IAEA Advisory Group Meeting on Nuclear Data for Radiation Damage and Safety, IAEA-TEC DOC-263, International Atomic Energy Agency, Vienna, Austria, pp. 115-121, 1981.

(Go81e) R. Gold, J. H. Roberts, C. C. Preston, and F. H. Ruddy, "Neutron Spectrometry with Nuclear Research Emulsions," LWR-PV-SDIP: PCA Experiments and Blind Test, NUREG/CR-1861, HEDL-TME 80-87, Sec. 3.3, Nuclear Regulatory Commission, Washington, DC, July 1981.

(Go82) R. Gold, J. H. Roberts and F. H. Ruddy, "Buffon Needle Method of Track Counting," Proc. of the 11th International Conference on Solid-State Nuclear Track Detectors, Bristol, UK, 1981, Pergamon Press, Oxford, UK, pp. 891-897, 1982.

(Go83) R. Gold et al., "Interactive System for Scanning Tracks in Nuclear Research Emulsions," Rev. Sci. Instrum. 54, pp. 183-192, 1983.

(Gr75b) J. A. Grundl and C. M. Eisenhauer, "Fission Spectrum Neutrons for Cross-Section Validation and Neutron Flux Transfer," Proc. of a Conference on Nuclear Cross Sections and Technology, NBS Special Publication 425, Vol. 1, National Bureau of Standards, Washington, DC, pp. 250-257, 1975.

(Gr77b) J. A. Grundl, V. Spiegel, C. M. Eisenhauer, H. T. Heaton, D. M. Gilliam and J. Bigelow, "A Californium-252 Fission Spectrum Irradiation Facility for Neutron Reaction Rate Measurements," Nucl. Technol. 32, p. 315, 1977.

(Gr78) J. A. Grundl and C. M. Eisenhauer, "Benchmark Neutron Fields for Reactor Dosimetry," Neutron Cross Sections for Reactor Dosimetry, IAEA-208, International Atomic Energy Agency, Vienna, Austria, Vol. I, pp. 53-104, 1978.

(Gr83a) P. W. Gray, "Random Sampling in the Scanning of Solid-State Track Recorders," Thesis, Imperial College, Univ. of London, Silwood Park, Ascot, UK, 1983.

(La69) N. L. Lark, "Spark Scanning for Fission Fragment Tracks in Plastic Foils," Nucl. Instrum. Methods 67, pp. 137-140, 1969.

(Mc83) J. P. McNeece, R. Gold, C. C. Preston and J. H. Roberts, "Automated Scanning of Solid-State Track Recorders: Computer-Controlled Microscope," Nucl. Tracks 7, pp. 39-45, 1983.

(Pr83) C. C. Preston, R. Gold, J. P. McNeece, J. H. Roberts and F. H. Ruddy, "Progress in Automated Scanning Electron Microscopy for Track Counting," Nucl. Tracks 7, pp. 53-61, 1983.

(Ro68a) J. H. Roberts, R. Gold and R. J. Armani, "Spontaneous-Fission Decay Constant of ^{238}U," Phys. Rev. 174, pp. 1482-1484, 1968.

(Ro83) J. H. Roberts, F. H. Ruddy, J. P. McNeece and R. Gold, "Automatic Scanning of Solid-State Track Recorders: Calibration," Nucl. Tracks 7, pp. 47-52, 1983

OAK RIDGE NATIONAL LABORATORY

(ORNL)

OAK RIDGE NATIONAL LABORATORY

A. LIGHT WATER REACTOR PRESSURE VESSEL (LWR-PV) BENCHMARK FACILITIES (PCA, ORR-PSF, ORR-SDMF) AT ORNL

F. B. K. Kam
F. W. Stallmann

Objectives

In order to serve as benchmarks, the neutron fields at PCA, ORR-PSF, ORR-SDMF, and BSR-HSST need to be known and controlled within sufficiently narrow uncertainty bounds. To achieve this objective, extensive measurements are combined with neutron physics calculations. Statistical uncertainty analysis and spectral adjustment techniques are used to determine uncertainty bounds. The results of this task will have a direct impact in the preparation of ASTM Standards for Surveillance of Nuclear Reactor Pressure Vessels. The objectives of these benchmark fields are:

1. PCA (in operation) - to validate and improve neutron transport calculations and dosimetry techniques in LWR-PV environments;

2. ORR-PSF (in operation) - to obtain reliable information from dosimetry measurements and neutron transport calculations and to correlate the spectral parameters with structural changes in the pressure vessel;

3. ORR-SDMF - to investigate results of current surveillance capsules so that dosimetry methods applied by vendors and service laboratories can be:

   a. validated and certified,
   b. improved by development of supplementary experimental data, and
   c. evaluated in terms of actual uncertainties; and

4. BSR-HSST - to study fracture toughness of irradiated pressure vessel materials.

A.1 PRESSURE VESSEL BENCHMARK FACILITY FOR IMPROVEMENT AND VALIDATION OF LWR PHYSICS CALCULATIONS AND DOSIMETRY (PCA)

C. A. Baldwin
R. E. Maerker
M. L. Williams

Summary

Calculated reaction rates, damage exposure parameters, and gamma flux densities from R. E. Maerker's coupled neutron-gamma calculations for the PCA 12/13 configuration are presented. A description of the calculation and comparisons with a similar calculation by G. Minsart have been reported in the April-June 1982 Quarterly Report.[1] The new calculation shows better agreement with experimental values compared to the old Blind Test[2] calculation.

Accomplishments and Status

Damage exposure parameters for the A1 through A6 locations of the PCA 12/13 configuration have been calculated and are listed in Table 1. With the exception of the A1 and A3M data for dpa, the new data in Table 1 are greater in magnitude than corresponding data reported for the PCA-PVF Blind Test. Ratios of new-to-old data are shown in parentheses next to the current data in Table 1.

Reaction rates have been calculated using the new neutron flux densities and are compared with the PCA-PVF Blind Test recommended integral results in Table 2.[3,4] The new C/E ratios demonstrate better agreement than was shown in the Blind Test results.[2] The old C/E ratios taken from the Blind Test are shown below the new C/E ratios in parentheses for comparison. A comparison of reaction rate ratios is presented in Table 3. The $^{58}Ni(n,p)^{58}Co$ reaction was chosen as the reference reaction rate. As can be seen, the calculations over predict the experimental values in general by 5 to 10%. There appear to be no obvious trends based on the threshold energies of the different reactions.

Finally, a tabulation of the calculated gamma flux densities for the A1 through A6 locations is given in Table 4. These data are part of the continuing documentation of the PCA benchmark facility, and are provided to assist in future gamma radiation measurements and the determination of photofission effects.

REFERENCES

(Ka83) 1. F. B. K. Kam, F. W. Stallmann, R. E. Maerker, and M. L. Williams, "Light Water Reactor Pressure Vessel (LWR-PV) Benchmark Facilities (PCA, ORR-PSF, ORR-SDMF) at ORNL," LWR Pressure Vessel Surveillance Dosimetry Improvement Program, Quarterly Progress Report, April-June 1982, HEDL-TME 82-19, Hanford Engineering Development Laboratory (January 1983).

(St81b) 2. F. W. Stallmann and F. B. K. Kam, "7.1 Compilation and Appraisal of PCA Blind Test C/E Data," LWR Pressure Vessel Surveillance Dosimetry Improvement Program: PCA Experiments and Blind Test, HEDL-TME 80-87, Hanford Engineering Development Laboratory (July 1981).

(Mc81f) 3. E. D. McGarry and A. Fabry, "8.2 Recommended Integral Results - Fission Chamber Measurements," LWR Pressure Vessel Surveillance Dosimetry Improvement Program: PCA Experiments and Blind Test, HEDL-TME 80-87, Hanford Engineering Development Laboratory (July 1981).

(Fa81c) 4. A. Fabry and L. S. Kellogg, "8.3 Recommended Integral Results - Radiometric Measurements," LWR Pressure Vessel Surveillance Dosimetry Improvement Program: PCA Experiments and Blind Test, HEDL-TME 80-87, Hanford Engineering Development Laboratory (July 1981).

TABLE ORNL-1 ORNL DWG 83-12851

DAMAGE EXPOSURE PARAMETERS FOR PCA 12/13 CONFIGURATION

Location	Flux Density[1] >1.0 MeV	Flux Density[1] >0.1 MeV	dpa[2] (ASTM)
A1	3.519-6 (1.04)	6.252-6 (1.04)	5.354-27 (0.74)
A2	3.886-7	7.754-7	5.963-28
A3M	1.297-7 (1.07)	2.294-7 (1.07)	2.015-28 (0.92)
A4	4.132-8 (1.04)	1.323-7 (1.11)	6.858-29 (1.05)
A5	1.881-8 (1.02)	8.653-8 (1.11)	3.737-29 (1.04)
A6	7.925-9 (1.01)	4.964-8 (1.08)	1.894-29 (1.02)

[1]Neutrons/cm^2/core neutron.

[2]Displacements/atom/core neutron.

TABLE ORNL-2

COMPARISON OF CALCULATED AND MEASURED REACTION RATES
(Reactions/Target Atom/Core Neutron) FOR PCA 12/13 CONFIGURATION

Location		^{235}U (n,f) F.P.*	^{237}Np (n,f) F.P.	^{115}In (n,n') ^{115m}In	^{103}Rh (n,n') ^{103m}Rh	^{238}U (n,f) F.P.	^{58}Ni (n,p) ^{58}Co	^{27}Al (n,α) ^{24}Na
A0	Cal.							
	Exp.						2.40-29	1.51-31
	C/E							
A1	Cal.	2.30-26	7.94-30	9.22-31	3.75-30	1.58-30	5.69-31	5.05-33
	Exp.	2.45-26	8.71-30	1.06-30	4.06-30		6.32-31	5.55-33
	C/E	0.94	0.91	0.87	0.92		0.90	0.91
			(0.82)	(0.86)			(0.89)	(0.90)
A2	Cal.	1.81-27	8.99-31	9.95-32	4.25-31	1.70-31	6.05-32	6.71-34
	Exp.			1.15-31			6.70-32	7.19-34
	C/E			0.87			0.90	0.93
A3M	Cal.	8.34-28	2.93-31	3.43-32	1.39-31	5.99-32	2.33-32	3.07-34
	Exp.	8.08-28	2.98-31	3.76-32			2.51-32	3.16-34
	C/E	1.03	0.98	0.91			0.93	0.97
			(0.83)	(0.86)			(0.89)	(0.92)
A4	Cal.	2.96-30	1.10-31	9.73-33	5.19-32	1.57-32	4.74-33	6.39-35
	Exp.		1.22-31	1.11-32	5.67-32	1.86-32	5.75-33	7.19-35
	C/E		0.90	0.88	0.92	0.84	0.82	0.89
			(0.87)	(0.84)		(0.77)	(0.80)	(0.85)
A5	Cal.	7.16-31	5.94-32	4.27-33	2.73-32	6.50-33	1.75-33	2.45-35
	Exp.		6.80-32	5.22-33	3.19-32	8.36-33	2.27-33	2.89-35
	C/E		0.87	0.82	0.85	0.78	0.77	0.85
			(0.85)	(0.80)		(0.74)	(0.75)	(0.81)
A6	Cal.	2.68-31	2.96-32	1.77-33	1.34-32	2.52-33	6.14-34	8.90-36
	Exp.		3.54-32	2.21-33	1.60-32	3.42-33	8.06-34	1.09-35
	C/E		0.84	0.80	0.84	0.74	0.76	0.82
			(0.83)	(0.77)		(0.69)	(0.74)	(0.78)
A7	Cal.							
	Exp.		9.51-33					
	C/E							

*Bare measurement and calculation.

TABLE ORNL-3

ORNL DWG 83-12853

COMPARISON OF REACTION RATE RATIOS FOR PCA 12/13 CONFIGURATION

Location	$^{235}U(n,f)F.P.*/^{58}Ni(n,p)^{58}Co$			$^{237}Np(n,f)F.P./^{58}Ni(n,p)^{58}Co$			$^{115}In(n,n')^{115m}In/^{58}Ni(n,p)^{58}Co$		
	Cal	Exp	C/E	Cal	Exp	C/E	Cal	Exp	C/E
A1	4.04+4	3.88+4	1.04	13.9	13.8	1.01	1.62	1.68	0.96
A2	2.99+4			14.8			1.64	1.72	0.95
A3M	3.58+4	3.22+4	1.11	12.6	11.9	1.06	1.47	1.50	0.98
A4	624.5			23.2	21.2	1.09	2.05	1.93	1.06
A5	409.1			33.9	29.9	1.13	2.44	2.30	1.06
A6	436.5			48.2	43.9	1.10	2.88	2.74	1.05

*Bare measurement and calculation.

Location	$^{103}Rh,(n,n')^{103m}Rh/^{58}Ni(n,p)^{58}Co$			$^{238}U(n,f)F.P./^{58}Ni(n,p)^{58}Co$			$^{27}Al(n,\alpha)^{24}Na/^{58}Ni(n,p)^{58}Co$		
	Cal	Exp	C/E	Cal	Exp	C/E	Cal	Exp	C/E
A1	6.59	6.42	1.03	2.78			8.87-3	8.78-3	1.01
A2	7.02			2.81			1.11-2	1.07-2	1.04
A3M	5.96			2.57			1.32-2	1.26-2	1.05
A4	10.9	9.86	1.10	3.31	3.23	1.02	1.35-2	1.25-2	1.08
A5	15.6	14.0	1.11	3.71	3.68	1.01	1.40-2	1.27-2	1.10
A6	21.8	19.8	1.10	4.10	4.24	0.97	1.45-2	1.35-2	1.07

TABLE ORNL-4

GAMMA FLUX DENSITIES FOR PCA 12/13 CONFIGURATION

Group	Upper energy (eV)	Gamma flux densities (photons/cm^2/core neutron)[a]					
		A1	A2	A3M	A4	A5	A6
1	1.400+07	1.326-10	2.238-11	1.460-11	2.035-12	5.162-13	1.254-13
2	1.000+07	2.658-07	7.632-08	4.215-08	4.706-09	1.063-09	2.390-10
3	8.000+06	1.232-06	2.370-07	1.549-07	2.198-08	5.219-09	1.139-09
4	7.000+06	4.456-07	8.805-08	5.800-08	9.293-09	2.486-09	6.155-10
5	6.000+06	7.706-07	1.301-07	8.769-08	1.417-08	3.796-09	9.271-10
6	5.000+06	1.544-06	2.098-07	1.434-07	2.266-08	5.995-09	1.435-09
7	4.000+06	2.608-06	3.406-07	2.315-07	3.650-08	9.681-09	2.305-09
8	3.000+06	1.834-05	1.552-06	1.050-06	9.586-08	2.179-08	4.779-09
9	2.000+06	5.836-06	7.332-07	4.956-07	7.014-08	1.682-08	3.754-09
10	1.500+06	1.001-05	1.102-06	7.338-07	1.021-07	2.410-08	5.331-09
11	1.000+06	6.222-06	6.672-07	4.353-07	6.306-08	1.594-08	3.988-09
12	8.000+05	3.893-06	3.931-07	2.596-07	3.535-08	8.349-09	1.901-09
13	7.000+05	4.807-06	4.685-07	3.106-07	4.137-08	9.650-09	2.179-09
14	6.000+05	1.592-05	1.593-06	1.059-06	1.570-07	3.700-08	8.457-09
15	4.000+05	3.799-05	3.123-06	2.191-06	2.580-07	6.037-08	1.373-08
16	2.000+05	4.959-05	3.247-06	2.502-06	1.572-07	3.679-08	8.373-09
17	1.000+05	3.192-05	1.625-06	1.399-06	1.243-08	2.903-09	6.619-10
18[b]	6.000+04	1.513-05	6.797-07	6.261-07	8.469-11	2.021-11	4.997-12
19	3.000+04	3.884-07	1.743-08	1.621-08	1.081-12	2.573-13	9.486-14
20	2.000+04	3.880-09	1.744-10	1.622-10	2.159-13	5.353-14	1.878-14
	1.000+04[c]						

[a]Multiply by 7.55 x 10^{10} to convert to (photons/cm^2/sec/watt).

[b]Gamma flux densities below 60 KeV may be inaccurate due to the coarse spatial mesh used in the transport calculation.

[c]Lower energy of Group 20.

A.2 PRESSURE VESSEL BENCHMARK FACILITY FOR LWR METALLURGICAL TESTING OF REACTOR PRESSURE VESSEL STEELS (ORR-PSF)

C. A. Baldwin
M. L. Williams
R. E. Maerker

Summary

Integral parameters have been calculated using flux densities from M. L. Williams and R. E. Maerker's Start-up Experiment calculations.[1] These parameters have been incorporated into the ORR-PSF metallurgical Blind Test and are presented here as well.

Accomplishments and Status

A coordinate system has been defined for the ORR-PSF Blind Test and is illustrated in Figure 1. Damage correlation parameters and reaction rates relative to this coordinate system are presented in Tables 5 through 8.

Expected Accomplishments in the Next Reporting Period

Integral parameters for the 1/4T left and 1/4T right positions will be calculated and reported.

REFERENCES

(Wi82) 1. M. L. Williams and R. E. Maerker, "Calculations of the Startup Experiments at the Poolside Facility," Proceedings of the Fourth ASTM-EURATOM Symposium on Reactor Dosimetry, Radiation Metrology Techniques, Data Bases, and Standardization, Volume I, NUREG/CP-0029, National Bureau of Standards (July 1982).

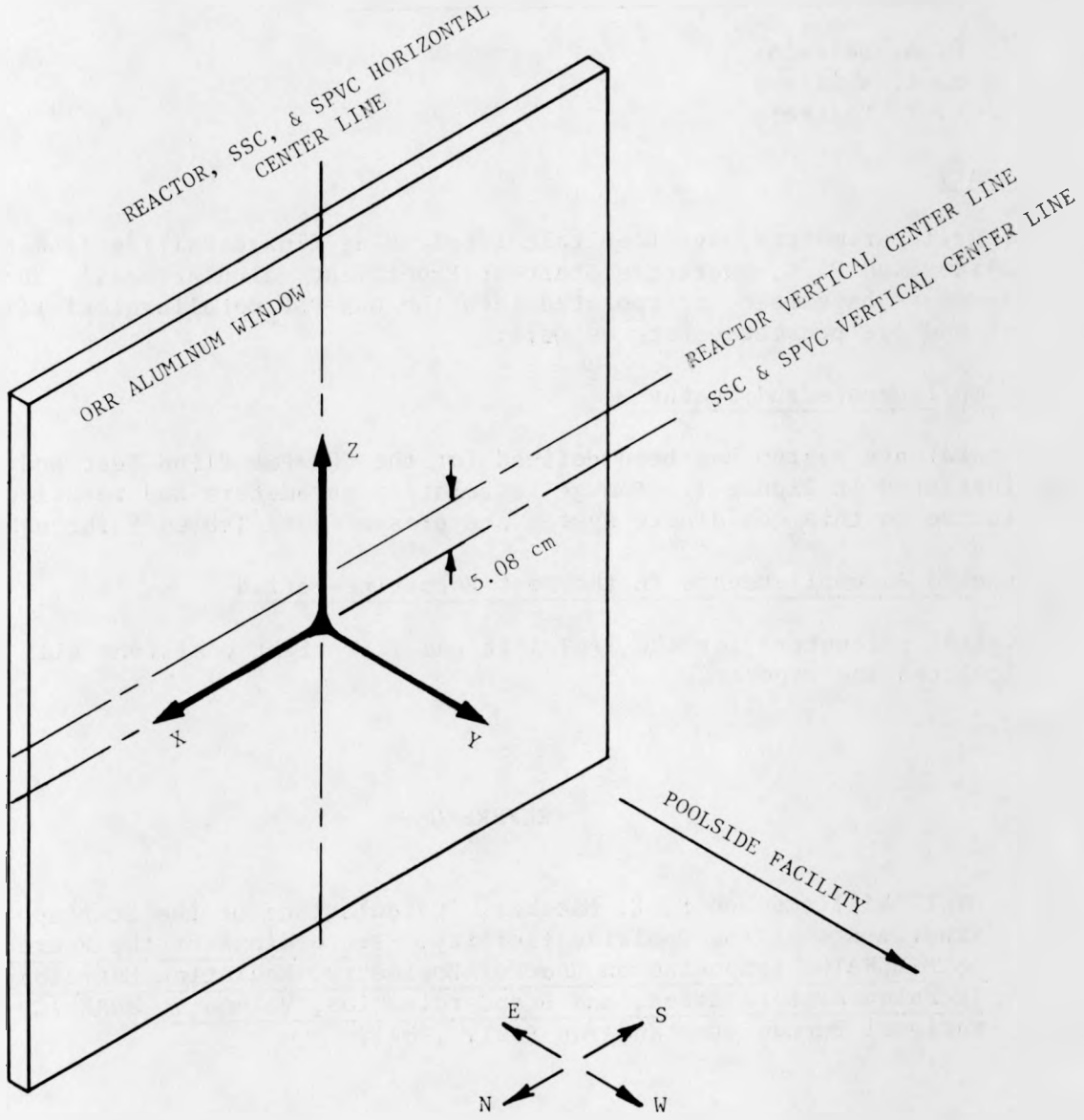

FIGURE ORNL-1. Coordinate System for ORR-PSF Blind Test.

TABLE ORNL-5

DAMAGE CORRELATION PARAMETERS AND REACTION RATES FOR ALUMINUM WINDOW AND SIMULATED SURVEILLANCE CAPSULE POSITIONS AT ORR POWER OF 30 MW

Coordinates			Damage correlation parameters			Reaction rates (reactions/sec/target atom)					
x	y	z	Fluence rate	Fluence rate	dpa	^{237}Np (n,f)	^{238}U (n,f)	^{46}Ti (n,p)	^{54}Fe (n,p)	^{58}Ni (n,p)	^{63}Cu (n,α)
(cm)	(cm)	(cm)	>1.0 MeV	>0.1 MeV	sec	F.P.	F.P.	^{46}Sc	^{54}Mn	^{58}Co	^{60}Co
0.00	-0.70	16.51	5.649+13	1.123+14	7.698-08	1.217-10	2.339-11	7.430-13	5.631-12	7.369-12	3.688-14
0.00	-0.70	11.43	6.675+13	1.328+14	9.097-08	1.439-10	2.763-11	8.753-13	6.643-12	8.695-12	4.339-14
0.00	-0.70	6.35	7.518+13	1.496+14	1.025-07	1.621-10	3.111-11	9.831-13	7.472-12	9.781-12	4.869-14
0.00	-0.70	1.27	8.046+13	1.602+14	1.097-07	1.735-10	3.329-11	1.051-12	7.991-12	1.046-11	5.200-14
0.00	-0.70	-1.27	8.167+13	1.626+14	1.113-07	1.761-10	3.379-11	1.066-12	8.108-12	1.061-11	5.274-14
0.00	-0.70	-6.35	8.104+13	1.614+14	1.104-07	1.747-10	3.352-11	1.056-12	8.040-12	1.053-11	5.225-14
0.00	-0.70	-11.43	7.596+13	1.513+14	1.035-07	1.638-10	3.141-11	9.888-13	7.530-12	9.858-12	4.891-14
0.00	-0.70	-16.51	6.652+13	1.326+14	9.065-08	1.435-10	2.750-11	8.657-13	6.589-12	8.628-12	4.284-14
0.00	13.30	16.19	4.254+12	1.257+13	6.405-09	1.107-11	1.498-12	3.696-14	2.860-13	3.846-13	2.006-15
0.00	13.30	11.43	5.144+12	1.582+13	7.854-09	1.364-11	1.778-12	4.188-14	3.291-13	4.443-13	2.265-15
0.00	13.30	6.35	5.743+12	1.782+13	8.801-09	1.529-11	1.980-12	4.630-14	3.649-13	4.929-13	2.500-15
0.00	13.30	1.27	6.086+12	1.890+13	9.330-09	1.620-11	2.097-12	4.902-14	3.865-13	5.222-13	2.645-15
0.00	13.30	-1.27	6.149+12	1.909+13	9.424-09	1.637-11	2.120-12	4.954-14	3.907-13	5.278-13	2.672-15
0.00	13.30	-6.35	6.037+12	1.866+13	9.235-09	1.604-11	2.083-12	4.873-14	3.842-13	5.190-13	2.628-15
0.00	13.30	-11.43	5.561+12	1.699+13	8.467-09	1.470-11	1.927-12	4.550-14	3.575-13	4.825-13	2.458-15
0.00	13.30	-16.19	4.620+12	1.358+13	6.942-09	1.199-11	1.630-12	4.029-14	3.118-13	4.191-13	2.184-15

TABLE ORNL-6

DAMAGE CORRELATION PARAMETERS AND REACTION RATES FOR PRESSURE VESSEL SURFACE AND PRESSURE VESSEL 0-T POSITIONS AT ORR POWER OF 30 MW

ORNL DWG 83-12856

Coordinates			Damage correlation parameters			Reaction rates (reactions/sec/target atom)					
			Fluence	Fluence		^{237}Np	^{238}U	^{46}Ti	^{54}Fe	^{58}Ni	^{63}Cu
x	y	z	rate	rate	dpa	(n,f)	(n,f)	(n,p)	(n,p)	(n,p)	(n,α)
(cm)	(cm)	(cm)	>1.0 MeV	>0.1 MeV	sec	F.P.	F.P.	^{46}Sc	^{54}Mn	^{58}Co	^{60}Co
0.00	22.12	16.19	7.075+11	1.890+12	1.057-09	1.712-12	2.756-13	9.365-15	6.206-14	8.185-14	5.566-16
0.00	22.12	11.43	7.680+11	2.134+12	1.161-09	1.891-12	2.949-13	9.683-15	6.479-14	8.568-14	5.767-16
0.00	22.12	6.35	8.312+11	2.334+12	1.261-09	2.055-12	3.182-13	1.038-14	6.955-14	9.204-14	6.188-16
0.00	22.12	1.27	8.707+11	2.445+12	1.321-09	2.153-12	3.333-13	1.087-14	7.282-14	9.636-14	6.480-16
0.00	22.12	-1.27	8.753+11	2.454+12	1.327-09	2.163-12	3.353-13	1.096-14	7.333-14	9.702-14	6.533-16
0.00	22.12	-6.35	8.564+11	2.387+12	1.295-09	2.111-12	3.285-13	1.075-14	7.195-14	9.519-14	6.413-16
0.00	22.12	-11.43	7.932+11	2.176+12	1.193-09	1.943-12	3.055-13	1.010-14	6.737-14	8.906-14	6.024-16
0.00	22.12	-16.19	6.940+11	1.826+12	1.031-09	1.669-12	2.713-13	9.296-15	6.135-14	8.088-14	5.539-16
0.00	23.97	16.19	6.065+11	1.785+12	9.291-10	1.543-12	2.250-13	6.949-15	4.714-14	6.269-14	4.142-16
0.00	23.97	11.43	6.593+11	2.030+12	1.026-09	1.713-12	2.404-13	7.138-15	4.896-14	6.534-14	4.263-16
0.00	23.97	6.35	7.103+11	2.215+12	1.111-09	1.856-12	2.581-13	7.606-15	5.226-14	6.979-14	4.545-16
0.00	23.97	1.27	7.419+11	2.314+12	1.161-09	1.939-12	2.696-13	7.942-15	5.457-14	7.287-14	4.747-16
0.00	23.97	-1.27	7.464+11	2.324+12	1.167-09	1.949-12	2.713-13	7.999-15	5.494-14	7.337-14	4.781-16
0.00	23.97	-6.35	7.289+11	2.252+12	1.136-09	1.897-12	2.654-13	7.847-15	5.386-14	7.190-14	4.691-16
0.00	23.97	-11.43	6.764+11	2.050+12	1.046-09	1.746-12	2.475-13	7.391-15	5.059-14	6.748-14	4.420-16
0.00	23.97	-16.19	5.936+11	1.719+12	9.035-10	1.501-12	2.209-13	6.863-15	4.643-14	6.173-14	4.097-16

TABLE ORNL-7

DAMAGE CORRELATION PARAMETERS AND REACTION RATES FOR PRESSURE VESSEL
1/4T and 1/2T POSITIONS AT ORR POWER OF 30 MW

ORNL DWG 83-12857

Coordinates			Damage correlation parameters			Reaction rates (reactions/sec/target atom)					
x (cm)	y (cm)	z (cm)	Fluence rate >1.0 MeV	Fluence rate >0.1 MeV	dpa sec	^{237}Np (n,f) F.P.	^{238}U (n,f) F.P.	^{46}Ti (n,p) ^{46}Sc	^{54}Fe (n,p) ^{54}Mn	^{58}Ni (n,p) ^{58}Co	^{63}Cu (n,α) ^{60}Co
0.00	28.38	16.19	3.395+11	1.315+12	5.818-10	9.872-13	1.139-13	3.066-15	2.119-14	2.862-14	1.878-16
0.00	28.38	11.43	3.618+11	1.485+12	6.363-10	1.084-12	1.184-13	3.009-15	2.113-14	2.870-14	1.851-16
0.00	28.38	6.35	3.859+11	1.612+12	6.850-10	1.167-12	1.256-13	3.156-15	2.222-14	3.022-14	1.943-16
0.00	28.38	1.27	4.005+11	1.675+12	7.111-10	1.211-12	1.303-13	3.275-15	2.305-14	3.135-14	2.018-16
0.00	28.38	-1.27	4.021+11	1.677+12	7.130-10	1.215-12	1.309-13	3.294-15	2.318-14	3.152-14	2.030-16
0.00	28.38	-6.35	3.923+11	1.618+12	6.917-10	1.179-12	1.280-13	3.237-15	2.275-14	3.092-14	1.996-16
0.00	28.38	-11.43	3.653+11	1.469+12	6.360-10	1.085-12	1.201-13	3.075-15	2.154-14	2.923-14	1.894-16
0.00	28.38	-16.19	3.297+11	1.250+12	5.588-10	9.509-13	1.110-13	2.988-15	2.066-14	2.790-14	1.829-16
0.00	33.52	16.19	1.608+11	8.478+11	3.244-10	5.473-13	4.866-14	1.158-15	8.077-15	1.110-14	7.373-17
0.00	33.52	11.43	1.684+11	9.474+11	3.524-10	5.947-13	4.941-14	1.093-15	7.787-15	1.078-14	7.001-17
0.00	33.52	6.35	1.775+11	1.021+12	3.764-10	6.346-13	5.162-14	1.124-15	8.034-15	1.115-14	7.211-17
0.00	33.52	1.27	1.829+11	1.055+12	3.884-10	6.549-13	5.314-14	1.156-15	8.261-15	1.147-14	7.427-17
0.00	33.52	-1.27	1.833+11	1.054+12	3.886-10	6.554-13	5.330-14	1.161-15	8.294-15	1.151-14	7.463-17
0.00	33.52	-6.35	1.788+11	1.014+12	3.759-10	6.350-13	5.219-14	1.144-15	8.157-15	1.131-14	7.349-17
0.00	33.52	-11.43	1.678+11	9.226+11	3.462-10	5.864-13	4.945-14	1.102-15	7.829-15	1.083-14	7.059-17
0.00	33.52	-16.19	1.552+11	7.934+11	3.075-10	5.216-13	4.720-14	1.125-15	7.854-15	1.079-14	7.141-17

TABLE ORNL-8

DAMAGE CORRELATION PARAMETERS AND REACTION RATES FOR THE PRESSURE VESSEL 3/4T AND VOID BOX POSITIONS AT ORR POWER OF 30 MW

ORNL DWG 83-12858

Coordinates			Damage correlation parameters			Reaction rates (reactions/sec/target atom)					
x (cm)	y (cm)	z (cm)	Fluence rate >1.0 MeV	Fluence rate >0.1 MeV	dpa sec	^{237}Np (n,f) F.P.	^{238}U (n,f) F.P.	^{46}Ti (n,p) ^{46}Sc	^{54}Fe (n,p) ^{54}Mn	^{58}Ni (n,p) ^{58}Co	^{63}Cu (n,α) ^{60}Co
0.00	38.98	16.19	6.841+10	4.728+11	1.634-10	2.718-13	1.884-14	4.036-16	2.816-15	3.937-15	2.684-17
0.00	38.98	11.43	7.077+10	5.206+11	1.760-10	2.922-13	1.886-14	3.735-16	2.666-15	3.764-15	2.501-17
0.00	38.98	6.35	7.370+10	5.560+11	1.865-10	3.090-13	1.942-14	3.757-16	2.697-15	3.819-15	2.524-17
0.00	38.98	1.27	7.541+10	5.712+11	1.913-10	3.170-13	1.983-14	3.827-16	2.747-15	3.892-15	2.574-17
0.00	38.98	-1.27	7.546+10	5.699+11	1.910-10	3.167-13	1.986-14	3.838-16	2.754-15	3.901-15	2.582-17
0.00	38.98	-6.35	7.370+10	5.480+11	1.846-10	3.068-13	1.948-14	3.793-16	2.717-15	3.845-15	2.550-17
0.00	38.98	-11.43	6.975+10	5.009+11	1.707-10	2.847-13	1.868-14	3.722-16	2.653-15	3.742-15	2.492-17
0.00	38.98	-16.19	6.562+10	4.363+11	1.529-10	2.562-13	1.821-14	3.928-16	2.742-15	3.829-15	2.603-17
0.00	70.88	16.51	9.521+09	6.719+10	2.310-11	3.914-14	2.620-15	6.878-17	4.262-16	5.887-16	4.976-18
0.00	70.88	11.43	1.053+10	7.231+10	2.511-11	4.257-14	2.938-15	7.901-17	4.873-16	6.710-16	5.697-18
0.00	70.88	6.35	1.118+10	7.594+10	2.645-11	4.494-14	3.121-15	8.329-17	5.160-16	7.108-16	5.999-18
0.00	70.88	1.27	1.102+10	7.596+10	2.630-11	4.472-14	3.044-15	7.935-17	4.950-16	6.836-16	5.718-18
0.00	70.88	-1.27	1.096+10	7.552+10	2.615-11	4.448-14	3.029-15	7.896-17	4.927-16	6.804-16	5.685-18
0.00	70.88	-6.35	1.091+10	7.385+10	2.576-11	4.378-14	3.052-15	8.157-17	5.059-16	6.966-16	5.857-18
0.00	70.88	-11.43	1.014+10	6.881+10	2.399-11	4.072-14	2.842-15	7.703-17	4.750-16	6.533-16	5.536-18
0.00	70.88	-16.51	9.030+09	6.238+10	2.161-11	3.665-14	2.510-15	6.742-17	4.160-16	5.729-16	4.864-18

A.3 NEUTRON SPECTRAL CHARACTERIZATION CALCULATIONS FOR THE FOURTH NUCLEAR REGULATORY COMMISSION HEAVY SECTION STEEL TECHNOLOGY 1T-CT IRRADIATION EXPERIMENTS

C. A. Baldwin

Summary

In support of the 4th series of NRC-HSST 1T-CT irradiations at the BSR, discrete ordinate neutron transport calculations have been performed. A flux density synthesis technique was used to obtain a three-dimensional flux-density distribution from the combination of two two-dimensional calculations. This technique appears very promising for this type of transport problem and is validated by comparison with experimental data. Comparison of absolute measured and calculated reaction rates indicate agreement to within 15% in most cases. Somewhat larger discrepancies are noted near the bottom of the metallurgical capsules.

Accomplishments and Status

Three-dimensional flux density synthesis calculations have been completed for the 4th series of NRC-HSST experiments at the BSR. A flow diagram of the calculational methodology is shown in Figure 2. This procedure is very similar to that used by R. E. Maerker and M. L. Williams for their Westinghouse Perturbation Experiment Calculations.[1] First, a three-dimensional diffusion theory calculation is performed to calculate a fission source distribution in the BSR core. The source distribution is then integrated over the appropriate directions to produce two-dimensional source distributions for two fixed source discrete ordinate transport calculations. The transport calculations model the core and experiment in the XY and YZ planes. The resulting calculated differential flux densities are combined in a synthesis program to produce differential flux densities at any location in the experiment. The synthesized differential flux densities are then folded with differential dosimetry cross-section data to produce reaction rates for comparisons with experiment.

Absolute comparisons of unadjusted calculations with iron gradient wire measurements are illustrated in Figs. 3 and 4 for capsules A and B respectively. The comparison shows that the $^{54}Fe(n,p)^{54}Mn$ reaction rates are in general predicted to within ±5% for the upper three-fifths of the specimens while an over prediction of 15 to 40% is observed for the lower two-fifths of the specimens at the plane of the 1T-CT specimen notch tips. The beginning-of-cycle (BOC) fission source distribution that was used is probably responsible for the high C/E ratios for the bottom two-fifths of the experiment. The BOC rod positions change significantly during the first two days of the BSR fuel cycle as Xe equilibrium is established.

Control rods 1 through 4, initally at 9.19 inches withdrawn for BOC and Xe free conditions are approximately 14 inches withdrawn after two days when Xe equilibrium is established. Thereafter rods 1 through 4 are withdrawn approximately 0.05 inches per day for the remainder of the two-month fuel cycle. With the rods further withdrawn from the core, the peak axial flux density would shift toward the midplane and away from the bottom of the core.

Ratios of different reaction rates at the same location can be used to uncover spectral biases in the calculated flux density spectra. This method of comparison effectively eliminates absolute magnitude differences while preserving spectral information. Tables 9 through 11 show calculated and experimental reaction rate ratios and a C/E comparison of the ratios. In these tables, the $^{54}Fe(n,p)^{54}Mn$ reaction (threshold energy 2.2 MeV)[2] has been chosen as the reference reaction rate. It can be seen that the reaction rate ratios with a reaction in the numerator that has a higher threshold energy than the reference [$^{63}Cu(n,\alpha)^{60}Co$ (6.1 MeV), $^{46}Ti(n,p)^{46}Sc$ (5.5 MeV), and $^{58}Ni(n,p)^{58}Co$ (2.9 MeV)] are under predicted relative to experimental values while reaction rate ratios with a reaction in the numerator that has a lower threshold energy than the reference [$^{238}U(n,f)$F.P. (1.45 MeV) and $^{237}Np(n,f)$F.P. (0.5 MeV)] are over predicted relative to experimental values. This indicates that the calculated spectra has under predicted high energy neutrons and over predicted low energy neutrons. This same trend was observed with the PCA-PVF Blind Test results,[3] and, as yet no certain cause for this phenomenon has been identified.

Expected Accomplishments in the Next Reporting Period

A final report giving details of the synthesis calculations and comparisons with experiment will be completed.[4]

REFERENCES

(Ma82e) 1. R. E. Maerker and M. L. Williams, "Calculations of the Westinghouse Perturbation Experiment at the Poolside Facility," Proceedings of the Fourth ASTM-EURATOM Symposium on Reactor Dosimetry, Radiation Metrology Techniques, Data Bases, and Standardization, Volume I, NUREG/CP-0029, National Bureau of Standards (July 1982).

(As79a) 2. American Society for Testing and Materials, 1979 Annual Book of ASTM Standards, Part 45, Nuclear Standards, p. 999 (1979).

(Mc81g) 3. W. N. McElroy, E. P. Lippincott, A. Fabry, F. W. Stallmann, and F. B. K. Kam, "7.0 Overview Analysis of Neutronic Calculations and Measurements," LWR Pressure Vessel Surveillance Dosimetry Improvement Program: PCA Experiments and Blind Test, HEDL-TME 80-87, Hanford Engineering Development Laboratory (July 1981).

(Ba83) 4. C. A. Baldwin, Neutron Spectral Characterization Calculations for the Fourth Nuclear Regulatory Commission Heavy Section Steel Technology 1T-CT Irradiation Experiments, NUREG/CR-3311, ORNL/TM-8782, June 1983.

ORNL-DWG-83-7952R

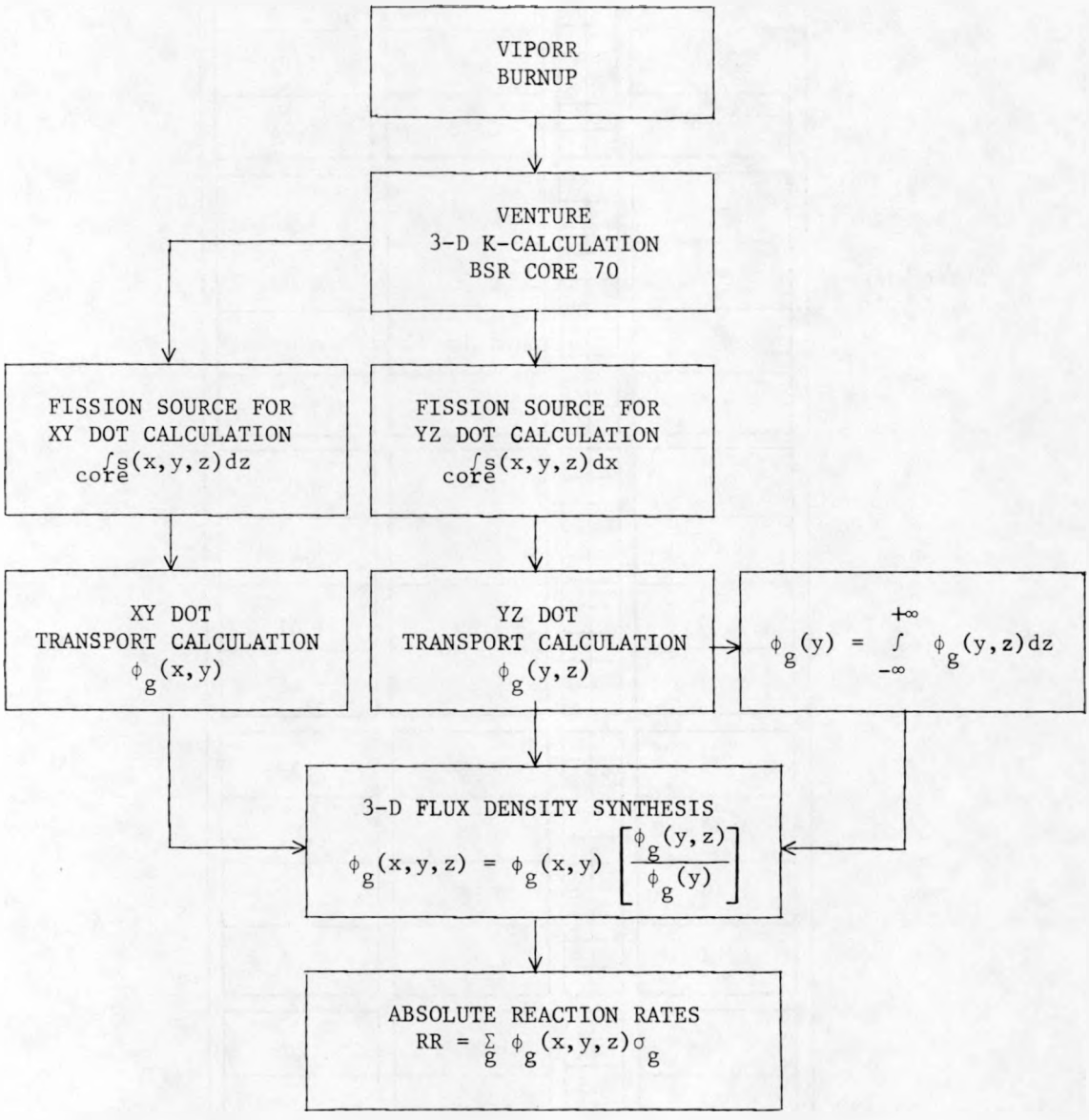

FIGURE ORNL-2. Three-Dimensional Flux Density Synthesis Procedure.

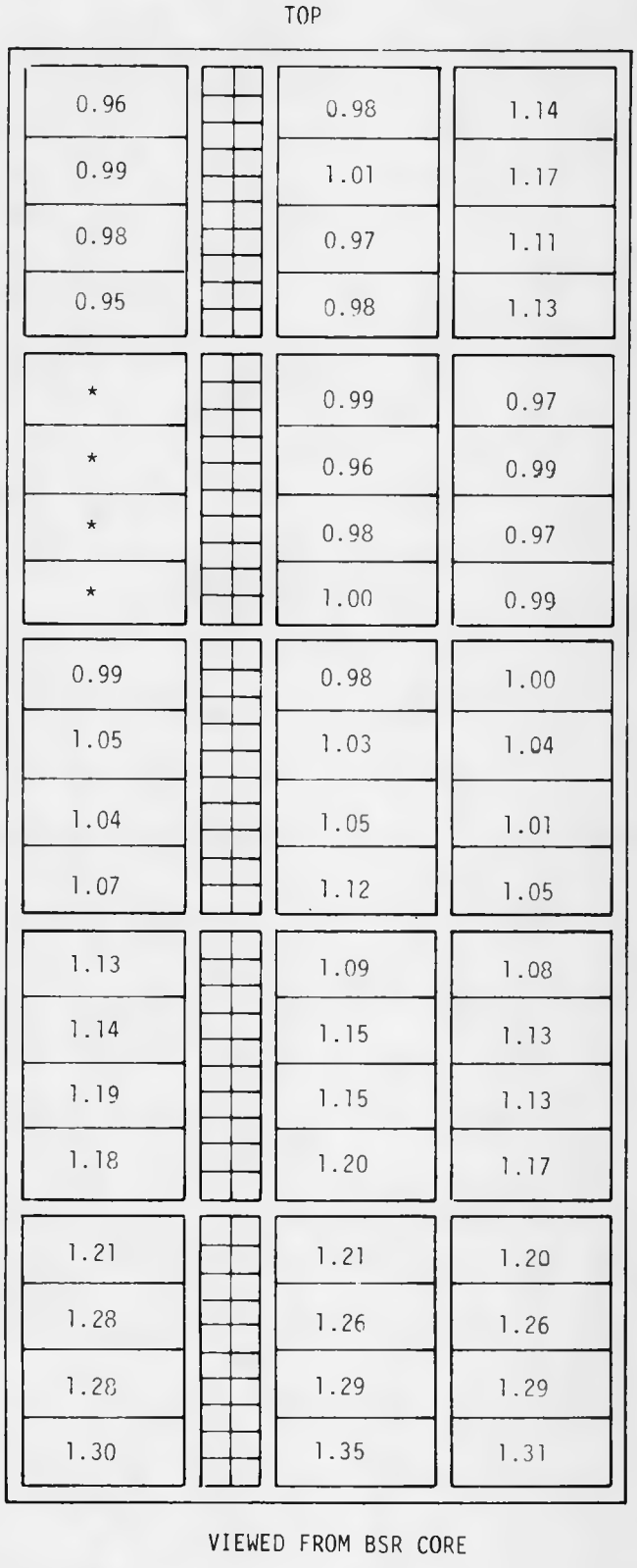

*Short Wire (3,2) Lost

FIGURE ORNL-3. Absolute $^{54}Fe(n,p)^{54}Mn$ Reaction C/E Ratios for Short-Wire Segments in BSR-HSST-4 Capsule A.

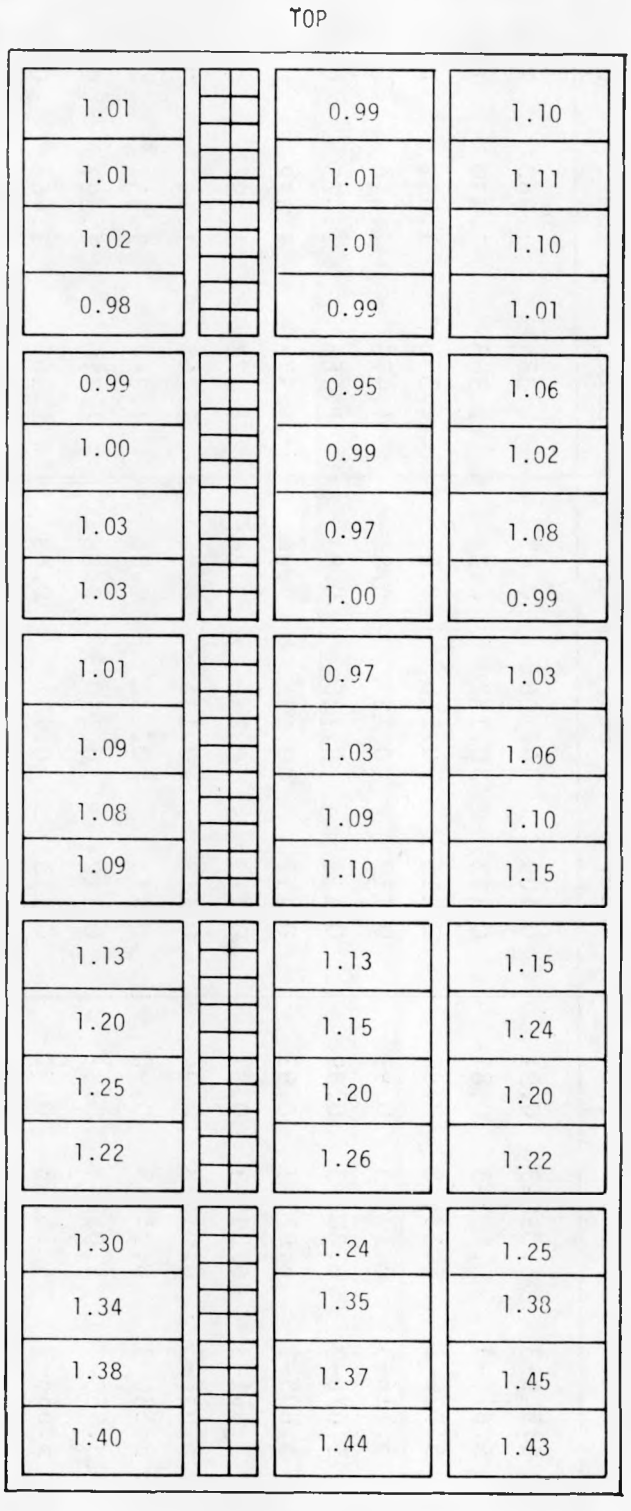

FIGURE ORNL-4. Absolute $^{54}Fe(n,p)^{54}Mn$ Reaction C/E Ratios for Short-Wire Segments in BSR-HSST-4 Capsule B.

TABLE ORNL-9

ORNL DWG 83-12859

REACTION RATE RATIOS FOR BSR-HSST-4 CAPSULE A

Monitor ID	$^{63}Cu(n,\alpha)^{60}Co/^{54}Fe(n,p)^{54}Mn$			$^{46}Ti(n,p)^{46}Sc/^{54}Fe(n,p)^{54}Mn$			$^{58}Ni(n,p)^{58}Co/^{54}Fe(n,p)^{54}Mn$		
	Calc.	Exp.	C/E	Calc.	Exp.	C/E	Calc.	Exp.	C/E
F01	5.549-3	6.090-3	0.91	0.109	0.126	0.87	1.385	1.362	1.02
F02	5.616-3	6.425-3	0.87	0.113	0.132	0.86	1.366	1.330	1.03
F03	5.728-3	6.384-3	0.90	0.116	0.136	0.85	1.355	1.381	0.98
NF1	5.716-3	6.172-3	0.93	0.112	0.131	0.86	1.375	1.416	0.97
NF2	5.676-3	6.383-3	0.89	0.113	0.136	0.83	1.366	1.425	0.96
NF3	5.605-3	6.017-3	0.93	0.112	0.131	0.86	1.372	1.422	0.96
NF4	5.561-3	6.393-3	0.87	0.112	0.130	0.86	1.372	1.388	0.99
NF5	5.658-3	6.014-3	0.94	0.113	0.135	0.84	1.368	1.467	0.93
NF6	5.630-3	6.246-3	0.90	0.113	0.132	0.86	1.364	1.357	1.01
NF7	5.558-3	6.042-3	0.92	0.112	0.130	0.86	1.370	1.397	0.98
NF8	5.653-3	6.151-3	0.92	0.113	0.137	0.83	1.365	1.465	0.93
NF9	5.686-3	6.542-3	0.87	0.113	0.134	0.84	1.369	1.435	0.95

TABLE ORNL-10

ORNL DWG 83-12860

REACTION RATE RATIOS FOR BSR-HSST-4 CAPSULE B

Monitor ID	$^{63}Cu(n,\alpha)^{60}Co/^{54}Fe(n,p)^{54}Mn$			$^{46}Ti(n,p)^{46}Sc/^{54}Fe(n,p)^{54}Mn$			$^{58}Ni(n,p)^{58}Co/^{54}Fe(n,p)^{54}Mn$		
	Calc.	Exp.	C/E	Calc.	Exp.	C/E	Calc.	Exp.	C/E
F04	5.572-3	6.203-3	0.90	0.109	0.136	0.80	1.386	1.363	1.02
NF14	5.755-3	6.453-3	0.89	0.114	0.133	0.86	1.364	1.404	0.97
F06	5.722-3	6.532-3	0.88	0.115	0.137	0.84	1.356	1.356	1.00
F05	5.788-3	6.339-3	0.91	0.113	0.128	0.88	1.374	1.377	1.00
NF10	5.849-3	6.452-3	0.91	0.115	0.134	0.86	1.364	1.417	0.96
MQ7	5.624-3	6.365-3	0.88	0.112	0.132	0.85	1.371	1.485	0.92
MF6	5.561-3	6.237-3	0.89	0.112	0.129	0.87	1.372	1.462	0.94
NF13	5.691-3	6.519-3	0.87	0.113	0.132	0.86	1.368	1.346	1.02
NF15	5.762-3	6.835-3	0.84	0.115	0.134	0.85	1.362	1.398	0.97
MF5	5.537-3	6.453-3	0.86	0.112	0.129	0.87	1.369	1.460	0.94
NF17	5.666-3	6.111-3	0.93	0.113	0.134	0.85	1.366	1.356	1.01
MQ4	5.692-3	6.578-3	0.87	0.113	0.131	0.86	1.369	1.452	0.94

TABLE ORNL-11

FISSION RATE RATIOS FOR BSR-HSST-4 CAPSULES A AND B

ORNL DWG 83-12861

Capsule	Monitor ID	$^{238}U(n,f)F.P./^{54}Fe(n,p)^{54}Mn$			$^{237}Np(n,f)F.P./^{54}Fe(n,p)^{54}Mn$		
		Calc.	Exp.	C/E	Calc.	Exp.	C/E
A	F01	6.45	6.29	1.03	63.7	52.1	1.22
	F02	5.92	5.54	1.07	48.4	40.4	1.20
	F03	5.57	5.54	1.01	42.1	37.9	1.11
B	F04	6.49	5.60	1.16	64.5	50.0	1.29
	F05	6.13	5.97	1.03	54.7	46.9	1.17
	F06	5.59	5.91	0.95	42.4	36.1	1.17
	MF5	6.02	5.89	1.02	49.9	42.9	1.16
	MF6	6.09	5.91	1.03	52.0	44.8	1.16

A.4 DOSIMETRY ANALYSIS AND THREE-DIMENSIONAL MAP OF DAMAGE EXPOSURE PARAMETER VALUES IN THE FOURTH NRC-HSST 1T-CT IRRADIATION EXPERIMENT

F. W. Stallmann

Summary

The dosimetry results and neutron transport calculations for the fourth HSST irradiation experiments were combined in the LSL spectrum adjustment method to obtain best estimates and uncertainties for the damage exposure parameter values $\phi > 1.0$ MeV, $\phi > 0.1$ MeV, and dpa. The values can be accurately fitted to a cosine-exponential three-dimensional map from which the damage exposure of individual metallurgical specimens can be determined.

Accomplishments and Status

A methodology for dosimetry analysis in material test reactors has been developed. A flow diagram of this methodology is shown in Figure 5. The procedure consists of two separate steps. First a spectrum adjustment method is applied to a combination of calculated and measured reaction rates in order to determine what corrections, if any, to the calculated spectrum need to be made. This adjustment is done "globally", that is calculated and measured values from all multiple foil measurements are processed simultaneously, resulting in an adjustment to the calculated ratios of $\phi > 1.0/^{54}Fe(n,p)$, $\phi > 0.1/^{54}Fe(n,p)$, and $dpa/^{54}Fe(n,p)$ which is common to every location in all 4 metallurgical capsules. The uncertainties in these ratios are also "global" so that any error in the adjusted values applies equally to the damage exposure parameter values at every location.

The three-dimensional maps of exposure parameter values are then obtained from the adjusted ratios times the measured $^{54}Fe(n,p)$ reaction rates from the gradient wires, which are located near the critical positions of the metallurgical specimen. These values can be fitted to a cosine-exponential model with cosine distributions along the two axis parallel to the core and an exponential attenuation along the axis perpendicular to the core. Local errors from local perturbations of the calculation, as well as, local measuring, and fitting errors must be combined with global errors to determine the uncertainties of the final estimates for the damage parameter values.

The final damage parameter values for each of the metallurgical specimens in all four capsules are listed in Tables 12 - 19. The global uncertainties are in the order of ±4% to ±6% relative standard deviation with local uncertainties in the order of ±3% to ±5% where the smaller values apply to the capsule centers and the larger ones to locations near the edges. These tables supersede the preliminary values in Reference 1.

Expected Accomplishments in the Next Reporting Period

A final report on the dosimetry analysis and three-dimensional damage parameter maps is being prepared and will be published soon in an ORNL/TM report.

REFERENCES

(Ka82) 1. F. B. K. Kam et al., "Neutron Exposure Parameters for the Fourth HSST Series of Metallurgical Irradiation Capsules," Proceedings of the Fourth ASTM-EURATOM Symposium on Reactor Dosimetry, Volume II, NUREG/CP-0029, National Bureau of Standards, p. 1023 (1982).

ORNL DWG 83-12862

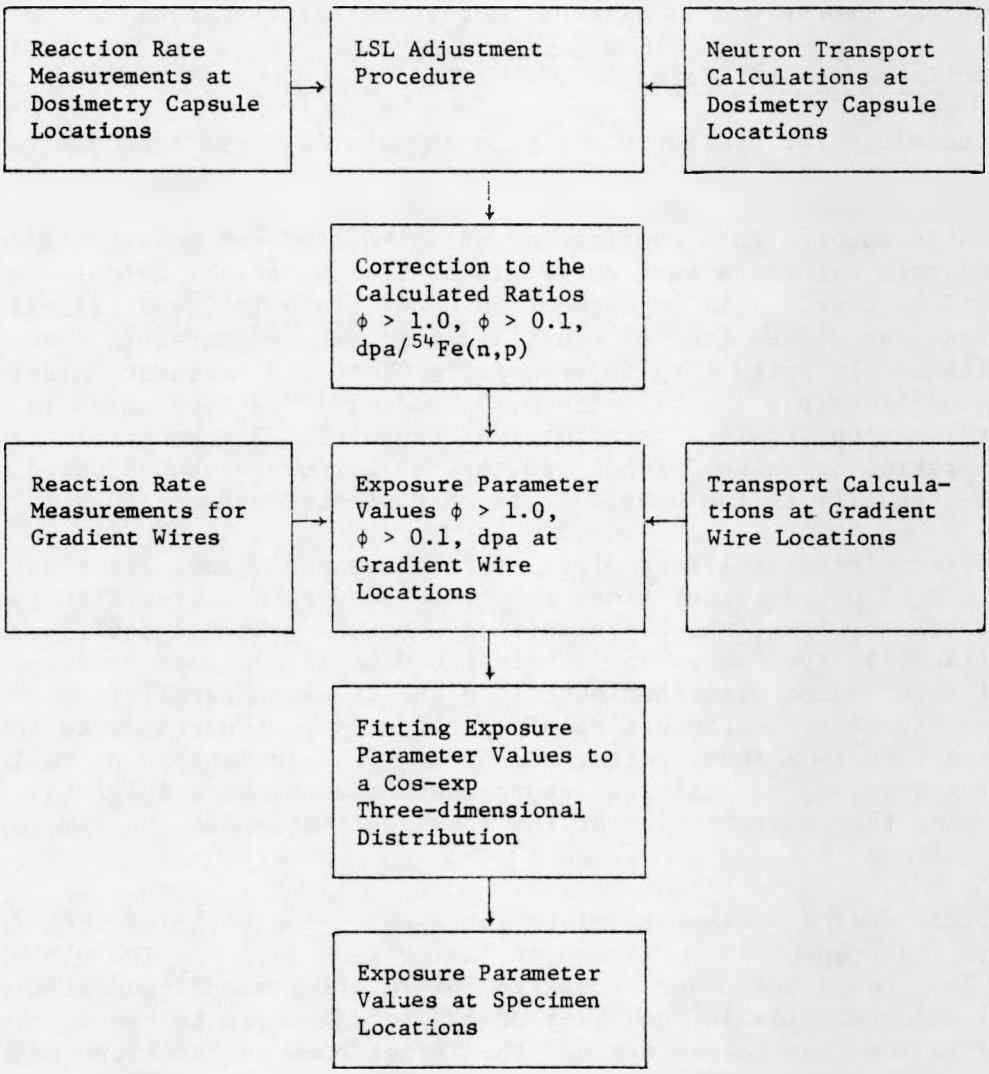

FIGURE ORNL-5. Methodology for Determining Exposure Parameter Values and Uncertainties.

TABLE ORNL-12

BSR-HSST-4 CAPSULE A PARAMETERS FOR COMPACT TENSION (IT-CT) SPECIMENS

ORNL DWG 83-12863

Specimen number	Damage exposure parameters			Specimen number	Damage exposure parameters			Specimen number	Damage exposure parameters		
	Fluence >1.0 MeV	Fluence >0.1 MeV	dpa (ASTM)		Fluence >1.0 MeV	Fluence >0.1 MeV	dpa (ASTM)		Fluence >1.0 MeV	Fluence >0.1 MeV	dpa (ASTM)
1	9.55+18	3.20+19	1.49-2	21	1.00+19	3.47+19	1.58-2	141	8.13+18	2.79+19	1.28-2
2	1.21+19	4.09+19	1.89-2	22	1.26+19	4.44+19	2.00-2	142	1.03+19	3.56+19	1.62-2
3	1.44+19	4.92+19	2.27-2	23	1.51+19	5.35+19	2.40-2	143	1.23+19	4.29+19	1.95-2
4	1.66+19	5.70+19	2.61-2	24	1.74+19	6.19+19	2.77-2	144	1.41+19	4.96+19	2.24-2
5	1.91+19	6.58+19	3.01-2	25	2.00+19	7.15+19	3.19-2	145	1.63+19	5.73+19	2.59-2
6	2.08+19	7.19+19	3.29-2	26	2.18+19	7.80+19	3.48-2	146	1.77+19	6.26+19	2.82-2
7	2.23+19	7.70+19	3.52-2	27	2.34+19	8.36+19	3.73-2	147	1.90+19	6.71+19	3.02-2
8	2.36+19	8.12+19	3.71-2	28	2.47+19	8.82+19	3.93-2	148	2.00+19	7.07+19	3.19-2
9	2.47+19	8.51+19	3.89-2	29	2.59+19	9.24+19	4.12-2	149	2.10+19	7.41+19	3.34-2
10	2.53+19	8.70+19	3.98-2	30	2.65+19	9.44+19	4.22-2	150	2.15+19	7.57+19	3.42-2
11	2.56+19	8.78+19	4.02-2	31	2.68+19	9.53+19	4.26-2	151	2.18+19	7.64+19	3.45-2
12	2.56+19	8.75+19	4.02-2	32	2.68+19	9.49+19	4.25-2	152	2.18+19	7.62+19	3.45-2
13	2.52+19	8.55+19	3.94-2	33	2.64+19	9.28+19	4.17-2	153	2.14+19	7.45+19	3.38-2
14	2.45+19	8.28+19	3.82-2	34	2.57+19	8.99+19	4.05-2	154	2.08+19	7.21+19	3.28-2
15	2.36+19	7.90+19	3.66-2	35	2.47+19	8.58+19	3.88-2	155	2.00+19	6.88+19	3.15-2
16	2.23+19	7.43+19	3.46-2	36	2.34+19	8.07+19	3.67-2	156	1.90+19	6.47+19	2.97-2
17	2.04+19	6.70+19	3.14-2	37	2.14+19	7.27+19	3.33-2	157	1.74+19	5.83+19	2.70-2
18	1.86+19	6.03+19	2.85-2	38	1.95+19	6.54+19	3.02-2	158	1.58+19	5.25+19	2.45-2
19	1.66+19	5.28+19	2.52-2	39	1.74+19	5.73+19	2.67-2	159	1.41+19	4.60+19	2.17-2
20	1.44+19	4.47+19	2.17-2	40	1.51+19	4.85+19	2.30-2	160	1.23+19	3.89+19	1.86-2

TABLE ORNL-13

BSR-HSST-4 CAPSULE A PARAMETERS FOR CHARPY SPECIMENS

Specimen number	Damage exposure parameters			Specimen number	Damage exposure parameters		
	Fluence >1.0 MeV	Fluence >0.1 MeV	dpa (ASTM)		Fluence >1.0 MeV	Fluence >0.1 MeV	dpa (ASTM)
41	8.00+18	2.86+19	1.28-2	42	7.83+18	2.80+19	1.25-2
43	8.90+18	3.21+19	1.43-2	44	8.72+18	3.14+19	1.40-2
45	9.79+18	3.55+19	1.57-2	46	9.59+18	3.47+19	1.54-2
47	1.07+19	3.88+19	1.72-2	48	1.04+19	3.79+19	1.68-2
49	1.15+19	4.20+19	1.86-2	50	1.13+19	4.11+19	1.82-2
51	1.23+19	4.52+19	1.99-2	52	1.21+19	4.42+19	1.95-2
53	1.32+19	4.83+19	2.13-2	54	1.29+19	4.72+19	2.08-2
55	1.39+19	5.13+19	2.25-2	56	1.36+19	5.01+19	2.21-2
57	1.47+19	5.42+19	2.38-2	58	1.44+19	5.29+19	2.33-2
59	1.54+19	5.69+19	2.50-2	60	1.51+19	5.57+19	2.44-2
61	1.67+19	6.18+19	2.71-2	62	1.64+19	6.04+19	2.65-2
63	1.74+19	6.42+19	2.81-2	64	1.70+19	6.28+19	2.75-2
65	1.80+19	6.66+19	2.91-2	66	1.76+19	6.51+19	2.85-2
67	1.86+19	6.88+19	3.01-2	68	1.82+19	6.72+19	2.94-2
69	1.91+19	7.09+19	3.10-2	70	1.87+19	6.93+19	3.03-2
71	1.97+19	7.28+19	3.18-2	72	1.92+19	7.12+19	3.12-2
73	2.01+19	7.46+19	3.26-2	74	1.97+19	7.29+19	3.19-2
75	2.06+19	7.63+19	3.33-2	76	2.02+19	7.45+19	3.26-2
77	2.10+19	7.78+19	3.40-2	78	2.06+19	7.60+19	3.33-2
79	2.14+19	7.91+19	3.46-2	80	2.09+19	7.74+19	3.39-2
81	2.20+19	8.13+19	3.55-2	82	2.15+19	7.94+19	3.48-2
83	2.22+19	8.22+19	3.60-2	84	2.18+19	8.03+19	3.52-2
85	2.25+19	8.29+19	3.63-2	86	2.20+19	8.11+19	3.55-2
87	2.26+19	8.35+19	3.66-2	88	2.22+19	8.17+19	3.58-2
89	2.28+19	8.40+19	3.68-2	90	2.23+19	8.21+19	3.60-2
91	2.29+19	8.43+19	3.69-2	92	2.24+19	8.24+19	3.62-2
93	2.29+19	8.44+19	3.70-2	94	2.25+19	8.25+19	3.62-2
95	2.30+19	8.44+19	3.70-2	96	2.25+19	8.25+19	3.62-2
97	2.29+19	8.42+19	3.70-2	98	2.25+19	8.23+19	3.62-2
99	2.29+19	8.38+19	3.68-2	100	2.24+19	8.19+19	3.60-2
101	2.27+19	8.27+19	3.64-2	102	2.22+19	8.08+19	3.56-2
103	2.25+19	8.19+19	3.61-2	104	2.20+19	8.00+19	3.53-2
105	2.23+19	8.09+19	3.57-2	106	2.18+19	7.91+19	3.49-2
107	2.20+19	7.98+19	3.53-2	108	2.15+19	7.80+19	3.45-2
109	2.17+19	7.85+19	3.47-2	110	2.12+19	7.67+19	3.40-2
111	2.14+19	7.71+19	3.42-2	112	2.09+19	7.53+19	3.34-2
113	2.10+19	7.55+19	3.35-2	114	2.05+19	7.38+19	3.28-2
115	2.06+19	7.37+19	3.28-2	116	2.01+19	7.21+19	3.21-2
117	2.01+19	7.19+19	3.20-2	118	1.97+19	7.03+19	3.13-2
119	1.96+19	6.99+19	3.12-2	120	1.92+19	6.83+19	3.05-2
121	1.86+19	6.58+19	2.95-2	122	1.82+19	6.43+19	2.89-2
123	1.80+19	6.34+19	2.85-2	124	1.77+19	6.20+19	2.79-2
125	1.74+19	6.09+19	2.75-2	126	1.70+19	5.96+19	2.69-2
127	1.68+19	5.83+19	2.64-2	128	1.64+19	5.70+19	2.58-2
129	1.61+19	5.56+19	2.53-2	130	1.57+19	5.44+19	2.47-2
131	1.54+19	5.28+19	2.41-2	132	1.51+19	5.16+19	2.35-2
133	1.46+19	4.98+19	2.28-2	134	1.43+19	4.87+19	2.23-2
135	1.39+19	4.68+19	2.16-2	136	1.36+19	4.58+19	2.11-2
137	1.31+19	4.37+19	2.02-2	138	1.28+19	4.27+19	1.98-2
139	1.23+19	4.05+19	1.89-2	140	1.20+19	3.96+19	1.85-2

TABLE ORNL-14

BSR-HSST-4 CAPSULE B PARAMETERS FOR COMPACT TENSION (IT-CT) SPECIMENS

ORNL DWG 83-12865

Specimen number	Damage exposure parameters			Specimen number	Damage exposure parameters			Specimen number	Damage exposure parameters		
	Fluence >1.0 MeV	Fluence >0.1 MeV	dpa (ASTM)		Fluence >1.0 MeV	Fluence >0.1 MeV	dpa (ASTM)		Fluence >1.0 MeV	Fluence >0.1 MeV	dpa (ASTM)
1	5.90+18	1.99+19	9.21-3	21	7.01+18	2.45+19	1.12-2	141	5.72+18	1.97+19	8.98-3
2	7.45+18	2.54+19	1.17-2	22	8.86+18	3.13+19	1.42-2	142	7.22+18	2.52+19	1.14-2
3	8.91+18	3.06+19	1.40-2	23	1.06+19	3.77+19	1.70-2	143	8.65+18	3.03+19	1.37-2
4	1.03+19	3.54+19	1.62-2	24	1.22+19	4.36+19	1.97-2	144	9.97+18	3.51+19	1.58-2
5	1.18+19	4.09+19	1.87-2	25	1.41+19	5.03+19	2.27-2	145	1.15+19	4.05+19	1.82-2
6	1.29+19	4.46+19	2.04-2	26	1.53+19	5.50+19	2.48-2	146	1.25+19	4.43+19	1.99-2
7	1.38+19	4.78+19	2.19-2	27	1.64+19	5.89+19	2.65-2	147	1.34+19	4.74+19	2.13-2
8	1.46+19	5.04+19	2.31-2	28	1.73+19	6.21+19	2.80-2	148	1.42+19	5.00+19	2.25-2
9	1.53+19	5.29+19	2.42-2	29	1.82+19	6.51+19	2.94-2	149	1.49+19	5.24+19	2.36-2
10	1.57+19	5.40+19	2.48-2	30	1.87+19	6.65+19	3.01-2	150	1.52+19	5.36+19	2.42-2
11	1.59+19	5.45+19	2.51-2	31	1.89+19	6.72+19	3.04-2	151	1.54+19	5.41+19	2.44-2
12	1.59+19	5.44+19	2.50-2	32	1.89+19	6.70+19	3.03-2	152	1.54+19	5.39+19	2.44-2
13	1.56+19	5.32+19	2.46-2	33	1.86+19	6.55+19	2.98-2	153	1.52+19	5.27+19	2.39-2
14	1.52+19	5.15+19	2.39-2	34	1.81+19	6.34+19	2.89-2	154	1.48+19	5.11+19	2.33-2
15	1.46+19	4.92+19	2.29-2	35	1.74+19	6.06+19	2.77-2	155	1.42+19	4.88+19	2.23-2
16	1.39+19	4.63+19	2.16-2	36	1.65+19	5.70+19	2.62-2	156	1.35+19	4.59+19	2.11-2
17	1.27+19	4.18+19	1.96-2	37	1.51+19	5.14+19	2.38-2	157	1.23+19	4.14+19	1.91-2
18	1.16+19	3.76+19	1.78-2	38	1.38+19	4.63+19	2.16-2	158	1.13+19	3.73+19	1.74-2
19	1.04+19	3.30+19	1.58-2	39	1.23+19	4.07+19	1.91-2	159	1.01+19	3.27+19	1.54-2
20	9.03+18	2.80+19	1.36-2	40	1.07+19	3.45+19	1.65-2	160	8.76+18	2.78+19	1.32-2

TABLE ORNL-15

BSR-HSST-4 CAPSULE B PARAMETERS FOR CHARPY SPECIMENS

Specimen number	Damage exposure parameters			Specimen number	Damage exposure parameters		
	Fluence >1.0 MeV	Fluence >0.1 MeV	dpa (ASTM)		Fluence >1.0 MeV	Fluence >0.1 MeV	dpa (ASTM)
41	5.75+18	2.07+19	9.26-3	42	5.64+18	2.03+19	9.06-3
43	6.41+18	2.32+19	1.03-2	44	6.28+18	2.27+19	1.01-2
45	7.05+18	2.56+19	1.14-2	46	6.91+18	2.51+19	1.12-2
47	7.68+18	2.80+19	1.25-2	48	7.52+18	2.74+19	1.22-2
49	8.29+18	3.04+19	1.35-2	50	8.12+18	2.97+19	1.32-2
51	8.90+18	3.27+19	1.45-2	52	8.71+18	3.19+19	1.42-2
53	9.48+18	3.49+19	1.54-2	54	9.29+18	3.41+19	1.51-2
55	1.00+19	3.70+19	1.64-2	56	9.84+18	3.62+19	1.60-2
57	1.06+19	3.91+19	1.73-2	58	1.04+19	3.83+19	1.69-2
59	1.11+19	4.11+19	1.82-2	60	1.09+19	4.02+19	1.78-2
61	1.21+19	4.46+19	1.97-2	62	1.18+19	4.36+19	1.93-2
63	1.25+19	4.64+19	2.05-2	64	1.23+19	4.54+19	2.00-2
65	1.30+19	4.81+19	2.12-2	66	1.27+19	4.70+19	2.07-2
67	1.34+19	4.97+19	2.19-2	68	1.31+19	4.86+19	2.14-2
69	1.38+19	5.12+19	2.26-2	70	1.35+19	5.01+19	2.21-2
71	1.42+19	5.26+19	2.32-2	72	1.39+19	5.14+19	2.27-2
73	1.45+19	5.39+19	2.38-2	74	1.42+19	5.27+19	2.32-2
75	1.49+19	5.51+19	2.43-2	76	1.46+19	5.39+19	2.38-2
77	1.52+19	5.62+19	2.48-2	78	1.48+19	5.49+19	2.42-2
79	1.54+19	5.71+19	2.52-2	80	1.51+19	5.59+19	2.47-2
81	1.59+19	5.87+19	2.59-2	82	1.55+19	5.74+19	2.54-2
83	1.61+19	5.94+19	2.62-2	84	1.57+19	5.81+19	2.57-2
85	1.62+19	5.99+19	2.65-2	86	1.59+19	5.86+19	2.59-2
87	1.64+19	6.03+19	2.67-2	88	1.60+19	5.90+19	2.61-2
89	1.65+19	6.07+19	2.69-2	90	1.61+19	5.94+19	2.63-2
91	1.65+19	6.09+19	2.70-2	92	1.62+19	5.96+19	2.64-2
93	1.66+19	6.10+19	2.70-2	94	1.62+19	5.97+19	2.64-2
95	1.66+19	6.10+19	2.70-2	96	1.63+19	5.96+19	2.64-2
97	1.66+19	6.08+19	2.70-2	98	1.62+19	5.95+19	2.64-2
99	1.65+19	6.06+19	2.69-2	100	1.62+19	5.93+19	2.63-2
101	1.64+19	5.98+19	2.66-2	102	1.61+19	5.85+19	2.60-2
103	1.63+19	5.92+19	2.64-2	104	1.59+19	5.79+19	2.58-2
105	1.61+19	5.85+19	2.61-2	106	1.58+19	5.72+19	2.55-2
107	1.59+19	5.77+19	2.58-2	108	1.56+19	5.65+19	2.52-2
109	1.57+19	5.68+19	2.54-2	110	1.54+19	5.56+19	2.48-2
111	1.55+19	5.58+19	2.50-2	112	1.51+19	5.46+19	2.44-2
113	1.52+19	5.46+19	2.45-2	114	1.49+19	5.34+19	2.40-2
115	1.49+19	5.34+19	2.40-2	116	1.46+19	5.22+19	2.35-2
117	1.46+19	5.21+19	2.34-2	118	1.43+19	5.09+19	2.29-2
119	1.42+19	5.06+19	2.28-2	120	1.39+19	4.95+19	2.23-2
121	1.35+19	4.77+19	2.16-2	122	1.32+19	4.67+19	2.11-2
123	1.31+19	4.60+19	2.09-2	124	1.28+19	4.50+19	2.04-2
125	1.27+19	4.42+19	2.01-2	126	1.24+19	4.33+19	1.97-2
127	1.22+19	4.23+19	1.93-2	128	1.19+19	4.14+19	1.89-2
129	1.17+19	4.04+19	1.85-2	130	1.15+19	3.95+19	1.81-2
131	1.12+19	3.84+19	1.76-2	132	1.10+19	3.75+19	1.72-2
133	1.07+19	3.62+19	1.67-2	134	1.05+19	3.55+19	1.64-2
135	1.01+19	3.41+19	1.58-2	136	9.91+18	3.33+19	1.55-2
137	9.56+18	3.18+19	1.49-2	138	9.36+18	3.11+19	1.45-2
139	8.97+18	2.95+19	1.39-2	140	8.79+18	2.89+19	1.36-2

TABLE ORNL-16

BSR-HSST-4 CAPSULE C PARAMETERS FOR COMPACT TENSION (IT-CT) SPECIMENS

ORNL DWG 83-12867

Specimen number	Damage exposure parameters			Specimen number	Damage exposure parameters			Specimen number	Damage exposure parameters		
	Fluence >1.0 MeV	Fluence >0.1 MeV	dpa (ASTM)		Fluence >1.0 MeV	Fluence >0.1 MeV	dpa (ASTM)		Fluence >1.0 MeV	Fluence >0.1 MeV	dpa (ASTM)
1	8.35+18	2.80+19	1.30-2	21	9.65+18	3.40+19	1.55-2	141	8.08+18	2.81+19	1.28-2
2	1.04+19	3.51+19	1.62-2	22	1.20+19	4.26+19	1.93-2	142	1.00+19	3.53+19	1.60-2
3	1.23+19	4.18+19	1.93-2	23	1.42+19	5.07+19	2.29-2	143	1.19+19	4.20+19	1.90-2
4	1.40+19	4.80+19	2.21-2	24	1.62+19	5.82+19	2.62-2	144	1.36+19	4.82+19	2.18-2
5	1.60+19	5.50+19	2.52-2	25	1.86+19	6.67+19	3.00-2	145	1.55+19	5.52+19	2.49-2
6	1.74+19	5.98+19	2.74-2	26	2.02+19	7.25+19	3.26-2	146	1.69+19	6.00+19	2.71-2
7	1.86+19	6.38+19	2.93-2	27	2.15+19	7.75+19	3.48-2	147	1.80+19	6.41+19	2.89-2
8	1.96+19	6.72+19	3.08-2	28	2.27+19	8.15+19	3.66-2	148	1.90+19	6.74+19	3.04-2
9	2.05+19	7.02+19	3.22-2	29	2.37+19	8.52+19	3.83-2	149	1.99+19	7.05+19	3.18-2
10	2.10+19	7.17+19	3.29-2	30	2.43+19	8.69+19	3.91-2	150	2.03+19	7.20+19	3.25-2
11	2.12+19	7.22+19	3.33-2	31	2.45+19	8.77+19	3.95-2	151	2.05+19	7.26+19	3.28-2
12	2.12+19	7.20+19	3.32-2	32	2.45+19	8.73+19	3.95-2	152	2.05+19	7.23+19	3.28-2
13	2.09+19	7.04+19	3.26-2	33	2.41+19	8.54+19	3.87-2	153	2.02+19	7.07+19	3.21-2
14	2.03+19	6.82+19	3.16-2	34	2.35+19	8.28+19	3.76-2	154	1.97+19	6.85+19	3.12-2
15	1.96+19	6.52+19	3.04-2	35	2.26+19	7.91+19	3.61-2	155	1.89+19	6.55+19	2.99-2
16	1.86+19	6.14+19	2.87-2	36	2.15+19	7.45+19	3.41-2	156	1.80+19	6.17+19	2.83-2
17	1.70+19	5.56+19	2.62-2	37	1.97+19	6.74+19	3.11-2	157	1.65+19	5.58+19	2.58-2
18	1.56+19	5.02+19	2.38-2	38	1.80+19	6.09+19	2.83-2	158	1.51+19	5.04+19	2.35-2
19	1.40+19	4.42+19	2.12-2	39	1.61+19	5.37+19	2.52-2	159	1.35+19	4.44+19	2.09-2
20	1.22+19	3.77+19	1.83-2	40	1.41+19	4.58+19	2.17-2	160	1.18+19	3.79+19	1.80-2

TABLE ORNL-17

BSR-HSST-4 CAPSULE C PARAMETERS FOR CHARPY SPECIMENS

Specimen number	Damage exposure parameters			Specimen number	Damage exposure parameters		
	Fluence >1.0 MeV	Fluence >0.1 MeV	dpa (ASTM)		Fluence >1.0 MeV	Fluence >0.1 MeV	dpa (ASTM)
41	7.98+18	2.91+19	1.30-2	42	7.84+18	2.85+19	1.27-2
43	8.81+18	3.22+19	1.44-2	44	8.65+18	3.16+19	1.41-2
45	9.62+18	3.54+19	1.57-2	46	9.45+18	3.47+19	1.54-2
47	1.04+19	3.84+19	1.70-2	48	1.02+19	3.77+19	1.67-2
49	1.12+19	4.14+19	1.83-2	50	1.10+19	4.06+19	1.80-2
51	1.20+19	4.43+19	1.96-2	52	1.17+19	4.34+19	1.92-2
53	1.27+19	4.71+19	2.08-2	54	1.25+19	4.62+19	2.04-2
55	1.34+19	4.98+19	2.20-2	56	1.32+19	4.89+19	2.16-2
57	1.41+19	5.25+19	2.32-2	58	1.39+19	5.15+19	2.27-2
59	1.48+19	5.50+19	2.43-2	60	1.45+19	5.40+19	2.38-2
61	1.59+19	5.95+19	2.62-2	62	1.57+19	5.83+19	2.57-2
63	1.65+19	6.17+19	2.72-2	64	1.62+19	6.05+19	2.67-2
65	1.71+19	6.38+19	2.81-2	66	1.68+19	6.26+19	2.76-2
67	1.76+19	6.58+19	2.90-2	68	1.73+19	6.46+19	2.84-2
69	1.81+19	6.77+19	2.98-2	70	1.78+19	6.64+19	2.93-2
71	1.86+19	6.95+19	3.06-2	72	1.83+19	6.82+19	3.00-2
73	1.91+19	7.11+19	3.13-2	74	1.87+19	6.98+19	3.07-2
75	1.95+19	7.26+19	3.20-2	76	1.91+19	7.12+19	3.14-2
77	1.98+19	7.40+19	3.26-2	78	1.95+19	7.26+19	3.20-2
79	2.02+19	7.52+19	3.31-2	80	1.98+19	7.38+19	3.25-2
81	2.07+19	7.72+19	3.40-2	82	2.03+19	7.57+19	3.34-2
83	2.10+19	7.80+19	3.44-2	84	2.06+19	7.65+19	3.37-2
85	2.12+19	7.87+19	3.47-2	86	2.08+19	7.72+19	3.40-2
87	2.13+19	7.92+19	3.49-2	88	2.09+19	7.77+19	3.43-2
89	2.14+19	7.96+19	3.51-2	90	2.11+19	7.81+19	3.45-2
91	2.15+19	7.99+19	3.53-2	92	2.11+19	7.83+19	3.46-2
93	2.16+19	8.00+19	3.53-2	94	2.12+19	7.84+19	3.47-2
95	2.16+19	7.99+19	3.53-2	96	2.12+19	7.84+19	3.47-2
97	2.16+19	7.97+19	3.53-2	98	2.12+19	7.82+19	3.46-2
99	2.15+19	7.94+19	3.52-2	100	2.11+19	7.78+19	3.45-2
101	2.13+19	7.83+19	3.48-2	102	2.09+19	7.68+19	3.41-2
103	2.11+19	7.76+19	3.45-2	104	2.08+19	7.61+19	3.38-2
105	2.09+19	7.67+19	3.41-2	106	2.06+19	7.52+19	3.35-2
107	2.07+19	7.56+19	3.37-2	108	2.03+19	7.42+19	3.30-2
109	2.04+19	7.45+19	3.32-2	110	2.01+19	7.30+19	3.26-2
111	2.01+19	7.31+19	3.26-2	112	1.97+19	7.17+19	3.20-2
113	1.98+19	7.17+19	3.20-2	114	1.94+19	7.03+19	3.14-2
115	1.94+19	7.01+19	3.14-2	116	1.90+19	6.87+19	3.08-2
117	1.90+19	6.84+19	3.07-2	118	1.86+19	6.71+19	3.01-2
119	1.85+19	6.65+19	2.99-2	120	1.82+19	6.53+19	2.93-2
121	1.76+19	6.28+19	2.83-2	122	1.73+19	6.16+19	2.78-2
123	1.71+19	6.06+19	2.74-2	124	1.68+19	5.95+19	2.69-2
125	1.65+19	5.83+19	2.64-2	126	1.62+19	5.72+19	2.59-2
127	1.59+19	5.59+19	2.54-2	128	1.56+19	5.48+19	2.49-2
129	1.53+19	5.34+19	2.44-2	130	1.50+19	5.24+19	2.39-2
131	1.46+19	5.08+19	2.33-2	132	1.44+19	4.98+19	2.28-2
133	1.40+19	4.81+19	2.21-2	134	1.37+19	4.72+19	2.17-2
135	1.33+19	4.53+19	2.09-2	136	1.30+19	4.44+19	2.05-2
137	1.26+19	4.24+19	1.97-2	138	1.23+19	4.16+19	1.93-2
139	1.18+19	3.95+19	1.84-2	140	1.16+19	3.87+19	1.81-2

TABLE ORNL-18

BSR-HSST-4 CAPSULE D PARAMETERS FOR COMPACT TENSION (IT-CT) SPECIMENS

ORNL DWG 83-12869

Specimen number	Damage exposure parameters			Specimen number	Damage exposure parameters			Specimen number	Damage exposure parameters		
	Fluence >1.0 MeV	Fluence >0.1 MeV	dpa (ASTM)		Fluence >1.0 MeV	Fluence >0.1 MeV	dpa (ASTM)		Fluence >1.0 MeV	Fluence >0.1 MeV	dpa (ASTM)
1	1.00+19	3.39+19	1.57-2	21	1.13+19	3.98+19	1.81-2	141	9.27+18	3.22+19	1.47-2
2	1.28+19	4.37+19	2.02-2	22	1.45+19	5.14+19	2.32-2	142	1.19+19	4.15+19	1.89-2
3	1.54+19	5.30+19	2.44-2	23	1.75+19	6.24+19	2.81-2	143	1.43+19	5.04+19	2.29-2
4	1.79+19	6.17+19	2.83-2	24	2.03+19	7.26+19	3.26-2	144	1.66+19	5.87+19	2.65-2
5	2.08+19	7.17+19	3.28-2	25	2.35+19	8.43+19	3.78-2	145	1.93+19	6.81+19	3.08-2
6	2.28+19	7.86+19	3.59-2	26	2.57+19	9.24+19	4.14-2	146	2.11+19	7.47+19	3.37-2
7	2.45+19	8.45+19	3.86-2	27	2.77+19	9.94+19	4.45-2	147	2.27+19	8.03+19	3.62-2
8	2.60+19	8.94+19	4.09-2	28	2.94+19	1.05+20	4.71-2	148	2.41+19	8.50+19	3.84-2
9	2.74+19	9.42+19	4.31-2	29	3.10+19	1.11+20	4.97-2	149	2.54+19	8.95+19	4.04-2
10	2.82+19	9.66+19	4.43-2	30	3.18+19	1.14+20	5.10-2	150	2.61+19	9.18+19	4.15-2
11	2.86+19	9.78+19	4.49-2	31	3.24+19	1.15+20	5.17-2	151	2.65+19	9.30+19	4.21-2
12	2.88+19	9.79+19	4.51-2	32	3.25+19	1.15+20	5.19-2	152	2.67+19	9.31+19	4.22-2
13	2.85+19	9.64+19	4.45-2	33	3.22+19	1.13+20	5.12-2	153	2.64+19	9.16+19	4.17-2
14	2.79+19	9.38+19	4.34-2	34	3.15+19	1.10+20	5.00-2	154	2.59+19	8.92+19	4.07-2
15	2.70+19	9.02+19	4.19-2	35	3.05+19	1.06+20	4.83-2	155	2.50+19	8.57+19	3.93-2
16	2.58+19	8.54+19	3.99-2	36	2.92+19	1.00+20	4.59-2	156	2.39+19	8.12+19	3.74-2
17	2.38+19	7.79+19	3.66-2	37	2.70+19	9.16+19	4.22-2	157	2.21+19	7.41+19	3.44-2
18	2.20+19	7.10+19	3.36-2	38	2.49+19	8.34+19	3.87-2	158	2.04+19	6.74+19	3.15-2
19	1.99+19	6.31+19	3.02-2	39	2.25+19	7.42+19	3.48-2	159	1.85+19	6.00+19	2.83-2
20	1.76+19	5.46+19	2.64-2	40	1.99+19	6.42+19	3.05-2	160	1.63+19	5.19+19	2.48-2

TABLE ORNL-19

BSR-HSST-4 CAPSULE D PARAMETERS FOR CHARPY SPECIMENS

Specimen number	Damage exposure parameters			Specimen number	Damage exposure parameters		
	Fluence >1.0 MeV	Fluence >0.1 MeV	dpa (ASTM)		Fluence >1.0 MeV	Fluence >0.1 MeV	dpa (ASTM)
43	1.03+19	3.75+19	1.67-2	44	1.01+19	3.67+19	1.64-2
45	1.14+19	4.16+19	1.85-2	46	1.11+19	4.07+19	1.81-2
47	1.24+19	4.57+19	2.03-2	48	1.22+19	4.47+19	1.98-2
49	1.35+19	4.97+19	2.20-2	50	1.32+19	4.86+19	2.15-2
51	1.45+19	5.36+19	2.37-2	52	1.42+19	5.24+19	2.32-2
53	1.55+19	5.74+19	2.53-2	54	1.52+19	5.61+19	2.48-2
55	1.65+19	6.10+19	2.69-2	56	1.62+19	5.97+19	2.64-2
57	1.74+19	6.46+19	2.85-2	58	1.71+19	6.32+19	2.79-2
59	1.84+19	6.80+19	3.00-2	60	1.80+19	6.66+19	2.93-2
61	2.00+19	7.41+19	3.26-2	62	1.96+19	7.25+19	3.19-2
63	2.08+19	7.71+19	3.39-2	64	2.04+19	7.55+19	3.32-2
65	2.16+19	8.01+19	3.52-2	66	2.11+19	7.83+19	3.45-2
67	2.23+19	8.28+19	3.64-2	68	2.19+19	8.11+19	3.56-2
69	2.30+19	8.55+19	3.76-2	70	2.26+19	8.36+19	3.68-2
71	2.37+19	8.79+19	3.86-2	72	2.32+19	8.60+19	3.78-2
73	2.43+19	9.02+19	3.96-2	74	2.38+19	8.83+19	3.88-2
75	2.49+19	9.24+19	4.06-2	76	2.44+19	9.04+19	3.97-2
77	2.54+19	9.43+19	4.15-2	78	2.49+19	9.23+19	4.06-2
79	2.59+19	9.61+19	4.22-2	80	2.54+19	9.41+19	4.14-2
81	2.67+19	9.90+19	4.35-2	82	2.62+19	9.68+19	4.26-2
83	2.71+19	1.00+20	4.41-2	84	2.66+19	9.81+19	4.32-2
85	2.74+19	1.01+20	4.46-2	86	2.69+19	9.91+19	4.37-2
87	2.77+19	1.02+20	4.50-2	88	2.71+19	1.00+20	4.41-2
89	2.79+19	1.03+20	4.53-2	90	2.74+19	1.01+20	4.44-2
91	2.81+19	1.03+20	4.56-2	92	2.75+19	1.01+20	4.47-2
93	2.82+19	1.04+20	4.58-2	94	2.76+19	1.02+20	4.48-2
95	2.83+19	1.04+20	4.59-2	96	2.77+19	1.02+20	4.49-2
97	2.83+19	1.04+20	4.59-2	98	2.78+19	1.02+20	4.49-2
99	2.83+19	1.04+20	4.58-2	100	2.77+19	1.01+20	4.48-2
101	2.81+19	1.03+20	4.55-2	102	2.76+19	1.00+20	4.45-2
103	2.80+19	1.02+20	4.51-2	104	2.74+19	9.96+19	4.42-2
105	2.78+19	1.01+20	4.48-2	106	2.72+19	9.86+19	4.38-2
107	2.75+19	9.96+19	4.43-2	108	2.69+19	9.75+19	4.34-2
109	2.72+19	9.83+19	4.37-2	110	2.66+19	9.61+19	4.28-2
111	2.68+19	9.67+19	4.31-2	112	2.63+19	9.46+19	4.22-2
113	2.64+19	9.50+19	4.24-2	114	2.59+19	9.29+19	4.15-2
115	2.60+19	9.31+19	4.16-2	116	2.55+19	9.11+19	4.08-2
117	2.55+19	9.10+19	4.08-2	118	2.50+19	8.91+19	3.99-2
119	2.50+19	8.88+19	3.99-2	120	2.45+19	8.69+19	3.90-2
121	2.39+19	8.42+19	3.80-2	122	2.34+19	8.24+19	3.72-2
123	2.32+19	8.15+19	3.69-2	124	2.27+19	7.97+19	3.61-2
125	2.25+19	7.86+19	3.57-2	126	2.21+19	7.70+19	3.49-2
127	2.18+19	7.56+19	3.44-2	128	2.13+19	7.40+19	3.37-2
129	2.10+19	7.25+19	3.31-2	130	2.06+19	7.09+19	3.24-2
131	2.02+19	6.92+19	3.17-2	132	1.98+19	6.77+19	3.11-2
133	1.93+19	6.58+19	3.03-2	134	1.90+19	6.44+19	2.97-2
135	1.85+19	6.23+19	2.88-2	136	1.81+19	6.10+19	2.82-2
137	1.76+19	5.87+19	2.73-2	138	1.72+19	5.74+19	2.67-2
139	1.66+19	5.49+19	2.57-2	140	1.63+19	5.37+19	2.52-2

DISTRIBUTION

R5

DOE-RL/Office of Asst Manager
for Advanced Reactor Programs
P.O. Box 550
Richland, WA 99352

KR Absher, Chief,
Technology Dev Branch

DOE-HQ/Office of Converter
Reactor Deployment
Nuclear Regulation & Safety Division
NE-12
Washington, DC 20545

JD Griffith, Deputy Director

DOE-HQ/Office of Breeder
Technology Projects (9)
NE-53
Washington, DC 20545

WA Nelson, Director, Office of
Breeder Technology Projects
H. Alter, Asst Director, Safety
FX Gavigan, Director,
Safety & Physics
PB Hemmig, Asst Director,
Reactor Physics Technology
JW Lewellen, Manager,
Core Analysis Technology
DK Magnus, Director,
Fuels & Core Materials
RJ Neuhold, Asst Director,
Core Systems & Materials
CM Purdy, Asst Director,
Materials & Structures Tech
A. Van Echo, Manager, Metallurgy,
Absorbers & Standards

Arizona State University (2)
College of Eng & Appl Sciences
Tempe, AZ 85287

B. Stewart
JW McKlveen

Argonne National Laboratory (2)
9700 South Cass Avenue
Argonne, IL 60439

RJ Armani
RR Heinrich, Bldg 316

Babcock & Wilcox Co.
Lynchburg Research Center (4)
P.O. Box 1260
Lynchburg, VA 24505

RH Lewis AA Lowe, Jr.
LB Gross CL Whitmarsh

Battelle
Pacific Northwest Laboratory
P.O. Box 999
Richland, WA 99352

EP Simonen

Battelle Memorial Institute
505 King Avenue
Columbus, OH 43201

M. Manahan

Bechtel Power Corporation
15740 Shady Grove Road
Gaithersburg, MD 20760

WC Hopkins

Brookhaven National Laboratory (3)
National Neutron Cross Section Center
Upton, Long Island, NY 11973

JF Carew BA Magurno
S. Pearlstein, Bldg T-197

DISTRIBUTION (Cont'd)

Burns & Roe, Inc.
633 Industrial Avenue
Paramus, NJ 07672

C. Celnik

Carolina Power & Light Co.
P.O. Box 1551
Raleigh, SC 27602

S. Grant

Centre d'Etude de l'Énergie Nucléaire
Studiecentrum voor Kernenergie (7)
Boeretang 200
B-2400 Mol, Belgium

J. Debrue
G. DeLeeuw
S. DeLeeuw
A. Fabry
G. Minsart
H. Tourwé
PH Van Asbroeck

Combustion Engineering Inc. (5)
1000 Prospect Hill Road
Windsor, CT 06095

S. Byrne
G. Cavanaugh
JJ Koziol
RG Shimko
D. Stephen

Comitato Nazional per Energia Nucleare
Centro di Studi Nucleari della Casaccia
Casella Postale 2400
Santa Maria di Galeria
I-00060 Rome, Italy

U. Farinelli

Commissariat a l'Energie Atomique
Centre d'Etudes Nucleaires de Saclay (6)
Boite Postale 2
91190 Gif-sur-Yvette, France

AA Alberman
C. Buchalet (Framatome)
JM Cerles
JP Genthon
P. Mas (Grenoble)
P. Petrequin

Commonwealth Edison
P.O. Box 767
Chicago, IL 60690

E. Steeve

EG&G Idaho, Inc. (3)
P.O. Box 1625
Idaho Falls, ID 83415

R. Greenwood
Y. Harker
JW Rogers

EG&G Ortec, Inc.
100 Midland Road
Oak Ridge, TN 37830

W. Zimmer

Electric Power Research Institute (6)
3412 Hillview Avenue
P.O. Box 10412
Palo Alto, CA 94304

TU Marston
O. Ozer
T. Passell
AD Rossin
R. Shaw
K. Stahlkopf

Energieonderzoek Centrum Nederland
Westerdionweg 3
NL-1755 ZG, Petten, Netherlands

WL Zijp

Engineering Services Associates
3320 Bailey
Buffalo, NY 14215

M. Haas

EURATOM
Joint Research Center Ispra (2)
I-21020 Ispra, Varese, Italy

R. Dierckx
H. Rief

DISTRIBUTION (Cont'd)

Fracture Control Corporation (2)
330 Kellogg Ave, Suite E
Goleta, CA 93017

J. Perrin
RA Wullaert

GE/Vallecitos Nuclear Center
P.O. Box 460
Pleasanton, CA 94566

GC Martin

IKE-Stuttgart (2)
Pfaffenwaldring 31
Postfach 801140
D-7000 Stuttgart 80 (Vaihingen)
Federal Republic of Germany

G. Hehn
G. Prillinger

International Atomic Energy Agency (2)
Wagramerstrasse 5
Postfach 100
A-1400 Vienna, Austria

A. Sinev
JJ Schmidt

IRT Corporation (3)
P.O. Box 80817
San Diego, CA 92183

NA Lurie WE Selph
C. Preskitt

Italian Atomic Power Authority
National Electric Energy Agency (2)
Viale Regina Margherita 137
Rome, Italy

M. Galliani
F. Remondino

Japan Atomic Energy Research Institute (2)
Tokai-mura, Naka-gun
Ibaraki-ken, Japan

S. Mizazono
K. Sakurai

Kernforschungsanlage Jülich GmbH (3)
Postfach 1913
D-517 Jülich 1
Federal Republic of Germany

D. Pachur L. Weise
W. Schneider

Kraftwerk Union Aktiengesellschaft (5)
Postfach 3220
D-8520 Erlangen
Federal Republic of Germany

A. Gerscha J. Koban
U. Groschel C. Leitz
W. Hofmann

Los Alamos National Laboratory (2)
P.O. Box 1663
Los Alamos, NM 87545

GE Hansen, Group N-2
L. Stewart

Maine Yankee Atomic Power Co.
Edison Drive
Augusta, MA 04336

HF Jones, Jr.

Materials Engineering Associates
111 Mel-Mara Drive
Oxen Hill, MD 20021

JR Hawthorne

DISTRIBUTION (Cont'd)

National Bureau of Standards
Center of Radiation Research (6)
Washington, DC 20234

RS Caswell
CM Eisenhauer
DM Gilliam
JA Grundl
G. Lamaze
ED McGarry

Naval Research Laboratory
Engineering Materials Division
Thermostructural Materials Branch
Code 6390
Washington, DC 20375

LE Steele

Nuclear Regulatory Commission (17)
Office of Nuclear Regulatory Research
Division of Engineering Technology
Materials Engineering Branch
NL-5650
Washington, DC 20555

Chief
Public Doc Rm (3)
M. Bolotski
M. Dunenseld
R. Gamble
W. Hazelton
KG Hoge
RE Johnson
L. Lois
S. Pawlicki
PN Randall
CZ Serpan
D. Sieno
A. Taboda
M. Vagin

Oak Ridge National Laboratory (8)
P.O. Box X
Oak Ridge, TN 37830

CA Balawin
RG Berggren
FBK Kam
AL Lotts
RE Maerker
LS Miller
R. Nanstad
FW Stallmann

Radiation Research Associates (2)
3550 Hulen Street
Fort Worth, TX 76107

RM Rubin
MB Wells

Rockwell International
Energy Systems Group (2)
P.O. Box 309
Canoga Park, CA 91304

H. Farrar IV
B. Oliver

Rolls-Royce & Associates Ltd. (4)
P.O. Box 31
Derby, UK

M. Austin
P. Burch
AF Thomas
TJ Williams

S.A. Cockerill-Ougree
Recherches et Developments
Division de la Construction Mecanique
B-4100 Seraing, Belgium

J. Widart

Science Applications Inc. (3)
P.O. Box 2325
La Jolla, CA 92037

W. Hagan
GL Simmons
VV Verbinski

Ship Research Institute
Takai Branch Office
Tokai-mura, Naka-gun
Ibaraki-ken, Japan

K. Takeuchi

DISTRIBUTION (Cont'd)

Southwest Research Institute
8500 Calebra Road
P.O. Box 28510
San Antonio, TX 78284

EB Norris

Swiss Federal Institute
for Reactor Research
CH-5303 Würenlingen, Switzerland

F. Hegedus

United Kingdom Atomic Energy Authority
Atomic Energy Research Establishment (3)
Harwell, Oxon, UK

LM Davies DR Harries
AJ Fudge

United Kingdom Atomic Energy Authority
Atomic Energy Establishment (4)
Winfrith, Dorchester, Dorset, UK

J. Butler AK McCracken
CG Campbell J. Sanders

University of Arkansas (2)
Dept of Mechanical Engineering
Fayetteville, AR 72701

CO Cogburn
L. West

University of California
at Santa Barbara (2)
Dept of Chem & Nucl Eng
Santa Barbara, CA 93106

G. Lucas
GR Odette

Univ of London Reactor Center
Silwood Park, Sunnyhill
Ascot, Berkshire, UK
SL57PY

JA Mason

University of Tokyo (2)
Dept of Nuclear Engineering
7-3-1, Hongo
Bunkyo-ku, Tokyo, 113 Japan

M. Nakazawa
J. Sekiguchi

Westinghouse
Nuclear Energy Systems (3)
P.O. Box 355
Pittsburgh, PA 15230

SL Anderson SE Yanichko
TR Mager

Westinghouse
Research and Development Center
1310 Beulah Road
Pittsburgh, PA 15235

JA Spitznagel

University of Missouri (2)
at Rolla
Dept of Nucl Eng
Building C
Rolla, MO 65401

DR Edwards
N. Tsoulfanidis

DISTRIBUTION (Cont'd)

HEDL (48)
c/o Document Processing Supervisor
P.O. Box 1970, W/C-123
Richland, WA 99352

HJ Anderson	W/C-39	WN McElroy (2)	W/C-39
RA Bennett	W/D-3	JP McNeece	W/C-39
TK Bierlein	W/A-64	JE Nolan	W/B-65
LD Blackburn	W/A-40	RE Peterson	W/C-80
DG Doran	W/A-57	CC Preston	W/C-39
EA Evans	W/C-23	JH Roberts	W/C-39
DS Gelles	W/A-64	FH Ruddy	W/C-39
R. Gold	W/C-39	JM Ruggles	W/C-36
GL Guthrie	W/A-40	RE Schenter	W/A-4
BR Hayward	W/C-44	FA Schmittroth	W/A-4
LA James	W/A-40	WF Sheely	W/A-62
LS Kellogg	W/C-39	FR Shober	W/E-3
NE Kenny	W/C-115	RL Simons	W/A-57
RL Knecht	W/A-40	HH Yoshikawa	W/C-44
JJ Laidler	W/B-107	Program Files (10)	W/C-39
EP Lippincott (2)	W/C-39	Central Files (3)	W/C-110
WY Matsumoto	W/C-33	Publ Services (2)	W/C-115

NRC FORM 335 (7-77)

U.S. NUCLEAR REGULATORY COMMISSION

BIBLIOGRAPHIC DATA SHEET

1. REPORT NUMBER *(Assigned by DDC)*
NUREG/CR-3391, VOL. 1
HEDL-TME 83-21

4. TITLE AND SUBTITLE *(Add Volume No., if appropriate)*
LWR Pressure Vessel Surveillance Dosimetry Improvement Program
Quarterly Progress Report - January 1983-March 1983

2. *(Leave blank)*

3. RECIPIENT'S ACCESSION NO.

7. AUTHOR(S)
E.P. Lippincott and W. N. McElroy

5. DATE REPORT COMPLETED
MONTH: September | YEAR: 1983

9. PERFORMING ORGANIZATION NAME AND MAILING ADDRESS *(Include Zip Code)*
Hanford Engineering Development Laboratory
P.O. Box 1970
Richland, WA 99352

DATE REPORT ISSUED
MONTH: November | YEAR: 1983

6. *(Leave blank)*

8. *(Leave blank)*

12. SPONSORING ORGANIZATION NAME AND MAILING ADDRESS *(Include Zip Code)*
Division of Engineering Technology
Office of Nuclear Regulatory Research
US Nuclear Regulatory Commission
Washington, DC 20555

10. PROJECT/TASK/WORK UNIT NO.

11. CONTRACT NO.
B5988-7

13. TYPE OF REPORT
Quarterly Progress Report

PERIOD COVERED *(Inclusive dates)*
January 1983 - March 1983

15. SUPPLEMENTARY NOTES

14. *(Leave blank)*

16. ABSTRACT *(200 words or less)*

The Light Water Reactor Pressure Vessel Surveillance Dosimetry Improvement Program (LWR-PV-SDIP) has been established by NRC to improve, test, verify, and standardize the physics-dosimetry-metallurgy, damage correlation, and the associated reactor analysis methods, procedures and data used to predict the integrated effect of neutron exposure to LWR pressure vessels and their support structures. A vigorous research effort attacking the same measurement and analysis problems exists worldwide, and strong cooperative links between the US NRC-supported activities at HEDL, ORNL, NBS, and MEA-ENSA and those supported by CEN/SCK (Mol, Belgium), EPRI (Palo Alto, USA), KFA (Jülich, Germany), and several UK laboratories have been extended to a number of other countries and laboratories. These cooperative links are strengthened by the active membership of the scientific staff from many participating countries and laboratories in the ASTM E10 Committee on Nuclear Technology and Applications. Several subcommittees of ASTM E10 are responsible for the preparation of LWR surveillance standards.

17. KEY WORDS AND DOCUMENT ANALYSIS

17a. DESCRIPTORS

17b. IDENTIFIERS/OPEN-ENDED TERMS

18. AVAILABILITY STATEMENT
Unlimited

19. SECURITY CLASS *(This report)*
Unclassified

21. NO. OF PAGES
89

20. SECURITY CLASS *(This page)*
Unclassified

22. PRICE
$

NRC FORM 335 (7-77)